EUB/AGS Special Report 72

Basement Structure in Central and Southern Alberta: Insights from Gravity and Magnetic Maps

Alberta Energy and Utilities Board

Alberta Geological Survey

AGS

EUB/AGS Special Report 72

Basement Structure in Central and Southern Alberta: Insights from Gravity and Magnetic Maps

H.V. Lyatsky[1], D.I. Pana[2] and M. Grobe[2]

[1]Lyatsky Geoscience Research & Consulting Ltd.
[2]Alberta Energy and Utilities Board/Alberta Geological Survey

October 2005

ISBN 0-7785-3858-3

Lyatsky, H.V., Pană, D.I. and Grobe, M. (2005): Basement structure in central and southern Alberta: insights from gravity and magnetic maps; Alberta Energy and Utilities Board, EUB/AGS Special Report 72, 76 p.

Author address:
Henry Lyatsky
Lyatsky Geoscience Research & Consulting Ltd.
4827 Nipawin Crescent NW
Calgary, AB T2K 2H8 Canada
Tel: (403) 282-5873

Published October 2005 by:
Alberta Energy and Utilities Board
Alberta Geological Survey
4th Floor, Twin Atria Building
4999 - 98th Avenue
Edmonton, Alberta
T6B 2X3
Canada

Tel: (780) 422-3767 (Information Sales)
Fax: (780) 422-1918
E-mail: EUB.AGS-Infosales@gov.ab.ca
Website: www.ags.gov.ab.ca

Contents

Figures

Maps

Acknowledgments

Nancy Crann, Chantel Bunnell and Dan Magee are thanked for able assistance with computer drafting. Public domain Canadian potential-field digital data have been obtained at low or no cost from Natural Resources Canada. The patient assistance of Doug Oneschuk at the Geological Survey of Canada, Ottawa office, is particularly noted and appreciated.

Aeromagnetic Data
Canadian Aeromagnetic Data Base
Continental Geoscience Division
Geological Survey of Canada
Earth Sciences Sector
Natural Resources Canada

Gravity Data
Canadian Geodetic Information System
Geodetic Survey Division
Geomatics Canada
Earth Sciences Sector
Natural Resources Canada
Contact: http://gdcinfo.agg.nrcan.gc.ca/contact_e.html#DataCentre

Abstract

Identification of brittle faults in the Alberta Basin is critical to hydrocarbon and mineral exploration, as well as to greenhouse gas geological sequestration studies. Many faults affecting the Phanerozoic sedimentary rocks of this basin are well known to be basement controlled. Potential-field data can give valuable information on the location of faults in the basement. These faults may have propagated into the overlying sedimentary rocks and influenced fluid flow and distribution of hydrocarbon traps and mineralization zones, as well as salt dissolution and carbonate alteration. The present study used regional, publicly available gravity and aeromagnetic data compiled and levelled by the Geological Survey of Canada to identify geophysical lineaments that may represent basement faults in central and southern Alberta (south of 56°N latitude).

The crystalline basement in central and southern Alberta includes Archean and Early Proterozoic ductile orogenic structures and Middle Proterozoic to Recent cratonic structures.

Although anomaly signatures of the ancient ductile basement structures predominate in potential-field maps, brittle, high-angle block-bounding faults that had the most influence on the evolution of the Alberta Basin. These steep, brittle basement faults are much more subtle and less easily detectable; many of them are subresolution seismically. Gravity and magnetic data processing and anomaly-enhancement experiments revealed many gravity and magnetic lineaments defined by gradient zones, alignments of separate local anomalies of various types and shapes, aligned breaks or discontinuities in the anomaly pattern, and so on. Such lineaments are commonly associated with brittle basement faults.

The results of gravity and magnetic data processing are provided here as a catalogue of maps with inferred lineaments, as well as geographically referenced geotiff files (potential-field maps) and DXF files (lineament maps).

1 Introduction

Identification of faults in the Alberta Basin is critical to hydrocarbon and mineral exploration, and potentially to meeting some environmental challenges. Many oil and gas fields and reservoir trends in the Alberta Basin have long been known to be linearly distributed along faults. Subsurface sequestration of greenhouse gases and waste storage, which are the focus of increasing research and policy attention in Western Canada and elsewhere (e.g., Friedmann and Homer-Dixon, 2004; White et al., 2004), also require knowledge of brittle faults.

Prevalence of basement faulting in cratonic regions has been recognized in classical geology since at least Stille (1924), and its oil exploration significance has been studied in Alberta for half a century (Garland and Bower, 1959). Fault-inducing lithospheric stresses in the pericratonic Alberta Basin were evidently the result of both local and external sources (Lyatsky et al., 1999). Local sources are always present due to the continental lithosphere's ability to produce radiogenic heat. Proximity to the Cordillera in this pericratonic region made for significant orogenic influences at various times, particularly in the western parts of the Alberta Basin. Whatever the causes of stress, it is well known that east of the Cordilleran deformation front, faults in the Phanerozoic cover were mostly defined by the patterns of faulting in the crystalline basement.

Essential for exploration, basement faults in various geological provinces and tectonic settings are routinely investigated at both regional and local scales with the help of potential-field data and other geophysical and geological information (e.g., Cohen et al., 1990; Friedman and Huffman, 1998; Gabrielsen et al., 2002; Marshak and Paulsen, 1996; Maughan and Perry, 1986; Piskarev and Tchernyshev, 1997; Steeples, 1989; Swanson, 1986; Vearncombe and Vearncombe, 2002; Wellman, 1985). Although examination of the underlying basement structure is a prerequisite in basin analysis, and such studies are a common part of exploration success in Western Canada and elsewhere, geophysical lineaments do not always exactly depict basement faults, and not all basement faults affected the overlying sedimentary rocks.

With the benefit of experience gained recently in northern Alberta (Lyatsky and Pană, 2003), the present study attempts to identify geophysical lineaments that may depict basement faults in the central and southern part of the province (south of 56°N latitude). Particular attention has been given to an area of potential interest for greenhouse-gas geological sequestration west of Edmonton (Figure 1). The processing and interpretation of gravity and magnetic data in southern Alberta, aiming to improve the understanding of basement influences on the sedimentary cover, is part of a longer-term multidisciplinary study coordinated by the Alberta Geological Survey (AGS).

The first sections of this report review the geological framework of southern Alberta, previous regional geophysical studies and relevant geophysical concepts routinely used in potential-field data processing and interpretation. The following sections describe the gravity and magnetic data used in this study, as well as various data processing and anomaly-enhancement techniques. The resulting processed gravity and magnetic maps with inferred geophysical lineaments that may depict basement faults are included in the attached catalogue. The report and the accompanying geophysical catalogue are delivered in PDF format on CD-ROM, which includes geographically referenced maps (geotiff files) and interpreted lineaments on each of these maps (DXF files).

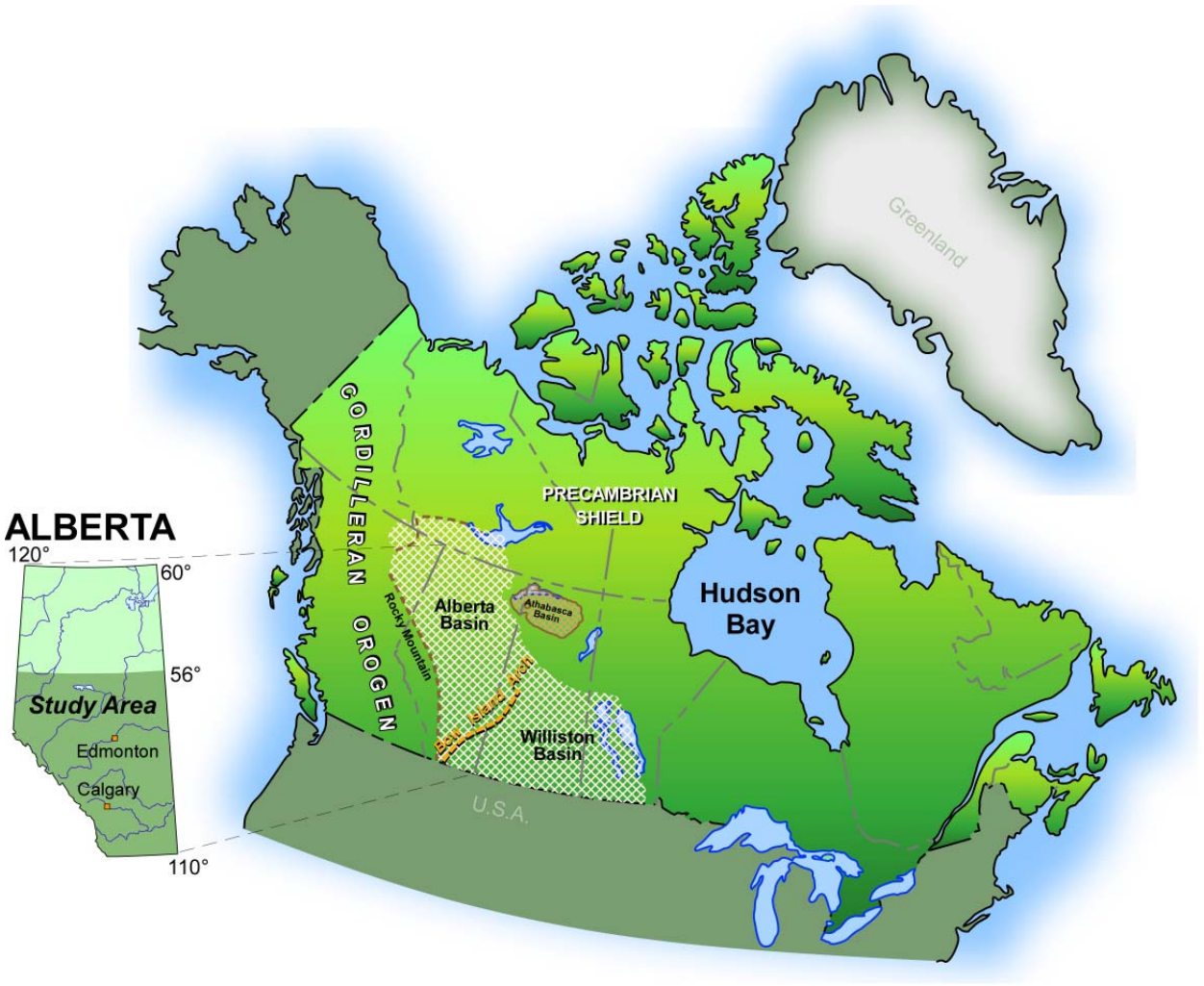

Figure 1. Index map showing the geological setting of the Alberta Basin, with the bounding crustal arches, Canadian Shield edge and the Cordilleran orogen, as well as political borders.

2 Geological Setting

The area under consideration encompasses the southern part of the Phanerozoic Alberta Basin in the Plains of Western Canada (Figure 1). Located in the pericratonic region in the western part of the North American craton, the essentially cratonic Alberta Basin was also subject to episodic Cordilleran structural and depositional influences, mainly from the Antler and Laramide orogenies. Some of the recent regional summaries of the Alberta Basin geology and evolution, offering a range of disparate tectonic ideas, have been published by Ricketts (1989); Mossop and Shetsen (1994); Cecile et al. (1997); Ross and Eaton (1999) and Lyatsky et al. (1999). Regional overviews of the relevant parts of Western Canada and the United States are also available in the Decade of North American Geology publications (Palmer, ed., 1982).

Boundaries of the Alberta Basin are generally thought to be large crustal weakness zones: the Tathlina Arch in the Northwest Territories, the Sweetgrass Arch near the Alberta-Saskatchewan border, and the Great Falls zone or Lewis and Clark zone in northern and central Montana. Across these weakness zones lie other sedimentary basins and geological provinces, with dissimilar geological history. The Alberta

Basin's western boundary is the Cordillera, whose east-verging Laramide thrust belt deforms the basin rocks in a system of large thrust sheets in the Front Ranges and Foothills, but does not involve the crystalline basement. In the northeast, across the erosional edge of the Phanerozoic sedimentary rocks of the Alberta Basin, lies the Early Proterozoic and Archean Canadian Shield, where crystalline rocks analogous to those underlying the Alberta Basin are exposed (Lewry and Stauffer, 1990).

From the sedimentary cover zero edge, the basin deepens towards the Cordillera to the southwest, reaching depths of more than five kilometres in the Laramide foredeep that runs parallel to the Cordillera. This entire region is covered by an assemblage of glacial tills and channel deposits related to several episodes of Wisconsinan and earlier glaciation.

3 Previous Regional Potential-field Geophysical Studies

Basement control on oilfield distribution in the Alberta and Williston basins has been examined with the help of potential-field data for decades (e.g., Garland and Bower, 1959). Regional studies by Edwards et al. (1998) and Lyatsky et al. (1998) used horizontal-gradient vector maps to highlight some aspects of the basement structure in central Alberta, as well as in the Williston Basin in southern Saskatchewan and Manitoba, and presented combined geological/geophysical examples of basement-fault control on the distribution of hydrocarbon traps in the sedimentary cover.

Hoffman (1988, 1989) used potential-field and geochronology data to extend geological and geophysical domains from the Canadian Shield into sediment-covered areas of North America and to develop a tectonic interpretation of the Canadian Shield. Ross et al. (1991) and Villeneuve et al. (1993) attempted to subdivide the Precambrian basement in Alberta and northeastern British Columbia into tectonic domains, based on their interpretation of potential-field data and isotope age determinations on basement core samples. These workers also sought corroboration for their interpretation in analogies with geophysical signatures of exposed geological provinces in the Canadian Shield and the inferred tectonic subdivisions of Hoffman. Ross et al. (1991) postulated several tectonic domains in the Alberta basement and proposed for them an accretion history; some of their supposed tectonic-domain boundaries seem to closely follow the zero contour in magnetic maps. Their methods and conclusions were strongly disputed by Lyatsky et al. (1999), who also stressed the difference between ancient ductile and younger brittle basement structures. Pilkington et al. (2000) used quantitative methods and anomaly enhancement (derivatives and shaded relief maps) to emphasize the internal character of domains and refine basement subdivisions.

Our first attempt to process data specifically to highlight lineaments that may represent brittle faults in the Alberta basement was the creation of a catalogue of gravity and magnetic maps for northern Alberta (Lyatsky and Pană, 2003). That catalogue was patterned in part on the Canadian Geophysical Atlas of the Geological Survey of Canada (1990), but it was created only for a relatively small region. One of the reasons for choosing northern Alberta for the initial study was the availability of geological constraints: presence of the Canadian Shield within and near that area permits one to geologically calibrate the interpretation of basement structures from geophysical data (Langenberg, 1983; Godfrey, 1986; Sprenke et al., 1986; Lewry and Stauffer, 1990).

4 Detection of Basement Structures with Potential-field Geophysical Data

4.1 Basement Structures and Their Potential-field Signatures

Two fundamentally different types of crystalline-basement structure, formed in different tectonic conditions, are recognized in the Alberta Basin (Lyatsky et al., 1999):

1) *Archean and Early Proterozoic (Hudsonian and older) ductile orogenic structures*, and
2) *Middle Proterozoic to Recent cratonic structures.*

The influence of ancient ductile basement structures on the Alberta Basin sedimentary cover is usually slight. It largely seems to be confined to the control on early Palaeozoic depositional and drape patterns exerted by pre-Phanerozoic erosional relief, which was formed when the future basement was exposed at the surface (Garland and Bower, 1959). This erosional basement relief is to some extent related to the distribution of resistant and recessive crystalline rocks, which may in turn bear some relation to the ductile, ancient structures. Overall, studies of the Hudsonian and older ductile basement structures are of secondary value to hydrocarbon and mineral exploration in the sedimentary cover.

Although anomaly signatures of the ancient ductile basement structures predominate in potential-field maps, it is brittle, high-angle block-bounding faults that had the most influence on the evolution of the Alberta Basin. The brittle faults partly follow the older ductile orogenic structures, but also commonly cut across them. Brittle cratonic faults and fractures are typical for the upper continental crust, above the mid-crustal brittle-ductile transition that usually lies at about 12 to 15 km depth, depending on geothermal gradients. Fault and block movements are dissipated in the lower crust, which is ductile and capable of flowage (e.g., Dohr, 1989).

Steep, brittle basement faults in the western Canadian platforms are much more subtle and less easily detectable than their famously huge equivalents in the spectacularly block-faulted United States Cordilleran foreland. Even when subresolution seismically, brittle faults and block movements nonetheless exerted considerable syn- and post-depositional influence on the sedimentary cover. Basement control on the sedimentary cover was partial, episodic, locally variable and commonly passive and indirect, particularly where even unreactivated brittle faults with zero offsets affected fluid flow, salt dissolution and carbonate alteration. Basement faults are known to have commonly influenced the distribution of hydrocarbon traps and mineralization zones in the sedimentary cover (Edwards et al., 1998; Lyatsky et al., 1998, 1999).

4.2 Gravity Exploration Methods

Gravity data are normally recorded on the ground, by taking gravimeter readings from station to station. The physical rock property that relates gravity anomalies to rocks is density, and gravity anomalies represent lateral variations in the density of rocks (Nettleton, 1971).

The gravity field is attractively simple: unipolar and almost perfectly vertical. Its measurable manifestation is acceleration due to gravity, measured commonly in Gals (1 Gal = 1 cm/s^2 = 0.01 m/s^2), or more commonly in geophysics, milliGals (1 mGal = 0.001 Gal) and occasionally gravity units (1 g.u. = 0.1 mGal). Gravity anomalies in the Bouguer reduction, used in this study as is commonly done in land areas, take account of the Earth's rotation, polar flattening, recording field station's latitude and elevation, and gravitational attraction of the rock mass lying above sea level.

The gravity data for this study were supplied by the Geological Survey of Canada (GSC) and Natural Resources Canada (Maps 1 and 2). Exact knowledge of every field station's elevation is essential for the accuracy of gravity data. The terrain correction was applied to the Bouguer gravity data by the GSC only in the high mountains of the Cordillera, but not in the flat topography Plains regions. Bouguer anomalies are generally considered to fairly represent the rock density variations in the crust and asthenosphere. Although isostatic anomalies may also be useful for some applications, Bouguer data were used in this study to enable easier comparison with previously published GSC maps.

From experience, gravity data in many parts of the Alberta and Williston basins are sensitive to local vertical offsets across high-angle faults where rocks with different densities are juxtaposed. Gravity lineaments therefore deserve attention in basement studies. On the other hand, high densities of some Palaeozoic sedimentary rocks just above the basement may smear out the subtle gravity signatures of basement faults. Notably, for whatever reason, in the Peace River Arch in northwestern Alberta, where vertical basement-fault offsets reach tens and hundreds of metres, the associated gravity anomalies are not as strong as might be expected.

4.3 Magnetic Exploration Methods

Much more complicated than gravity are the geophysically relevant aspects of the magnetic field. Data acquisition also presents many different challenges. Flight line levelling requires exact knowledge of aircraft position at any moment in the survey. The quality of magnetic data strongly depends on the removal of diurnal magnetic-field variations, corrections for aircraft noise, etc.

The physical rock property that relates magnetic anomalies to rocks is total magnetization (Nettleton, 1971; Reynolds et al., 1990), and magnetic anomalies represent lateral variations in the total magnetization of rocks. Total rock magnetization is usually unpredictably complex and composite, and highly variable over short distances. It may consist of an indecipherable variety of poorly understood remanent magnetizations of various types and ages, as well as magnetization induced by the ambient geomagnetic field. The ambient field itself, and hence the anomalies it induces, may be altered by nearby magnetic anomalies in a phenomenon known as coupling. Regional magnetic anomalies may be sourced variously in the crust or in the Earth's core, whose dynamics apparently create broad magnetic anomalies as well.

Rock magnetization is often carried by certain minerals – commonly but far from exclusively magnetite – whose distribution may have little relation to the bulk lithological and structural patterns in the rock mass. Rocks lose their ability to support magnetization when heated above the Curie temperature (575°C for magnetite). In cratonic regions, the Curie isotherm is commonly thought to lie in the lower crust or uppermost mantle, depending on the geothermal gradients, and rocks deeper than this isotherm are not represented in the magnetic anomalies.

The magnetic field itself is complex: dipolar and non-vertical. The standard unit of magnetic measurements used in exploration geophysics is NanoTesla (nT). The total-field aeromagnetic data for this study were supplied by the GSC, with the International Geomagnetic Reference Field reduction that subtracts from the recorded magnetic values the theoretical values computed for an assumed laterally uniform earth (Map 20).

The complexity (compared to gravity) of the magnetic field and of its anomaly-lithology relationships often complicates the interpretation of magnetic anomalies. Even a simple rock source may produce indecipherably complex anomalies.

On a regional scale, the supra-basement sedimentary cover in the Alberta Basin is generally considered almost non-magnetic, and the anomalies are sourced overwhelmingly in the crystalline basement. Local intra-sedimentary anomaly sources may be related to depositional concentrations of magnetic minerals in some clastic rocks, or to secondary magnetization of sedimentary rocks by circulating brines. Igneous buttes and dikes are found locally in southern Alberta, and volcanic and volcaniclastic rocks are known locally in the Front Ranges.

4.4 Geological Meaning of Geophysical Anomalies

An anomaly is the difference between the observed (measured) local value of a potential-field and the field's theoretical value predicted for the same location if the earth were more laterally uniform than it actually is. Geological sources of geophysical anomalies are variations in specific physical properties of rocks, within or between rock bodies.

The anomaly-lithology relationship is not direct (Lyatsky, 2004). An anomaly indicates, indirectly and non-uniquely, some perturbation in the geometric distribution of a particular physical property of underlying rocks. These physical properties are affected by the rocks' entire history, as well as present state, and may be unrelated to variations in bulk lithology. By itself, an anomaly says nothing about the nature, lithology or age of its rock-made source.

The bane of interpretation is non-uniqueness. In the physical theory, an infinite number of different sources can produce the same anomaly. For this reason, advance if partial knowledge of geological targets is essential for the interpretation to be geologically realistic. Interpretation is inherently a geological procedure, in which mathematical data processing and modelling can usefully assist but must never take the lead. No amount of computer power can replace the eye and mind of an experienced interpreter.

4.5 Geological Meaning of Potential-Field Lineaments

The gravity and magnetic lineaments picked from the presented data are included in this report as 'stick maps.' Such picks are inevitably somewhat subjective, reflecting a particular interpreter's experience and biases: the lineaments picked by another interpreter from the same map would inevitably be to some degree different. Derivative maps created with different processing or display parameters might also yield different lineament picks. The users of this report are encouraged to experiment with making derivative maps and lineament picks on their own.

The relationship between gravity and magnetic lineaments and brittle faults should not be expected to be 1:1. Some magnetic lineaments might represent ancient ductile structures, or cultural (infrastructure-related) or flight line noise, or just an interpreter's fancy. The non-vertical inclination of rock magnetization, both remanent and induced, may laterally offset the anomalies from their sources. Dipolarity of the magnetic field also complicates target location from anomalies. Because anomalies are much broader than their geological sources, the exact location of the source from an anomaly may be complicated. A pattern or family of several geophysical lineaments with the same orientation is more interpretationally compelling than a single lineament. Also compelling is the occurrence of the same lineaments in not one but several derivative potential-field maps. On the other hand, some faults may have no geophysical signature at all.

The ultimate test of the geological meaning of a geophysical anomaly comes from geological evidence. For example, stratigraphic studies of a particular Phanerozoic interval may reveal which faults were active at that time. Comparison of basement-sourced anomalies with surface topographic lineaments may also indicate the type and timing of fault activity. No interpretation is possible without adequate geological constraints.

In the search for steep brittle faults in the Alberta Basin, many of the largest gravity and especially magnetic anomalies are undesirable, as they represent the ductile, healed orogenic basement structures of Early Proterozoic and older age. These undesirable anomalies commonly dominate the potential-field maps and obscure the desirable subtle features. Steep brittle faults, formed and reactivated at different times after the cratonization of this part of North America, are associated with potential-field anomalies that tend to be very subtle. Identification of subtle gravity and magnetic lineaments, which may be related to brittle basement faults, is the primary objective of this study.

4.6 Data Display

Display of derivative maps sometimes matters almost as much as data processing for anomaly delineation. A poor map display can obscure the desirable anomalies, whereas a well-chosen display may actually highlight subtle anomalies that are otherwise hidden. As with processing, the optimal display options are found through experimentation and from experience, and the subjective preferences may vary from one user to another. The choice of data display options may require a great deal of experimentation to select the methods and parameters that make the desirable anomalies the most vivid.

Many data display options and methods are available in modern data processing packages. Often, but not always, the experienced software vendor's default options turn out to produce the best results. As with processing options, those display methods that are preferred are clearly explained in the manuals or known from general geophysics texts; the simplest methods should always be given preference.

A very simple way to sharpen anomaly display is to combine line contours with colour map images (Map 1). This approach is particularly valuable where the anomalies are relatively sparse and broad in relation to the map size. Yet, depending on the contour interval and line type, in areas of crowded anomalies contours may actually obscure the anomaly picture.

The choice of colour palette can also highlight or obscure particular anomalies. Histogram equalization is commonly the optimal – and best-known – method to assign colours or shades of grey to anomaly-amplitude values. The choice of hues is almost endless, particularly since colours can be mixed. Display and processing experiments can continue even on the same dataset endlessly, and it is up to the processor and the interpreter to make their best choices.

4.7 Detection of Subtle Lineaments in Processed Potential-Field Maps

Visual identification of lineaments is the most reliable when done by an experienced interpreter familiar with both the geological targets and the local specifics of the anomaly field. Automatic anomaly identification techniques do exist, but they rely on advance parameterization of desirable anomalies that may be too rigid to generate the most geologically meaningful anomaly picks.

Maps in this study were reviewed for lineaments in hardcopy and then again on computer screen. A good visual method to identify subtle lineaments from anomaly-enhanced derivative maps is to view these hardcopy maps at a low angle on a table, as one would sometimes view a seismic section. Rotating the map on the table, to change the interpreter's viewing direction, reveals lineaments and anomaly breaks with various orientations. Viewing a map from above helps to see the distribution of anomaly patterns and domains.

Particularly valuable, but hard to detect, are the aligned slight disruptions of an otherwise consistent anomaly field. Because the brittle cratonic faults commonly run through the ancient ductile basement structures without causing significant offsets, such sharp but extremely subtle disruptions of the magnetic or gravity anomaly pattern are a prime target for interpretation. More vivid discontinuities, across which the overall anomaly pattern noticeably changes, may be related not to the brittle but to the ancient ductile structures. These large discontinuities should be noted, nevertheless, because some of the large brittle structures are aligned with large ductile ones.

Any linear potential-field feature that runs for hundreds of kilometres, across large parts of the study region, is of interest. Such straight trans-regional features commonly represent major crustal shear zones and faults of various types and ages.

The potential-field manifestation of even a large fault may not be consistent along its trace, as it depends on the locally specific anomaly sources the fault runs through or past. An alignment of discontinuous, multiple local anomalies should be, therefore, of interest to the interpreter because such alignments may represent desirable faults.

5 Data Coverage and Preparation

Gravity and magnetic data in Alberta were compiled by the GSC from surveys recorded at different times, with different parameters, precision, instruments, technologies and specifications.

The current study area was defined by AGS to include all of Alberta south of 56°N latitude, west of the Cordilleran deformation front. Because gravity anomalies in the mountain regions are indeed significantly different from the Plains, due to complex geological structure and high topography, most of the deformed-belt region was removed from the dataset. The Foothills and Front Ranges magnetic data, in contrast, were found to be reasonably quiet due to relative absence of large, shallow anomaly sources, and the magnetic map area was successfully extended into the Rocky Mountains even beyond the Alberta-British Columbia provincial boundary.

The southern boundary of the map area is the Alberta-Montana (Canada-U.S.) border at 49°N, and no U.S. data were available for inclusion in the downloaded dataset supplied from the GSC. Elsewhere, in order to avoid bringing map-edge effects into the Alberta study area, the map area was extended by up to half a degree latitude or longitude north of 56°N or beyond the Alberta borders.

The GSC coverage standard for land gravity data of one station per 10 km (almost exactly, one station per township) is usually not maintained in northern Alberta, where road access tends to be poor, but it is commonly maintained or even exceeded in the central and southern parts of the province that have a better road system (Map 2). More closely spaced gravity data are sometimes found along roads, rivers and lakeshores, as well as along the Lithoprobe transect. Even with the sparse gravity data, lineaments longer than several field-station intervals – as many fault-related anomalies are – can be detected with careful data processing.

The GSC aeromagnetic data are compiled from surveys recorded over many decades, with different instruments and flight specifications. Some of these surveys overlap. Fortunately, common flight line spacing in modern surveys is quite tight: 800 metres or (almost identically) half a mile. Older surveys tend to be less detailed, with the flight line spacing as wide as three miles in some exceptional cases. Common flight line orientations are east-west in northern Alberta, and northwest-southeast in the Front Ranges, Foothills and adjacent parts of the western Plains.

Because the depth to principal magnetic-anomaly sources increases with basement depth, the shortest wavelength magnetic anomalies are found in the northeastern corner of Alberta, where the basement is exposed at the surface or is very shallow. Regardless of basement composition and structure, the magnetic anomalies become markedly smoother as the basement deepens to the southwest, and the definition of subtle anomalies correspondingly loses its sharpness.

With the gridded gravity and magnetic data obtained from the GSC, the cell size had to be small enough to capture the available anomaly details where the data were recorded at a tight spacing, without needlessly creating enormous data files that may slow down the data processing, transmission and storage. In a large region where survey parameters and the dominant anomaly wavelength vary from one area to another, a compromise grid-cell size needed to be chosen, adequate for areas of both detailed and sparse field surveys and of crowded and smooth anomalies. For the gravity data, optimal grid-cell size was

chosen to be 2000 metres, but due to a persistent glitch in the data source website, the data arrived with a cell size of 2540 metres. This cell size was deemed acceptable because, in virtually the entire map area, the recording station spacing and basement depth exceeded this value. The magnetic data arrived with our specified optimal cell size of 1000 metres.

Tight gridding does not make up for sparse survey coverage, and it may create artifacts of its own. Subtle gridding artifacts around some of the sparse gravity field stations, in particular, become more pronounced when anomaly enhancement is applied. In magnetic data, variations in the anomaly wavelength content may be related to variable survey parameters (such as flight line spacing and altitude), as well as to variations in basement depth, structure and composition. False magnetic lineaments can potentially be created along the boundaries of dissimilar surveys merged into a common dataset. Imperfect flight line levelling of the GSC aeromagnetic data sometimes causes east-west and northwest-southeast corrugation in the derivative maps, which can be mistaken for lineaments.

Where possible, the projected and plotted total-field aeromagnetic and Bouguer gravity data, as well as some of the derivative maps, were compared with published potential-field maps for the study area. This comparison served as first-order quality control, to ensure the correct position and shape of major anomalies.

6 Regional Potential-Field Anomaly Pattern

Large confusion surrounds the notion of 'domain' in the crystalline basement, commonly due to insufficient discrimination between fundamentally different notions of *geophysical anomaly domain* and *geological domain*. The former is defined based on some common characteristics of geophysical anomalies, the latter based on some common rock features.

In this study, we use potential-field maps to delineate *geophysical anomaly domains* and *zones*. A geophysical domain or zone is defined by some common major characteristics of gravity or magnetic anomalies within it: orientation, dimensions, wavelength, amplitude, etc. (cf. Thomas et al., 1987). These characteristics may be related to the composition and deformation patterns of basement rocks, but perhaps also to some secondary patterns of rock alteration or just basement depth. A geophysical domain's boundaries may or may not be distinct, as sometimes the anomaly pattern changes gradually from one domain to another. On the other hand, a large geological change within the rock mass may not be associated with a significant change in the character of geophysical anomalies.

Given the extreme scarcity of basement rock samples in Alberta, speculations about the geological meaning of these geophysical anomaly domains are avoided here, although some projections are possible from the geologically mapped areas in the Canadian Shield. Many of the principal anomaly domains or bands in central and southern Alberta overlap with and intersect one another. Such an anomaly pattern does not suggest some kind of collage of disparate, accreted crustal units with contrasting prior geological histories (e.g., Ross et al., 1991). Rather, it suggests a complex, common, regional history of multiple episodes of Archean and Early Proterozoic orogenic mobilization, varying in age, duration and extent (Lyatsky et al., 1999). Regional continuity of many anomaly zones, and diffuse and gradational boundaries between potential-field domains, seem to suggest multiple, partly overlapping orogenic episodes affecting all or parts of the study area at different times and with various intensity. Yet, these orogenic structures were mainly ductile, and they are not the primary focus of this study.

The main regional northeast-southwest magnetic and gravity anomaly band in central Alberta is the Snowbird Anomaly Zone (Figure 2), known from geological studies in the Canadian Shield to be related to mainly ductile Precambrian deformation (Lewry and Stauffer, 1990). Intriguingly, in Alberta, within

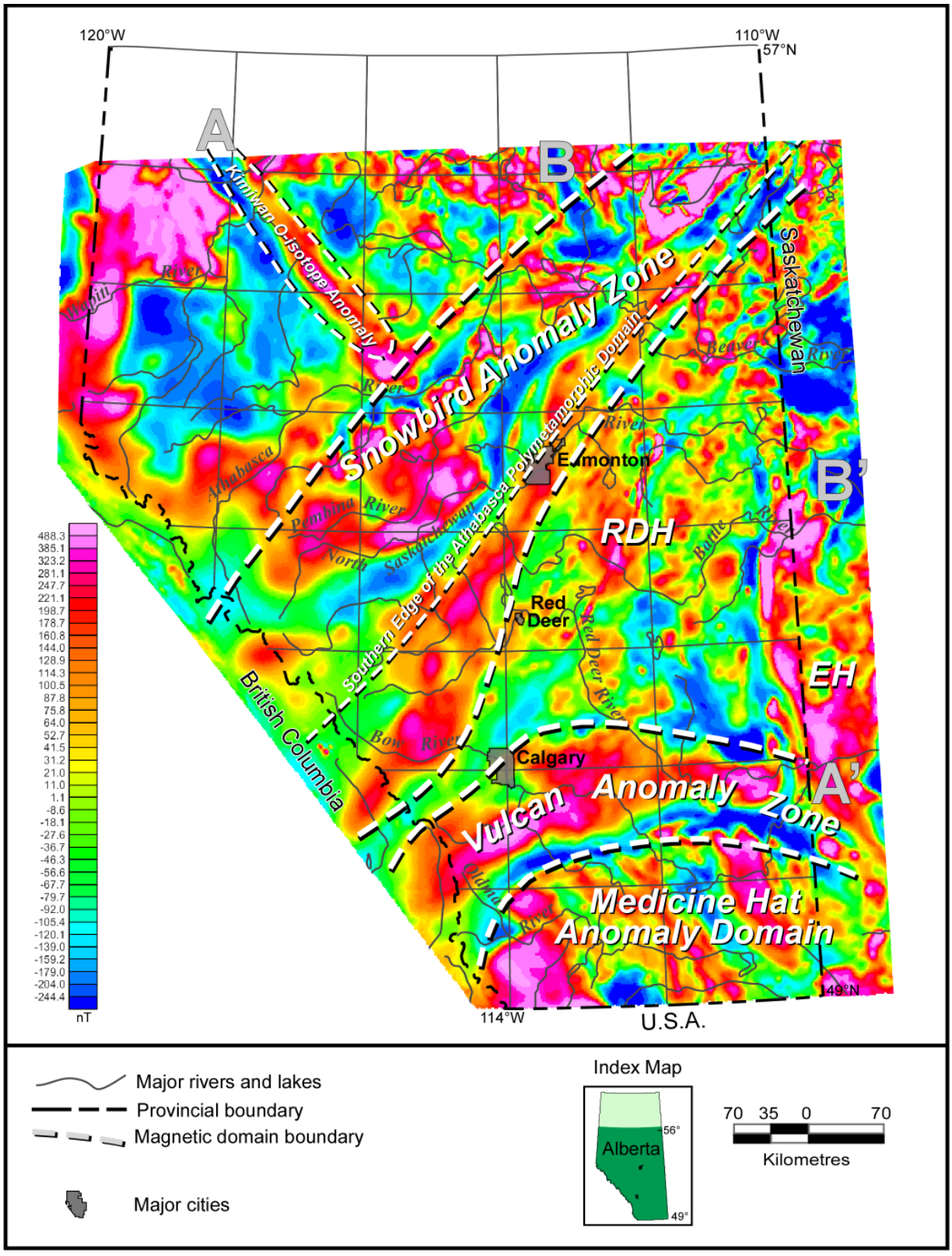

Figure 2. Map of gravity and magnetic anomaly domains of southern and central Alberta Basin, superimposed on a total-field magnetic map. RDH - Red Deer Magnetic High; EH - Eyehill magnetic high.

this zone and with the same orientation lies the southern boundary of the Athabasca polymetamorphic basement domain of Burwash et al. (1993).

In southern Alberta lies the Medicine Hat Anomaly Domain, considered by some workers to be a northward extension of the Archean Wyoming Craton (e.g., Thomas et al., 1987). Its northern boundary seems to be the curved Vulcan Anomaly Zone, across which the principal anomaly pattern changes substantially and whose westward continuation appears to coincide with large crustal-scale structures that regionally affected the miogeosynclinal Phanerozoic evolution of the eastern Cordillera.

Elsewhere in southern and central Alberta, the main anomaly orientation seems to be northwest-southeast, including a large zone of magnetic anomalies (A-A' in Figure 2). In regional maps, it runs across the Snowbird Anomaly Zone and the Hay River-Great Slave Lake fault system, from northeastern British Columbia to northern Montana. Intriguingly, in west-central Alberta it coincides for part of its length with the Proterozoic (approximately 1760 million years before present) Kimiwan oxygen isotope anomaly in basement rocks (e.g., Chacko et al., 1995), which is the oldest known instance of the 'Cordilleran' tectonic trend in this region. A smaller northwest-southeast anomaly zone runs through the northeastern part of the map area (B-B' in Figure 2).

Westward deepening of the basement into the Laramide foredeep causes a decrease of Bouguer gravity values in that direction, as well as a decline in the dominant wavelength of magnetic anomalies. These geophysical variations are unrelated to changes in basement composition and structure and must not be mistaken for geological domains.

7 Processing of the Gravity and Magnetic Data to Highlight Lineaments

Processing of geophysical data depends on the anomaly forms and on the specific geological needs of interpretation. Its aim is to highlight and enhance those anomalies that reveal desirable information about the geological target. In this study, the target is high-angle basement faults, and their potential-field signatures are known to commonly be lineaments.

Many anomaly-enhancement methods were experimented with in the production of this atlas, and many maps were generated as a result. Of those numerous processing products, only the most geologically meaningful were selected. This section describes the methods used to produce the maps included in this atlas and explains the reasons for their selection. The Geosoft data processing package residing at Lyatsky Geoscience was used for the computations and initial data display. Detailed mathematical descriptions of the processing methods can be found in Geosoft manuals. The selected maps were then exported as geotiff files that can be used in GIS software packages. Canvas drafting software at the Alberta Geological Survey was used to assemble and print the set of maps included in this report.

Of course, other interpreters may have other processing and display preferences. The choices made in this study are intended not as a final word, but rather as an illustration of a geologically minded gravity and magnetic approach to fault detection. The users are encouraged to experiment with the data on their own. Since the creation of the northern Alberta atlas (Lyatsky and Pană, 2003), the Geosoft software used was upgraded.

Because the basement is usually much deeper in the current map area than in the north, the dominant anomaly wavelength (particularly in magnetic maps) is generally longer, especially in the western part of the area. Because a particular processing or display technique might successfully highlight the subtle anomalies in some domains but not in others, the multitude of diverse anomaly domains within the map area required more processing products than had been deemed sufficient for the smaller area in northern

Alberta. The processing and display parameters in this study were chosen independently from the choices made previously for the data in northern Alberta, based instead on the tests and experiments designed to resolve subtle anomalies in the current region under investigation.

At all stages in data preparation and processing, steps that, in theory, could generate anomaly-like linear artifacts were kept to a minimum. In particular, we aimed to minimize the use of bandpass wavelength filtering because linear artifacts can be created due to Gibbs ringing.

7.1 Potential-Field Definition of Steep, Brittle Basement Faults

Because the Alberta Basin sedimentary cover is known to be mostly non-magnetic (on a regional scale, at any rate) and lacking large lateral density contrasts, potential-field anomalies are sourced overwhelmingly in the crystalline basement. Steep, straight faults are commonly expressed as potential-field lineaments. Lineaments can be gradient zones, alignments of separate local anomalies of various types and shapes, aligned breaks or discontinuities in the main anomaly pattern, etc.

The common subtlety of desirable, fault-related anomalies necessitates detailed and careful processing of potential-field data, using a wide range of anomaly-enhancement techniques and display parameters. Different processing and display methods reveal different aspects of the same anomaly field. Which methods of anomaly enhancement and display will yield the most geologically meaningful results is often hard to predict in advance, although prior experience in the region offers useful guidance. Furthermore, central and southern Alberta are geophysically very diverse, with many gravity and magnetic domains having different anomaly patterns and thus requiring different enhancement methods.

A proper exploration and research practice is to experiment by processing and displaying the data with a multitude of procedures and parameters. Such extensive experimentation, combined with prior experience, offers a chance to reveal all anomalies of practical interest.

Data processing aims to separate useful anomaly signal from undesirable noise and to enhance the signal to make it more vivid and interpretable. The definition of signal and noise is partly subjective. Signal is those parts of anomalies that contain interpretable information about the geological target of interest (basement faults in this case). The rest is noise. The choice of processing steps depends on which aspects of the anomaly field one regards as signal and aims to enhance, as well as on the results of experimentation needed to create the most geologically meaningful potential-field maps.

Because the signal and noise anomaly characteristics commonly overlap, complete separation between them may be impossible: either noise is retained and even enhanced, or useful signal is inadvertently altered or removed. Noise artifacts, such as Gibbs ringing or edge effects, may be accidentally introduced, contaminating the processed data. The danger of introducing anomaly-like linear artifacts is a particular concern when the target of a study is subtle lineaments. Unexpected consequences and side effects, as well as mistakes, are almost inevitable in processing, but all too often, they go unnoticed. Furthermore, it may be hard to know in advance which anomalies are desirable. In a map with several dissimilar anomaly domains, different processing and display choices may be required for each particular domain.

The best practice is to keep the processing to a minimum, to avoid ill-described ‘black-box’ techniques, and to rely on mathematically simple and intuitive procedures. Particular care must be taken to minimize the use of techniques that could conceivably generate artifacts. As much as possible, the processed and enhanced anomalies should be easy to relate back to the original anomaly shapes. Enhancement of local, low-amplitude and short-wavelength anomalies generally helps to detect the subtle gravity and magnetic lineaments.

7.2 Suppression of Short-Wavelength Noise

Short-wavelength noise in the data, such as gridding artifacts or flight line corrugation, may interfere with geologically meaningful lineaments. Cultural magnetic noise is caused by man-made infrastructure, including false 'lineaments' along roads and pipelines. Glacially transported erratic rocks from the Canadian Shield sometimes create undesirable, if slight, magnetic anomalies, as does glacial till (if it is magnetic; Gay, 2004). Aliasing may give false shapes to under-sampled anomalies.

Anomaly enhancement that boosts subtle and short-wavelength anomalies also boosts the short-wavelength noise. This undesirable noise should therefore be suppressed before anomaly enhancement is applied. Unfortunately, such noise suppression has an inevitable price of sacrificing some components of useful anomalies.

Bandpass wavelength filtering has several drawbacks: it requires assuming the cut-off wavelengths, can smear the separation due to non-vertical filter roll-off and can contaminate the data by Gibbs ringing.

Noise suppression can also be achieved by slightly upward continuing the data, or with smoothing convolution filters. By experimentation and from prior experience, upward continuation by 1 or 2 km was found to be the most effective for the gravity data in the study area, and two passes of the Hanning convolution filter for the magnetic data. These processing steps were taken before the enhancement of subtle anomalies.

7.3 Horizontal-Gradient Maps

Horizontal-gradient maps are vivid yet simple and intuitive derivative products to reveal the anomaly texture of potential-field maps and to highlight discontinuities in the anomaly pattern.

No reduction of the magnetic data to the pole was undertaken prior to the horizontal-gradient computation. The pole reduction uses phase rotation to simulate the appearance of anomalies if the area were located at the magnetic pole where the ambient anomaly-inducing field is vertical. The reason for this omission was twofold:

(1) Alberta lies at fairly high magnetic latitudes, so the change to the data would be small (some tests suggest a maximum of <1 km displacement in anomaly positions; Pilkington et al., 2000); and

(2) Pole reduction assumes all rock magnetization to be induced and remanence-free, but studies in the Canadian Shield in northeastern Alberta (Sprenke et al., 1986) show these crystalline rocks carry both induced and remanent magnetization. As always in data manipulation, where a processing step is avoidable, it is best avoided.

Horizontal-gradient maxima occur over the steepest parts of potential-field anomalies, and horizontal-gradient minima over the flattest parts. Short-wavelength anomalies are enhanced (Maps 7 and 27). More than vertical-gradient or analytic-signal maps, horizontal-gradient maps are very intuitive, as they can be easily related to the original potential-field anomalies. If an anomaly map is thought of as a relief, then a horizontal-gradient map contours the steepness of the anomaly relief's slope.

The horizontal gradient at each grid node is computed by

(1) computing the partial directional derivatives of the data in two mutually orthogonal horizontal directions;

(2) squaring the resulting values;

(3) adding the squares; and

(4) taking the square root of the sum.

Remarkably, even with the comparatively sparse gravity data in the Alberta and Williston basins, experience often shows horizontal-gradient maps to be one of the very best tools for the detection of basement faults.

7.4 Vertical-Gradient (Vertical-Derivative) Maps

Vertical-derivative (vertical-gradient) maps accentuate short-wavelength components of the anomaly field, whereas de-emphasizing long-wavelength components (Maps 8 and 28). The vertical gradient can be thought of as the rate of change of anomaly values as the potential-field data are upward continued (in fact, in the past some vertical-gradient maps used to be generated by upward continuing the data slightly, and then dividing the difference between the original and upward-continued data by the height of upward continuation).

Vertical-derivative maps are not particularly intuitive, and they may be harder than horizontal-gradient maps to relate to the original anomaly shapes. Nonetheless, vertical-gradient maps are useful tools for highlighting the details of anomaly texture, as well as the discontinuities and breaks in the anomaly pattern. In some cases, the second-order vertical derivative is also computed to better highlight subtle anomalies (Map 29).

7.5 Total-Gradient (Analytic-Signal) Maps

Total-gradient (or analytic-signal) maps help reveal the anomaly texture of potential-field maps and highlight discontinuities in the anomaly pattern. Short-wavelength anomalies are enhanced. Total-gradient maps are not intuitive because they incorporate the vertical derivative, and they may be harder than horizontal-gradient maps to relate to the original anomaly shapes (Maps 9 and 30).

The total gradient at each grid node is computed by

(1) computing the partial horizontal derivatives of the data in two mutually orthogonal directions;

(2) computing the vertical gradient of the data;

(3) squaring the resulting partial-gradient values;

(4) adding the three squares; and

(5) taking the square root of the sum.

No pole reduction was performed on the magnetic data prior to the total-gradient computation, for the reasons stated above.

7.6 Automatic Amplitude Gain Control

To highlight the local anomaly details, automatic gain control (AGC) boosts amplitudes in areas with low anomaly 'relief.' Such enhancement of the local anomaly relief usefully sharpens the anomaly shapes and subtle breaks in the anomaly pattern (Map 6, Maps 23 to 26).

Gain is estimated by using a sliding square filter window of specified size, centred on each grid node in

turn. A maximum gain correction is specified to prevent the procedure from 'blowing up' in the areas of low signal. Anomalies with the wavelength exceeding the window size are comparatively little affected by the AGC calculation, whereas anomalies equal to or smaller than the window are affected more strongly.

Local AGC was found, by experimentation, to be particularly effective in the study area. Inside the filter window centred at each position, the best-fit plane is calculated, which minimizes the RMS (root-mean-square) misfit with the data. The average RMS difference between the data and plane values within the window is the local signal gain. Signal at the grid node in the centre of the window is the difference between the data value and the plane value at that position. The first pass over the grid determines the signal and gain for each position, and records the largest gain encountered. In the second pass, the signal at each position is multiplied by the ratio of the largest to local gain, not exceeding the specified maximum correction (chosen to be 10, as per the software provider's default). The new, gained signal is then added to the original background value to obtain the final signal value.

The full AGC correction is somewhat coarser. In the first pass, the RMS average of anomaly amplitudes within a window (local gain) is recorded for each window position. The largest gain value for the map area is also recorded. In the second pass, anomaly values at all points are multiplied by the ratio of the largest gain to the local gain, not exceeding the maximum gain correction (specified as 10).

The optimal window size and the choice of local or full AGC are determined by experimentation. From among the many maps generated, the following window sizes and AGC types were selected for inclusion in this compilation.

For magnetic data:

- 7 grid nodes (square window 6 km on the side, with local AGC);
- 11 grid nodes (10 km on the side, with local AGC);
- 17 grid nodes (16 km on the side, with local AGC); and
- 29 grid nodes (28 km on the side, with full AGC).

For gravity data:

- 11 grid nodes (25.4 km on the side, with full AGC).

7.7 Separation of Local From Regional Anomalies

To highlight local anomalies, the regional component of the gravity or magnetic anomaly field is commonly subtracted from the data, generating a residual map. The definition of regional vs. local anomaly field is inevitably subjective. Regional-local anomaly separation can be achieved by bandpass wavelength filtering, but that procedure requires assuming the cut-off wavelengths, can smear the separation due to non-vertical filter roll-off, and can contaminate the data by Gibbs ringing. A much simpler and more intuitive alternative is to compute from the gridded data the best-fit smooth surface, of a selected low order, and then remove that smooth surface as the regional component.

A best-fit surface of too-low order may leave behind too much of the regional field. An order too high may cause the desirable local anomaly components to be removed. Good results in the western Canadian platforms, including this area, are often obtained by computing and subtracting from the data a third-order best-fit surface (Garland and Bower, 1959). Gravity data, which contain a strong regional down-the-southwest gradient that obscures local anomalies, benefited from this procedure the most (Map 5).

7.8 Shadowgrams (Shaded-Relief Maps)

Shadowgrams reveal variations in the dominant anomaly wavelengths and trends between regions. The computational procedure treats a potential-field map as a relief and computes the shadow pattern that would be created if this relief were illuminated by the sun from a user-specified angle (Maps 10 to 19 and 31 to 56).

The effect is analogous to taking aerial photographs of a terrain illuminated by the sun. Subtle, local and short-wavelength anomalies are emphasized. Side lighting (illuminating from a non-vertical angle) acts as a directional filter, highlighting anomalies oriented at an angle to the 'sun' azimuth and suppressing azimuth-parallel anomalies. Such a directional bias is avoided in shadowgrams computed with a vertical sun angle, and the resulting vertical shadowgram simulates a horizontal-gradient map (steepest gradients are darkest). Vertical shadowgrams are vivid when plotted on their own or as layers on top of colour-coded potential-field maps (Maps 10, 11, 31 and 32).

Although vertical shadowgrams are comparable to horizontal-gradient maps, they are far from identical. These two computational procedures are dissimilar in their nature and treatment of the data, and the differences between the products seem to be greater when the data are sparse. The output data grids may contain dissimilar local details and dynamic ranges, and they are plotted with different display parameters. Similar anomalies may thus be enhanced and highlighted differently. Beneficially for interpretation, vertical shadowgrams and horizontal-gradient maps are not redundant but complementary. In highlighting similar anomaly shapes and patterns, they reveal different information.

Side lighting 'loses' anomalies that are parallel to the 'sun' azimuth, and many shadowgrams with various sun angles need to be generated for each dataset to reveal variously oriented anomalies.

By experimentation, the optimal 'sun' inclination for the study-area gravity data was found to be 20° from the horizon. Diversity of magnetic anomaly domains, with different anomaly characteristics, caused us to include suites of side-lit magnetic shadowgrams with three different inclinations: 20°, 45° and 70°. For each of these chosen inclinations, a sweep of shadowgrams was generated, with the 'sun' illumination from the north (0°), northeast (45°), east (90°), southeast (135°), south (180°), southwest (225°), west (270°) and northwest (315°).

7.9 Upward-Continued Maps

The large-scale regional anomaly pattern is revealed by upward continuation. Comparing the upward-continued gravity data with the raw data clearly shows which of the anomalies survive the filtering, and thus, can be inferred to probably have large rock sources. The anomalies that do not survive the upward continuation lack long-wavelength components and (presumably) large and massive sources. Principal orientations of geological features in the crust are revealed by the orientation of potential-field anomalies in upward-continued maps (Maps 3, 4, 21 and 22).

The largest crustal features tend to be ductile, ancient and orogenic-related, and big gravity anomalies may even reflect the geometry of the Moho. Yet, regional structural trends sometimes appear also on a local scale, and upward-continued maps help with their identification.

This procedure uses wavelength filtering with no sharp cut-offs to simulate the appearance of potential-field maps if the data were recorded at a higher altitude than they actually were. For example, land data can be filtered to calculate what the same map would look like with the data flown at a user-specified high nominal altitude. The very smooth shape of the filter avoids creating artifacts. Short-wavelength anomalies are suppressed preferentially, whereas anomalies with a significant long-wavelength component remain. Such anomalies can be supposed to have large rock sources.

The fundamental physical assumption that no anomaly sources exist between the real and simulated (nominal) recording levels holds well in the Canadian Plains, especially when the nominal level is taken to be very much higher than any topography. Where the topographic relief is greater, as in the Foothills and Front Ranges, upward continuation to a nominal height far above the highest peaks allows us to pretend the no-source assumption holds approximately.

Upward continuation is rather intuitive. It is easy to understand while avoiding arbitrarily defined bandpass filters or the possibility of Gibbs ringing. From experience across Western Canada and northwestern U.S., the bulk structure of the upper crust, where the brittle faults chiefly reside, is often revealed by upward continuing gravity and magnetic data to a nominal altitude of 20 km. This nominal altitude was found to be effective with the data in the study area. The resultant maps show the largest anomalies as well as the principal anomaly trends.

8 Conclusions and Recommendations

Geophysical basement mapping with public domain gravity and magnetic data are an inexpensive and valuable regional exploration tool. Its responsible use is in combination with geological, remote sensing and seismic data (Edwards et al., 1998; Lyatsky et al., 1998, 1999). Such integrated studies offer the best chance to map the structure of the crystalline basement and to unravel its influence on the basin above.

In each particular area, suspected fault influences on the sedimentary cover must be investigated locally. Of significant exploration interest are situations where hydrocarbon-reservoir trends coincide with basement-related potential-field lineaments. Locations where such lineaments continue into undrilled areas might be of exploration interest and warrant further local attention.

Topographic lineaments are commonly a useful component of regional and local fault studies. Although not all basement faults reach the surface, and not all surface faults are basement related, inclusion of topographic lineaments enriches fault-detection exercises.

Most importantly, subsurface geological studies and seismic surveys are essential in unravelling the exact influence the detected faults might have had at various stratigraphic intervals in any particular area. These influences vary from interval to interval and from area to area. Regional and local stratigraphic, lithofacies and structural studies are needed, in conjunction with geophysical fault detection, to help unravel and predicatively delineate the distribution of reservoirs and traps.

Note: The gravity and magnetic data in this study were processed with the specific objective to highlight subtle lineaments to assist in fault delineation. Different anomaly shapes may matter in the search for geological features other than faults, but highlighting such anomalies may require different processing. Delineation of round anomalies, in particular, may benefit from different enhancement methods, as can the resolution of tight anomaly clusters.

9 References

Burwash, R.A., Green, A.G., Jessop, A.M. and Kanasewich, E.R. (1993): Geophysical and petrophysical characteristics of the basement rocks of the Western Canada sedimentary basin; *in* Sedimentary Cover of the Craton in Canada, D.F. Stott and J.D. Aitken (ed.), Geological Society of America, The Geology of North America, v. D-1, p. 55-77.

Cecile, M.P., Morrow, D.W. and Williams, G.K. (1997): Early Palaeozoic (Cambrian to Early Devonian) tectonic framework, Canadian Cordillera; Bulletin of Canadian Petroleum Geology, v. 45/1, p. 54-74.

Chacko, T., King, R.W., Muehlenbachs, K. and Burwash, R.A. (1995): The Kimiwan isotope anomaly, a low ^{18}O zone in the Precambrian basement of Alberta: constraints on the timing of ^{18}O depletion from K-Ar and Rb-Sr data; *in* Alberta Basement Transects Workshop, G.M. Ross (ed.), Lithoprobe Report 47, p. 336-339.

Cohen, Z., Kaptsan, V. and Flexer, A. (1990): The tectonic mosaic of the southern Levant: implications for hydrocarbon prospects; Journal of Petroleum Geology, v. 13, p. 437-462.

Dohr, G. (1989): Deep seismic - a tool in the recognition and interpretation of large geological elements, the starting point for deterministic basin modelling; Geologische Rundschau, v. 78, p. 21-48.

Edwards, D.J., Lyatsky, H.V. and Brown, R.J. (1998): Regional interpretation of steep faults in the Alberta Basin from public-domain gravity and magnetic data: an update; Recorder (Canadian Society of Exploration Geophysicists), v. 23, no. 1, p. 15-24.

Friedman, J.D. and Huffman, A.C. (1998): Laccolith complexes of southeastern Utah: time of emplacement and tectonic setting - workshop proceedings; U.S. Geological Survey, Bulletin 2158, p. 253-254.

Friedmann, S.J. and Homer-Dixon, T. (2004): Out of the energy box; Foreign Affairs, v. 83, no. 6, p. 72-83.

Gabrielsen, R.H., Braathen, A., Dehls, J. and Roberts, D. (2002): Tectonic lineaments of Norway; Norwegian Journal of Geology, v. 82, p. 153-174.

Garland, G.D. and Bower, M.E. (1959): Aeromagnetic anomalies in northeastern Alberta; Oilweek, June 19/59, p. 32-40.

Gay, S.P. (2004): Glacial till: a troublesome source of near-surface magnetic anomalies; The Leading Edge, v. 23, p. 542-547.

Geological Survey of Canada (1990): Canadian Geophysical Atlas, 15 maps.

Godfrey, J.D. (1986): Geology of the Precambrian Shield of northeastern Alberta; Alberta Research Council, Map 1986-1, scale 1:250,000.

Hoffman, P.F. (1988): United plates of America, the birth of a craton: early Proterozoic assembly and growth of Laurentia; Annual Review Earth and Planetary Science, v. 16, p. 543-603.

Hoffman, P.F. (1989): Precambrian geology and tectonic history of North America; *in* The Geology of North America - an Overview; A.W. Bally and A.R. Palmer (ed.), Geological Society of America, v. A, p. 447-512.

Langenberg, C.W. (1983): Polyphase deformation in the Canadian Shield of northeastern Alberta; Alberta Research Council, Alberta Geological Survey, Bulletin 45, 33 p.

Lewry, J.F. and Stauffer, M.R. (1990): The Early Proterozoic Trans-Hudson Orogen of North America; Geological Association of Canada, Special Paper 37, 505 p.

Lyatsky, H.V. (2004): The meaning of anomaly; Recorder, Canadian Society of Exploration Geophysicists, v. 29, no. 6, p. 50-51.

Lyatsky, H.V., Dietrich, J.R. and Edwards, D.J. (1998): Analysis of gravity and magnetic horizontal-gradient vector data over the buried Trans-Hudson Orogen and Churchill-Superior Boundary Zone in southern Saskatchewan and Manitoba; Geological Survey of Canada, Open File 3614, 34 p.

Lyatsky, H.V., Friedman, G.M. and Lyatsky, V.B. (1999): Principles of practical tectonic analysis of cratonic regions; Lecture Notes in Earth Sciences, v. 84, Springer-Verlag, 369 p.

Lyatsky, H.V. and Pană, D.I. (2003): Catalogue of selected regional gravity and magnetic maps of northern Alberta; Alberta Energy and Utilities Board/Alberta Geological Survey, Special Report 56, 40 p.

Marshak, S. and Paulsen, T. (1996): Mid-continent U.S. fault and fold zones: a legacy of Proterozoic intracratonic extensional tectonism?; Geology, v. 24, p. 151-154.

Maughan, E.K. and Perry, Jr., W.J. (1986): Lineaments and their tectonic implications in the Rocky Mountains and adjacent Plains regions; *in* Paleotectonic and Sedimentation in the Rocky Mountains Region, J.A. Peterson (ed.), American Association of Petroleum Geologists, Memoir 41, p. 41-53.

Mossop, G.D. and Shetsen, I. (1994): Geological atlas of the Western Canada Sedimentary Basin; Canadian Society of Petroleum Geologists and Alberta Research Council, 510 p.

Nettleton, L.L. (1971): Elementary gravity and magnetics for geologists and seismologists; Society of Exploration Geophysicists, Tulsa, OK, USA, 121 p.

Palmer, A.R. (1982): Perspectives in regional geological synthesis - planning for *the geology of North America*; The Geology of North America, Geological Society of America, Boulder Colorado, US, 176 p.

Pilkington, M., Miles, W.F., Ross, G.M. and Roest, W.R. (2000): Potential-field signatures of buried Precambrian basement in the Western Canada Sedimentary Basin; Canadian Journal of Earth Sciences, v. 37, no. 11, p. 1453-1471.

Piskarev, A.L. and Tchernyshev, M.Y. (1997): Magnetic and gravity anomaly patterns related to hydrocarbon fields in northern west Siberia; Geophysics, v. 62, p. 831-841.

Reynolds, R.L., Rosenbaum, J.G., Hudson, M.R. and Fishman, N.S. (1990): Rock magnetism, the distribution of magnetic minerals in the Earth's crust, and aeromagnetic anomalies; *in* Geological Applications of Modern Aeromagnetic Surveys, W.F. Hanna (ed.), U.S. Geological Survey, Bulletin 1924, p. 24-45.

Ricketts, B.D. (1989): Western Canada Sedimentary Basin, a case history; Canadian Society of Petroleum Geologists, Special Publication 30, 320 p.

Ross, G.M. and Eaton, D.E. (1999): Basement reactivation in the Alberta Basin: observational constraints and mechanical rationale; Bulletin of Canadian Petroleum Geology, v. 47/4, p. 391-411.

Ross, G.M., Parrish, R.R., Villeneuve, M.E. and Bowring, S.A. (1991): Geophysics and geochronology of the crystalline basement of the Alberta Basin, Western Canada; Journal of Earth Sciences, v. 28, p. 512-522.

Sprenke, K.F., Wavra, C.S. and Godfrey, J.D. (1986): Geophysical expression of the Canadian Shield in northeastern Alberta; Alberta Research Council, Alberta Geological Survey, Bulletin 52, 54 p.

Steeples, D.W. (1989): Geophysics in Kansas; Kansas Geological Survey, Bulletin 226, 54 p.

Stille, H. (1924): Grundfragen der Vergleichenden Tektonik; Gebrüder Bornträger, Berlin, 443p.

Swanson, M.T. (1986): Preexisting fault control for Mesozoic basin formation in eastern North America; Geology, v. 14, p. 419-422.

Thomas, M.D., Sharpton, V.L. and Grieve, R.A.F. (1987): Gravity patterns and Precambrian structure in the North American Central Plains; Geology, v. 15, p. 489-492.

Vearncombe, S. and Vearncombe, J.R. (2002): Tectonic controls on kimberlite location, southern Africa; Journal of Structural Geology, v. 24, p. 1619-1625.

Villeneuve, M.E., Ross, G.M., Parrish, R.R., Theriault, R.J., Miles, W. and Broome, J. (1993): Tectonic subdivisions, U-Pb geochronology and Sm-Nd isotope geochemistry of the crystalline basement of the Western Canada Sedimentary Basin, Alberta and northeastern British Columbia; Geological Survey of Canada, Bulletin 447, 85 p.

Wellman, P. (1985): Block structure of continental crust derived from gravity and magnetic maps, with Australian examples; *in* The Utility of Gravity and Magnetic Anomaly Maps, W.J. Hinze (ed.), Society of Exploration Geophysicists, p. 102-108.

White, D.J., Burrowes, G., Davis, T., Hajnal, Z., Hirsche, K., Hutcheon, I., Majer, E., Roston, B. and Whittaker, S. (2004): Greenhouse gas sequestration in abandoned oil reservoirs: the International Energy Agency Weyburn pilot project; GSA Today, v. 14, no. 7, p. 4-10.

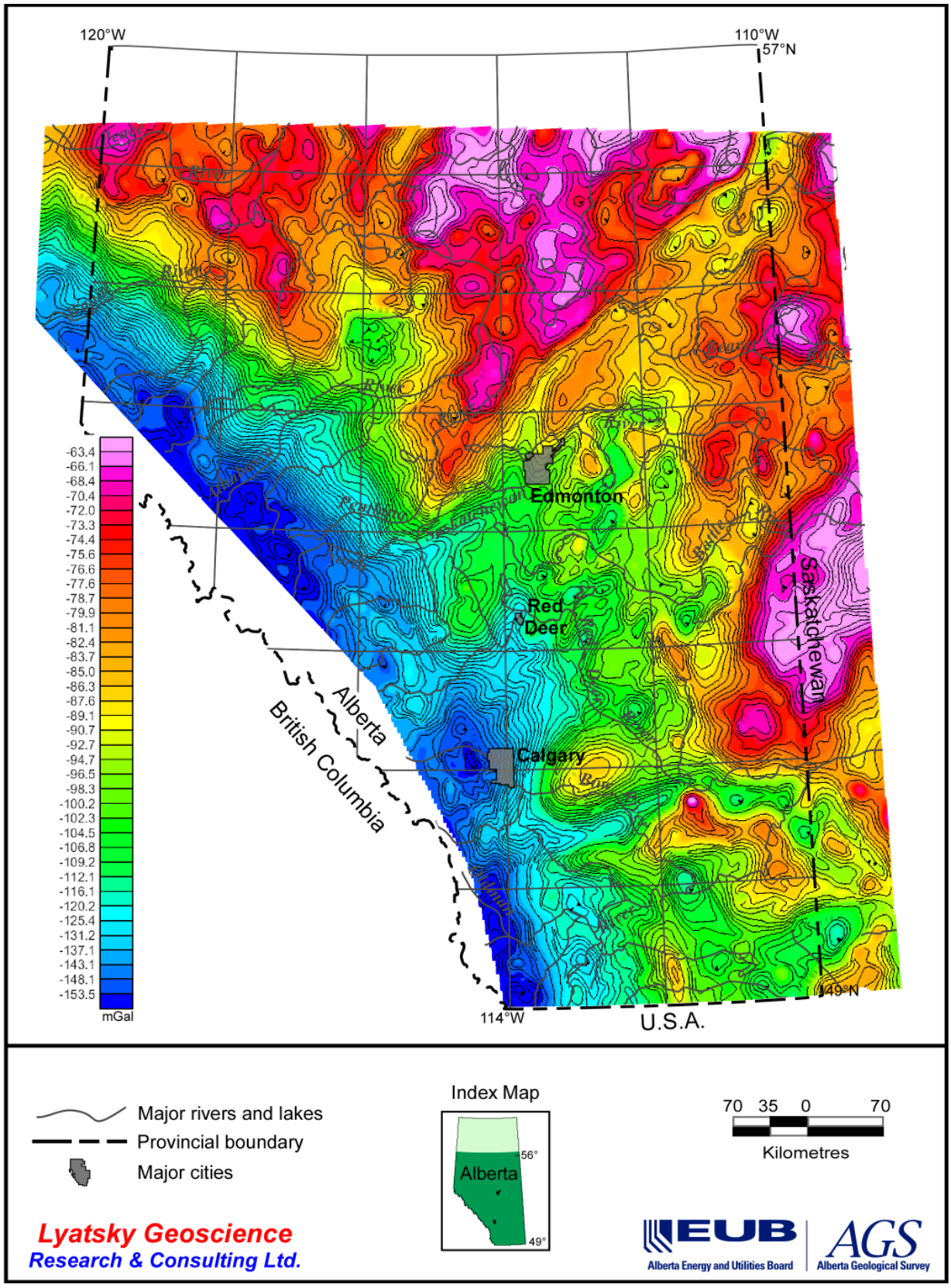

Map 1. Contoured Bouguer gravity data.

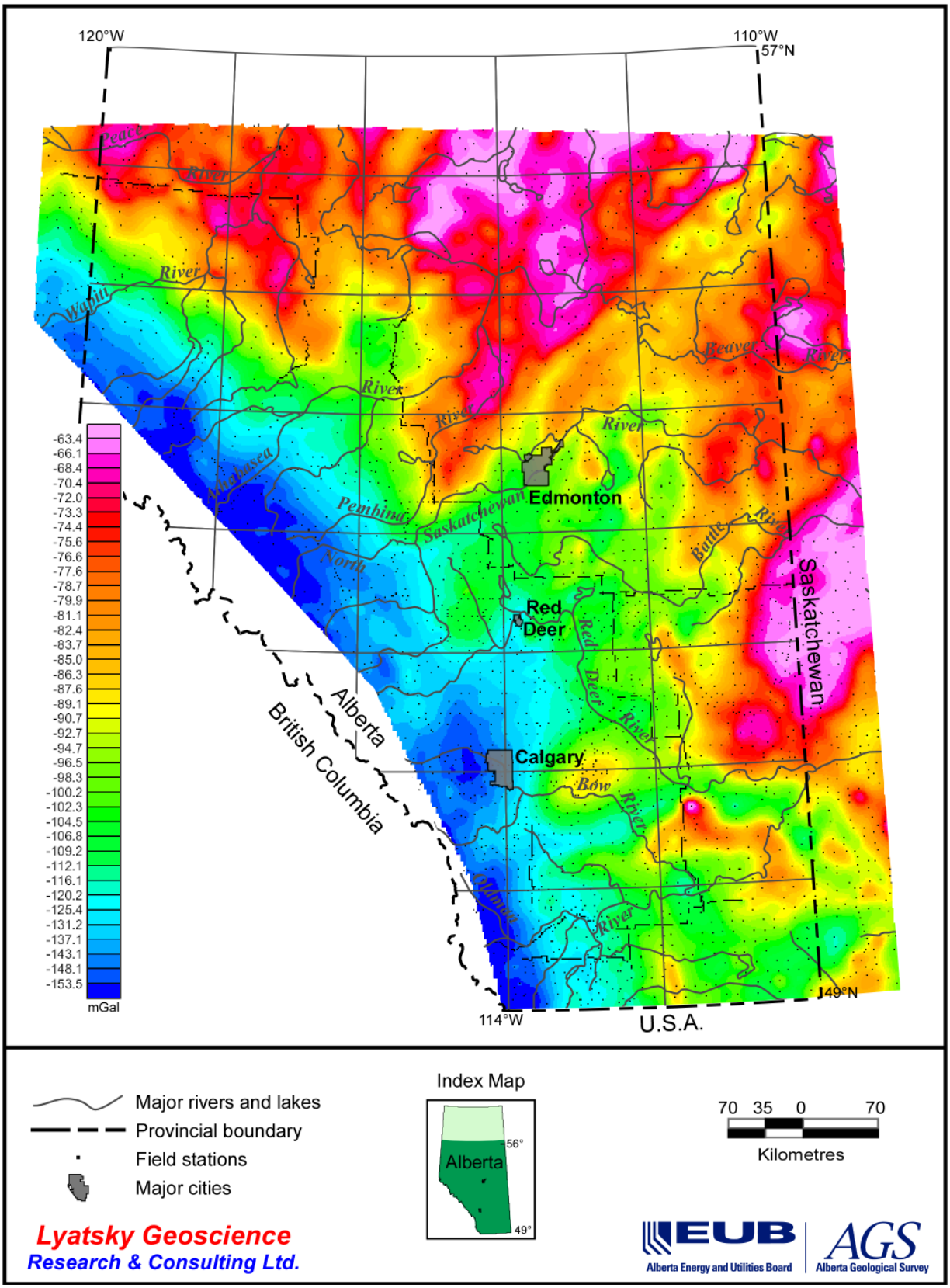

Map 2. Bouguer gravity map with field stations.

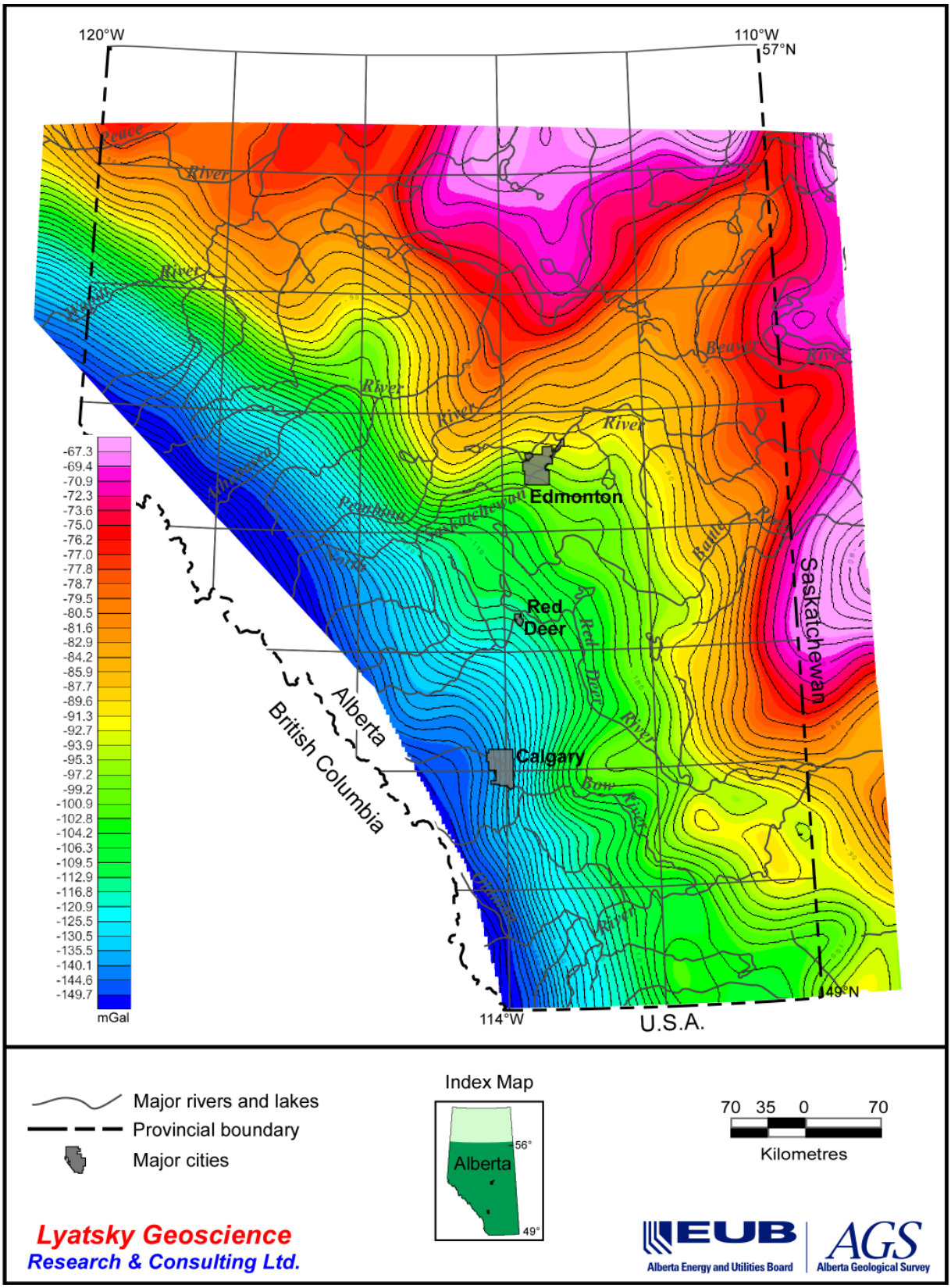

Map 3. Gravity map upward continued to 20 km.

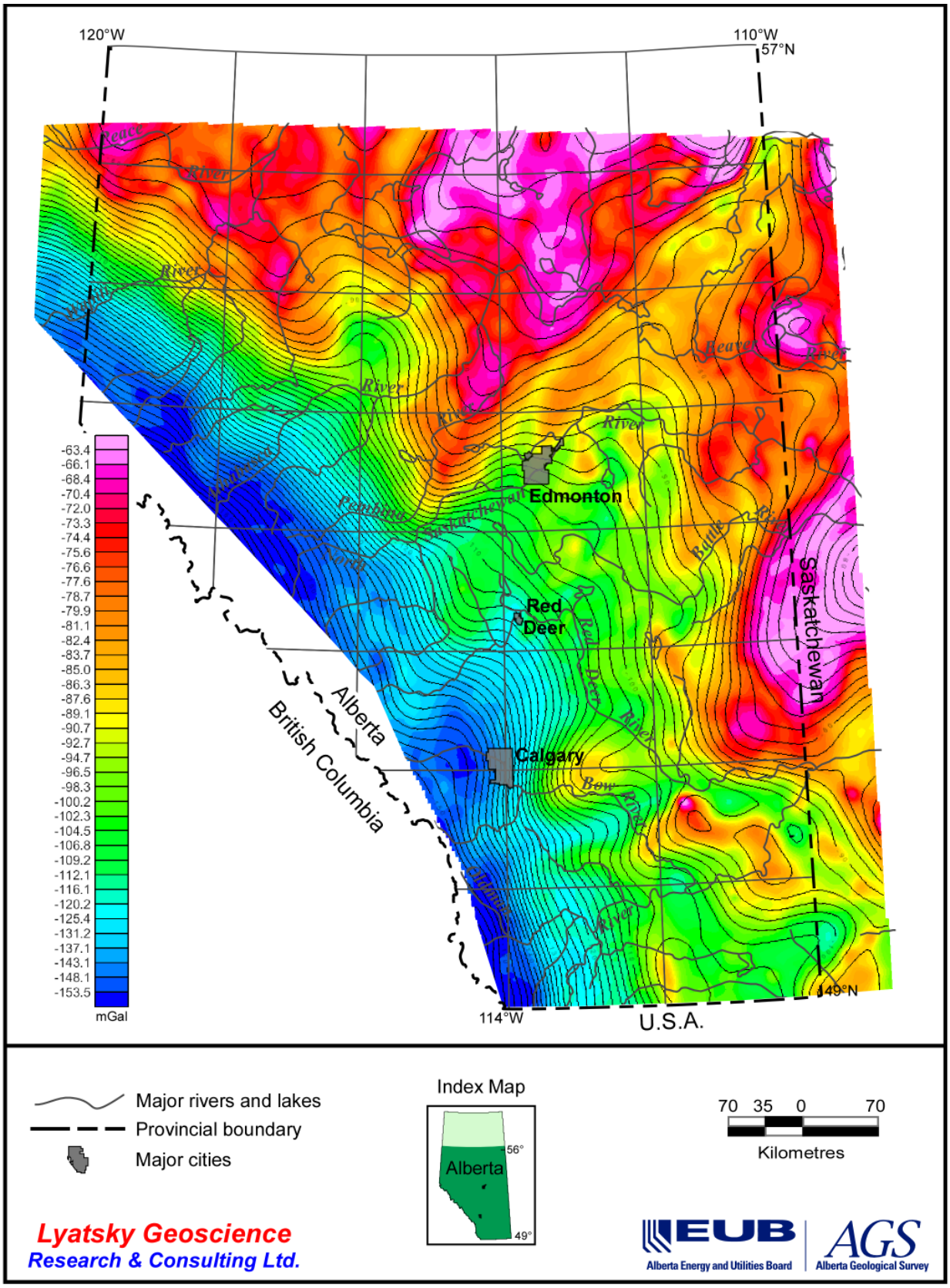

Map 4. Gravity data with contours of the data upward continued to 20 km.

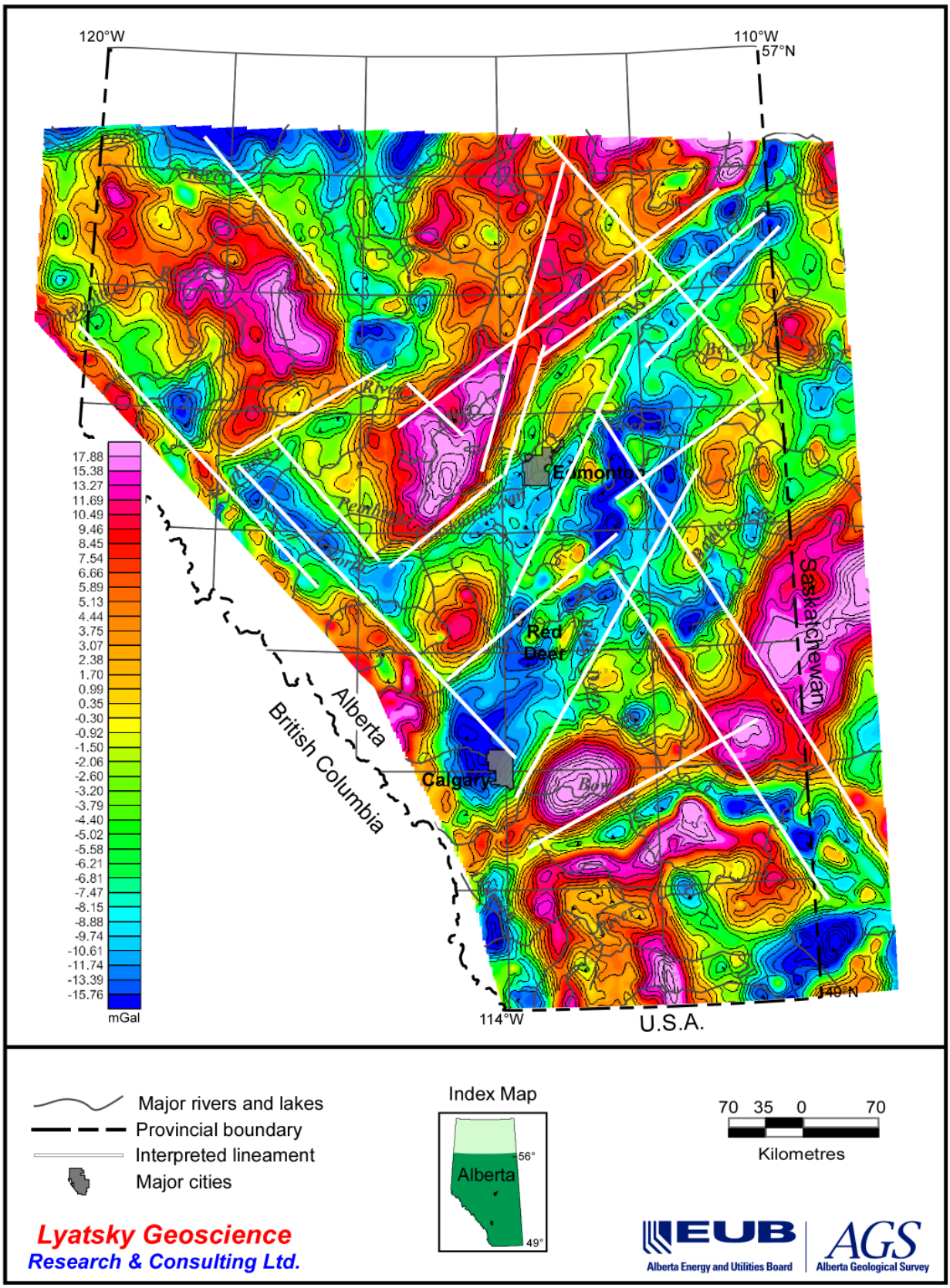

Map 5. Gravity map with third-order trend removed.

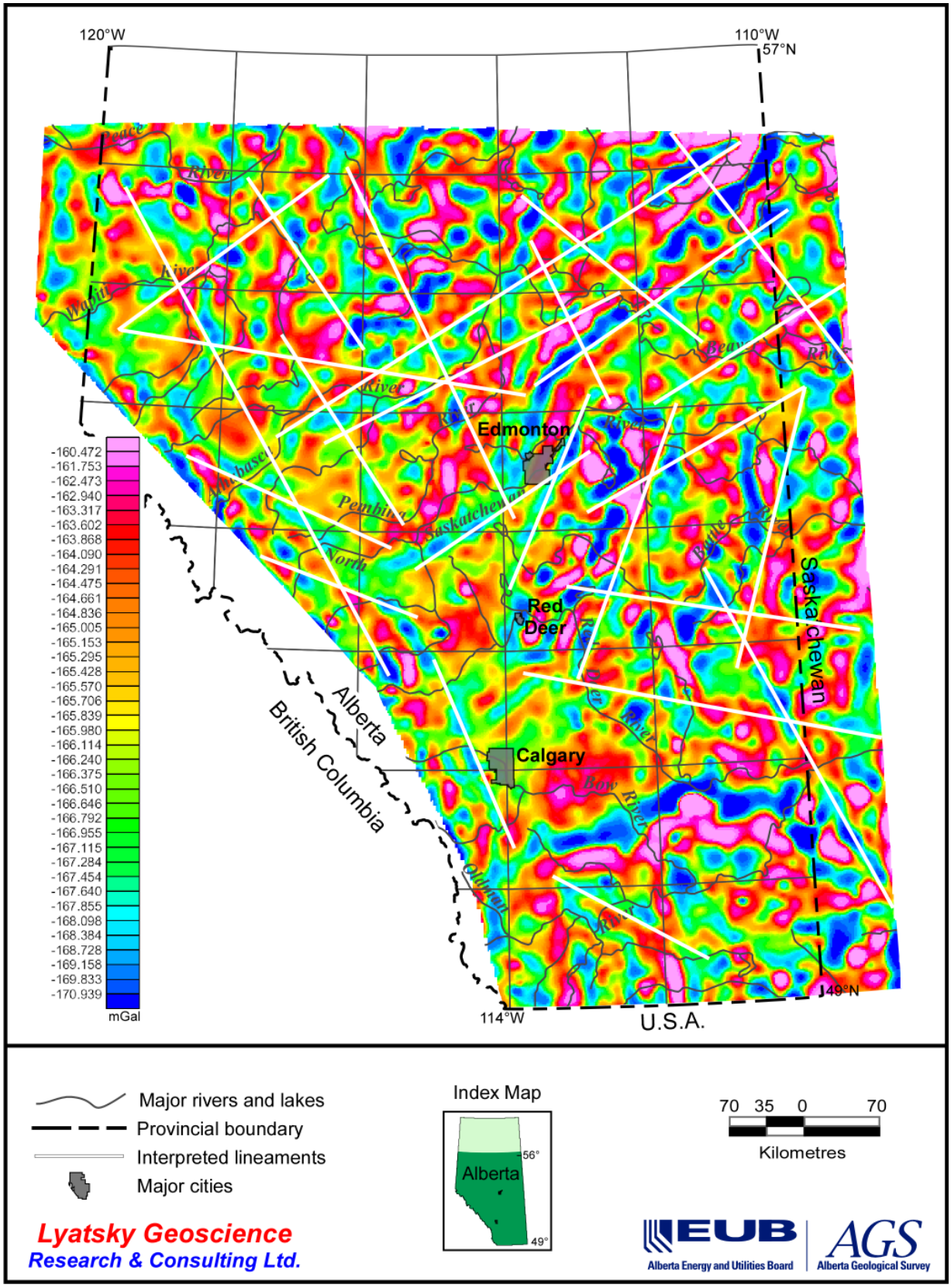

Map 6. Gravity map with automatic amplitude gain (full AGC, window size = 11 grid cells).

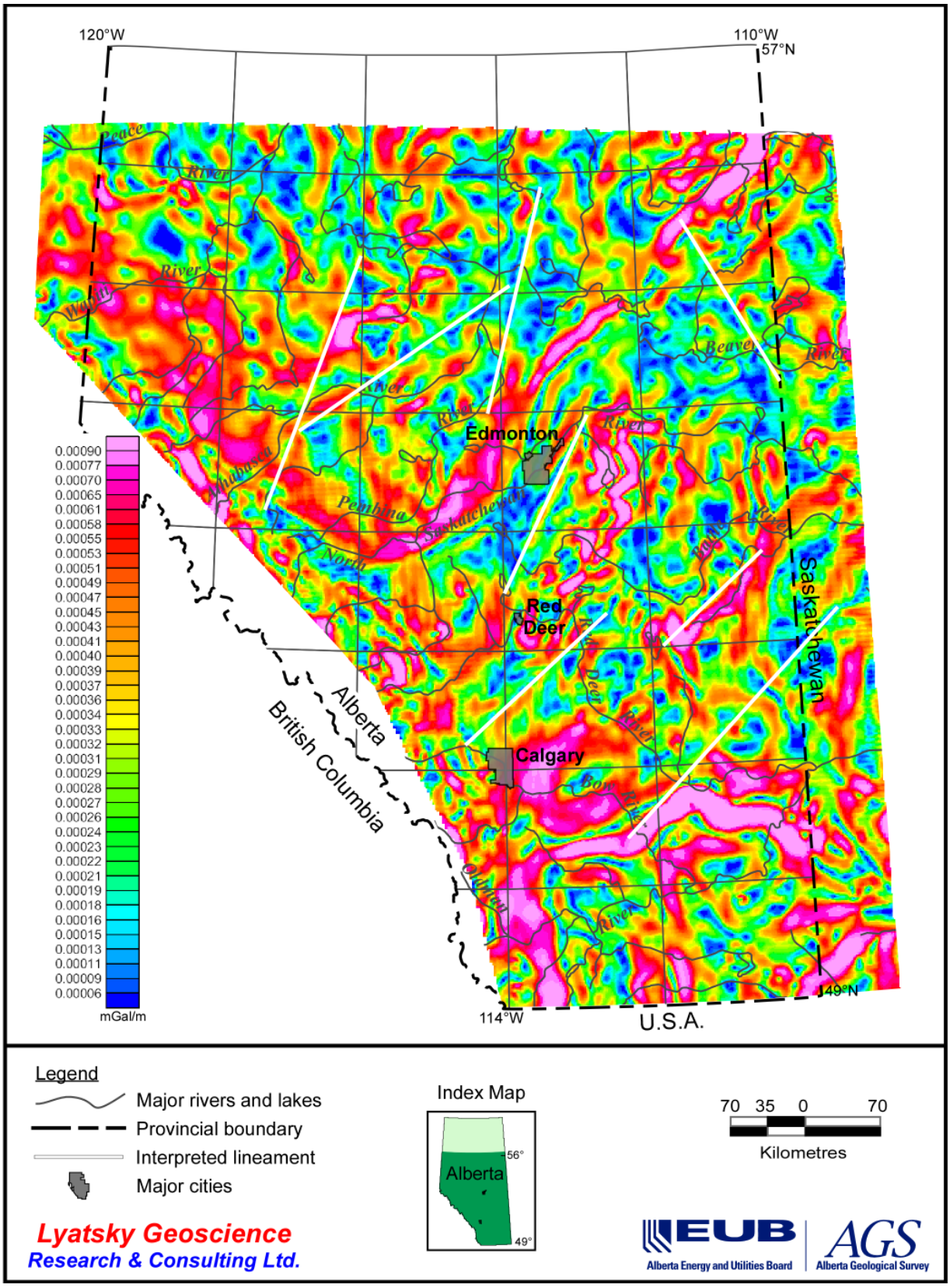

Map 7. Horizontal gradient of gravity data.

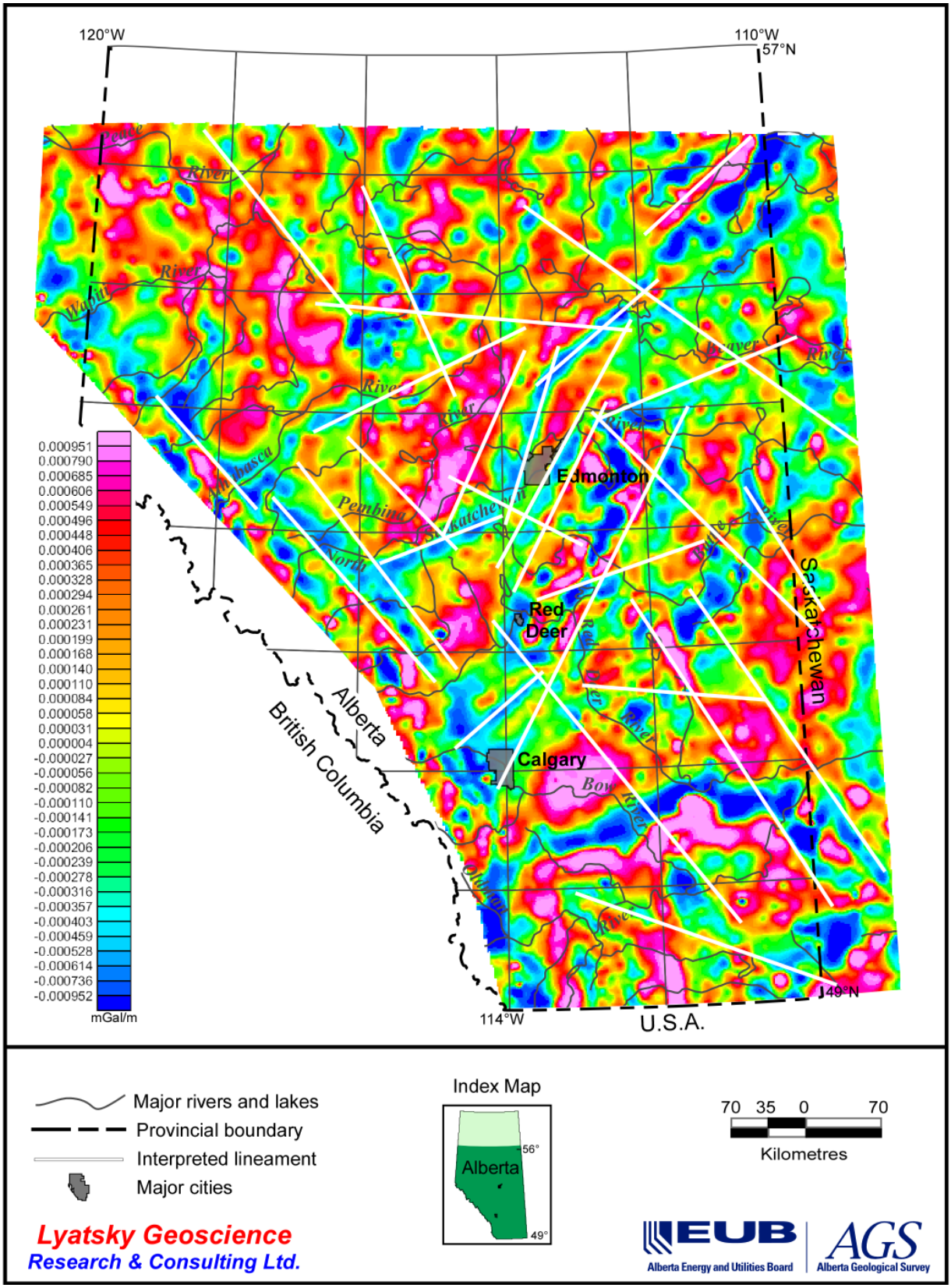

Map 8. First vertical derivative of gravity data.

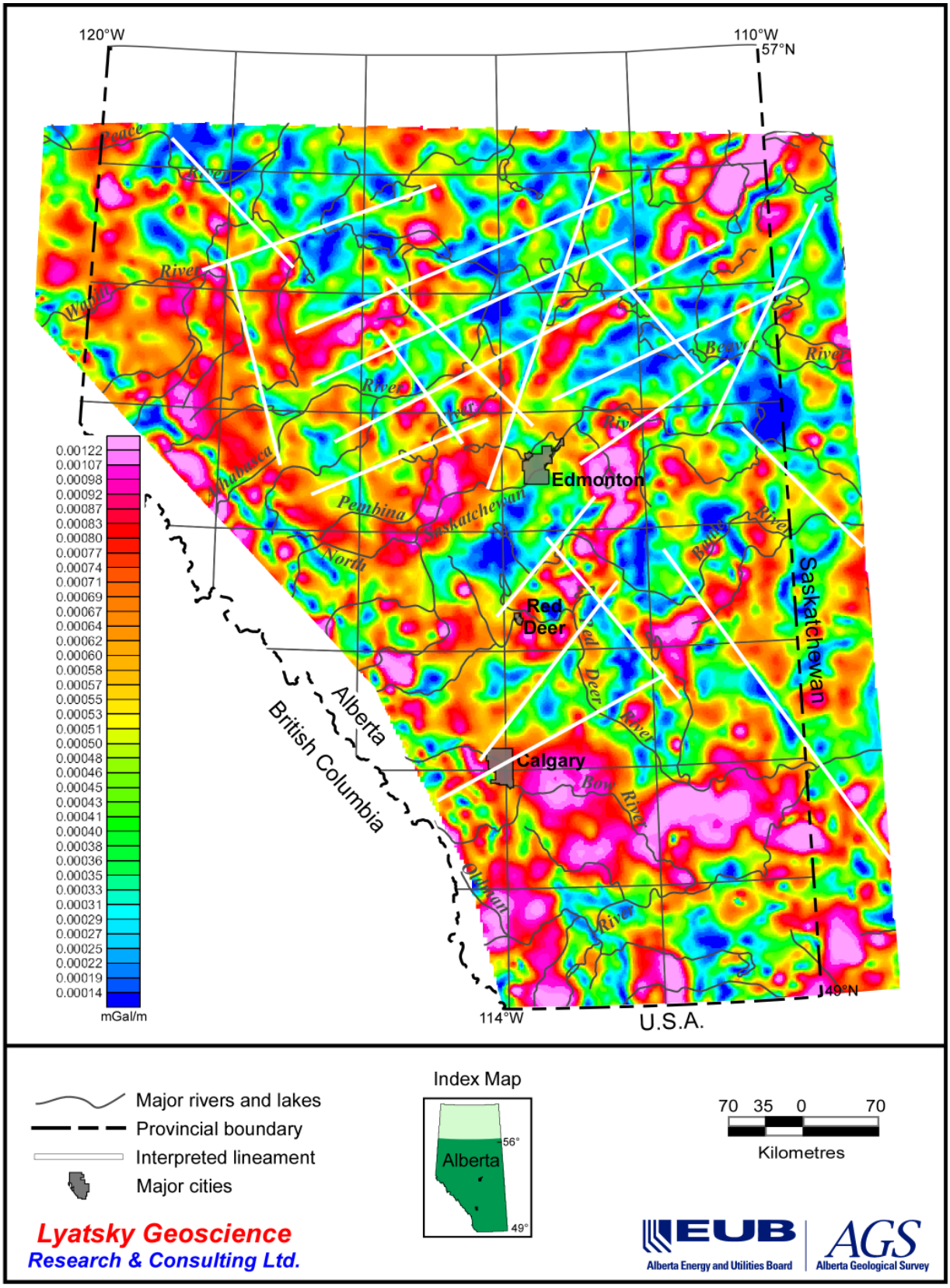

Map 9. Total gradient (analytic signal) of gravity data.

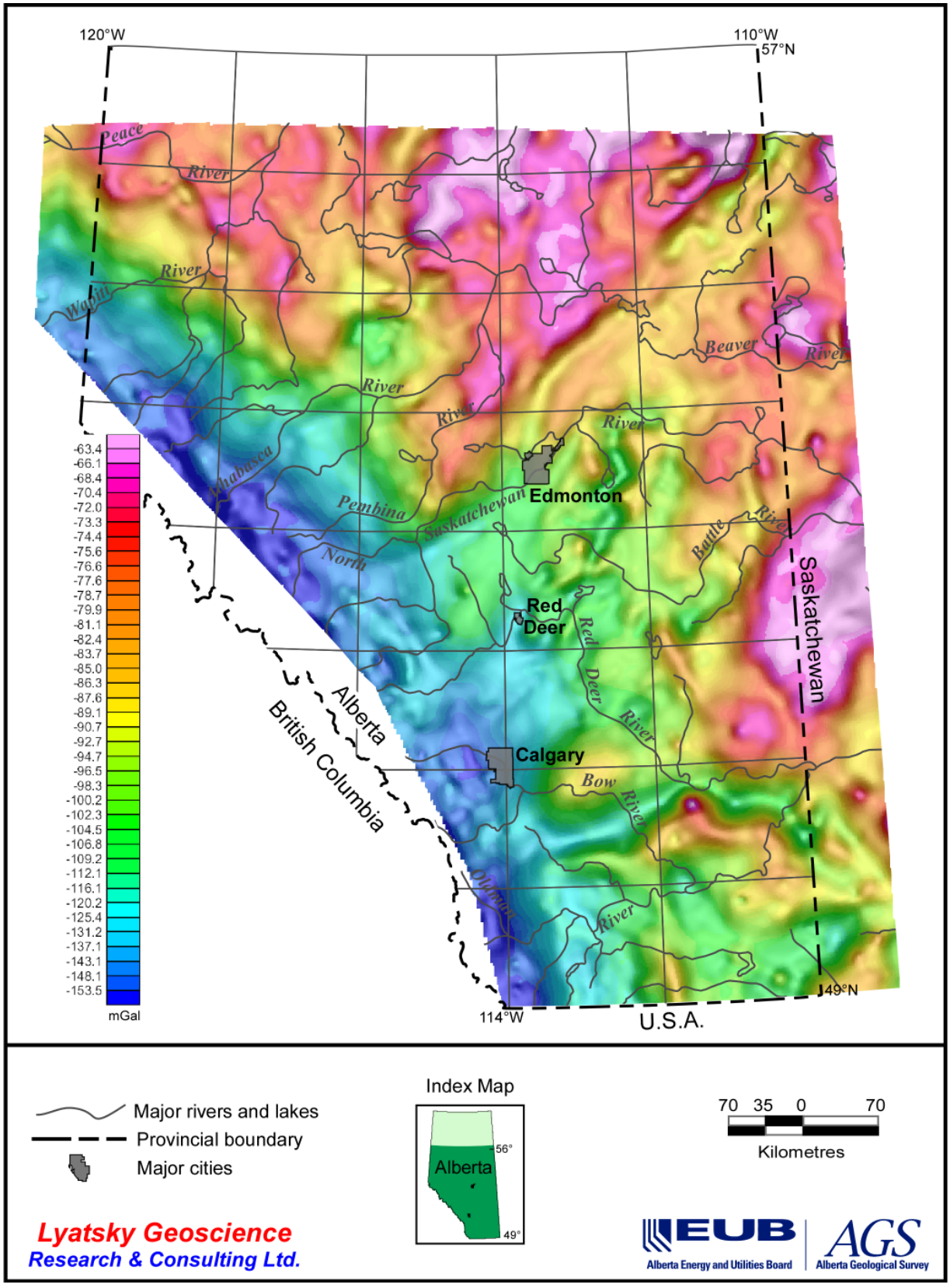

Map 10. Gravity data with vertical shadowgram superimposed.

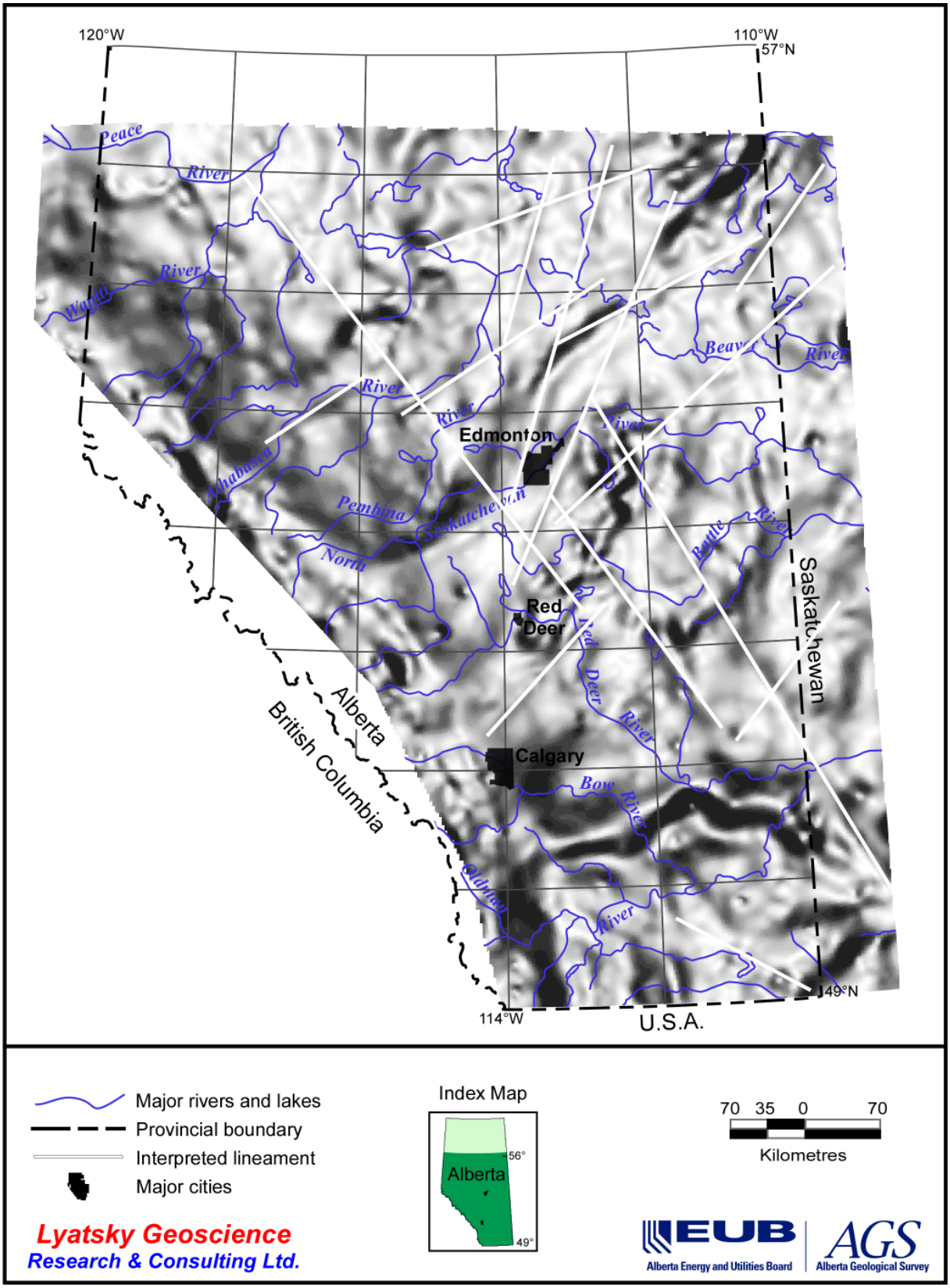

Map 11. Vertical-sun-angle shadowgram of gravity data.

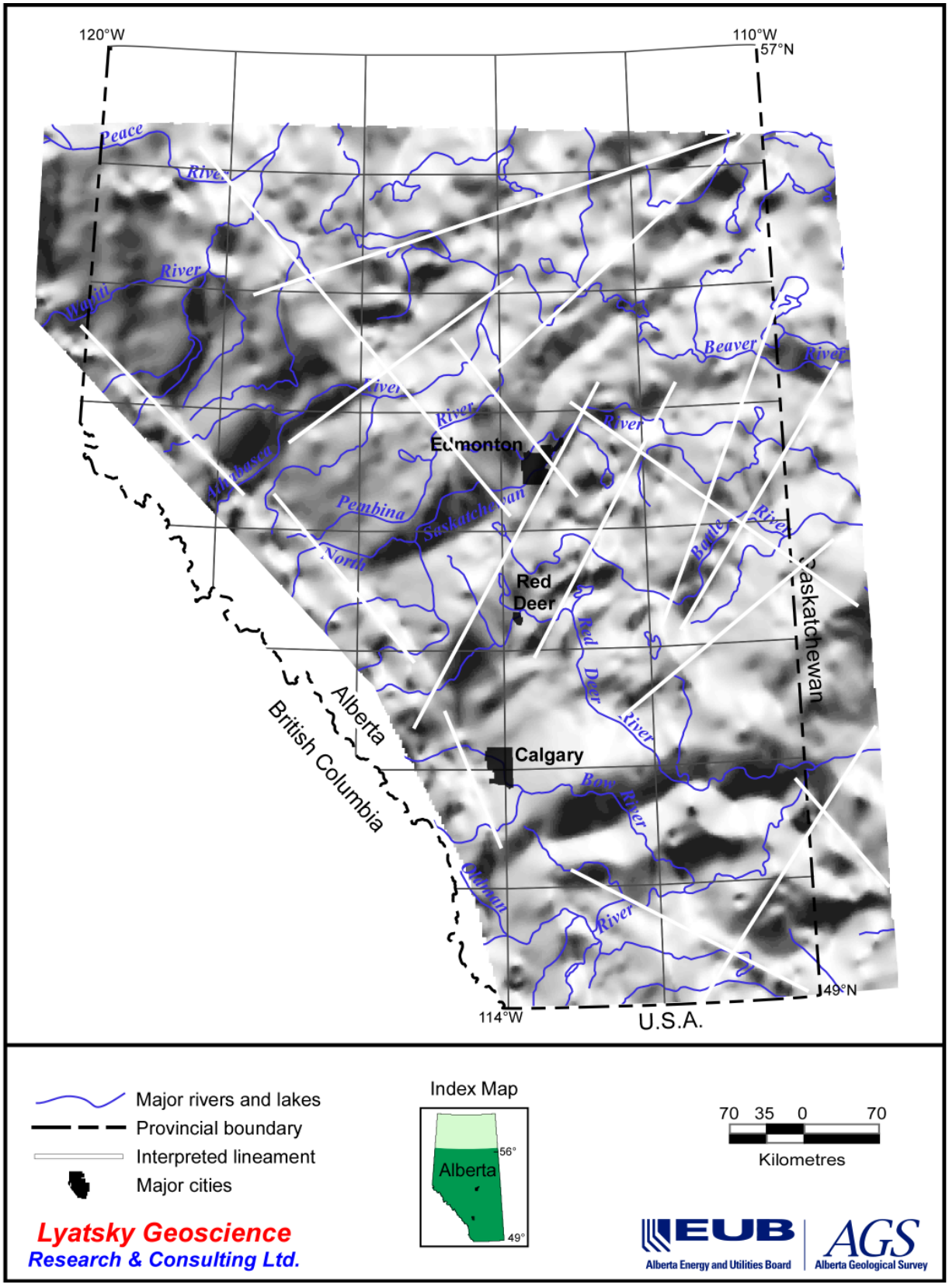

Map 12. Gravity shadowgram illuminated from the north with a 20° 'sun' inclination.

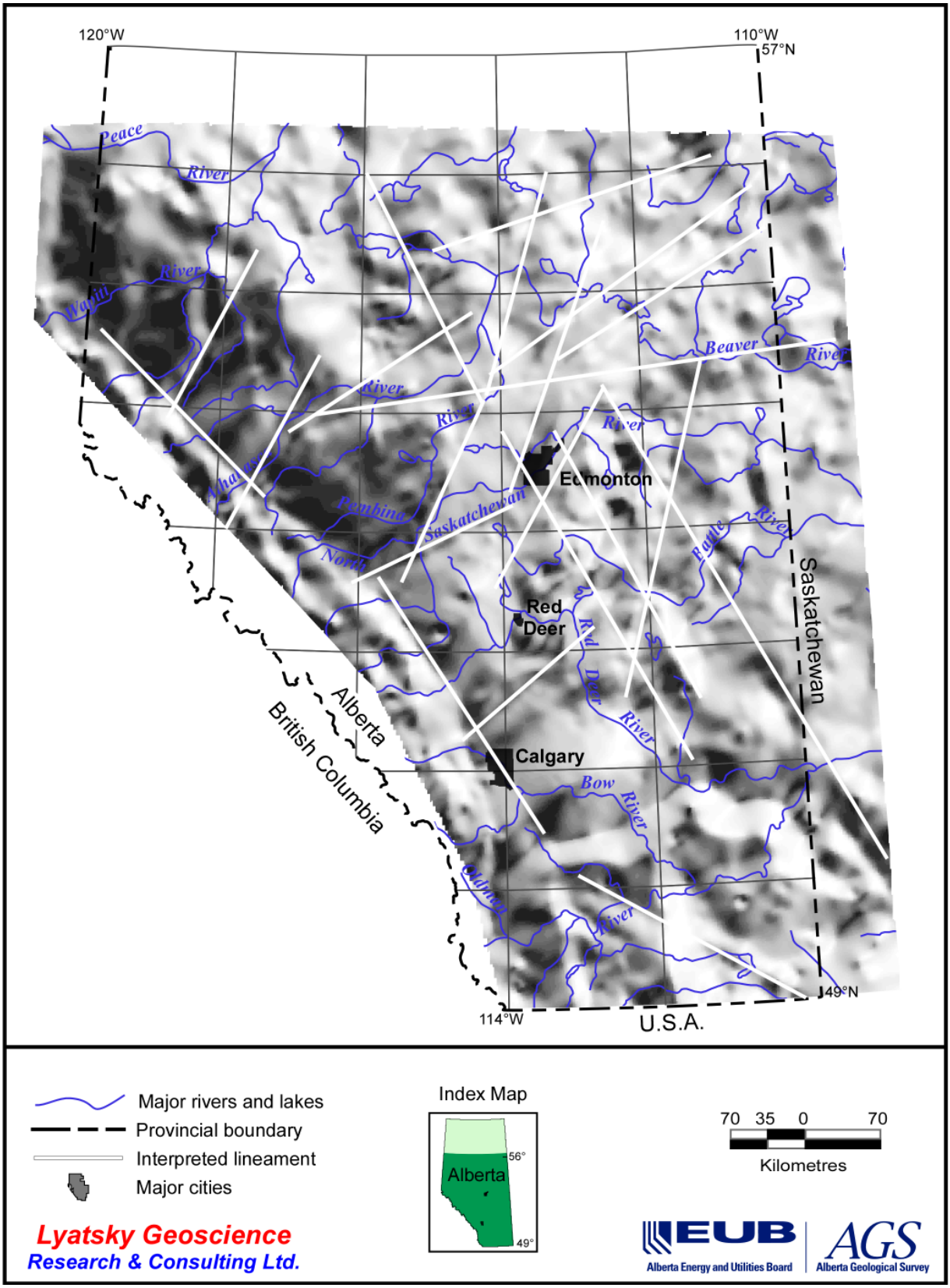

Map 13. Gravity shadowgram illuminated from the northeast with a 20° 'sun' inclination.

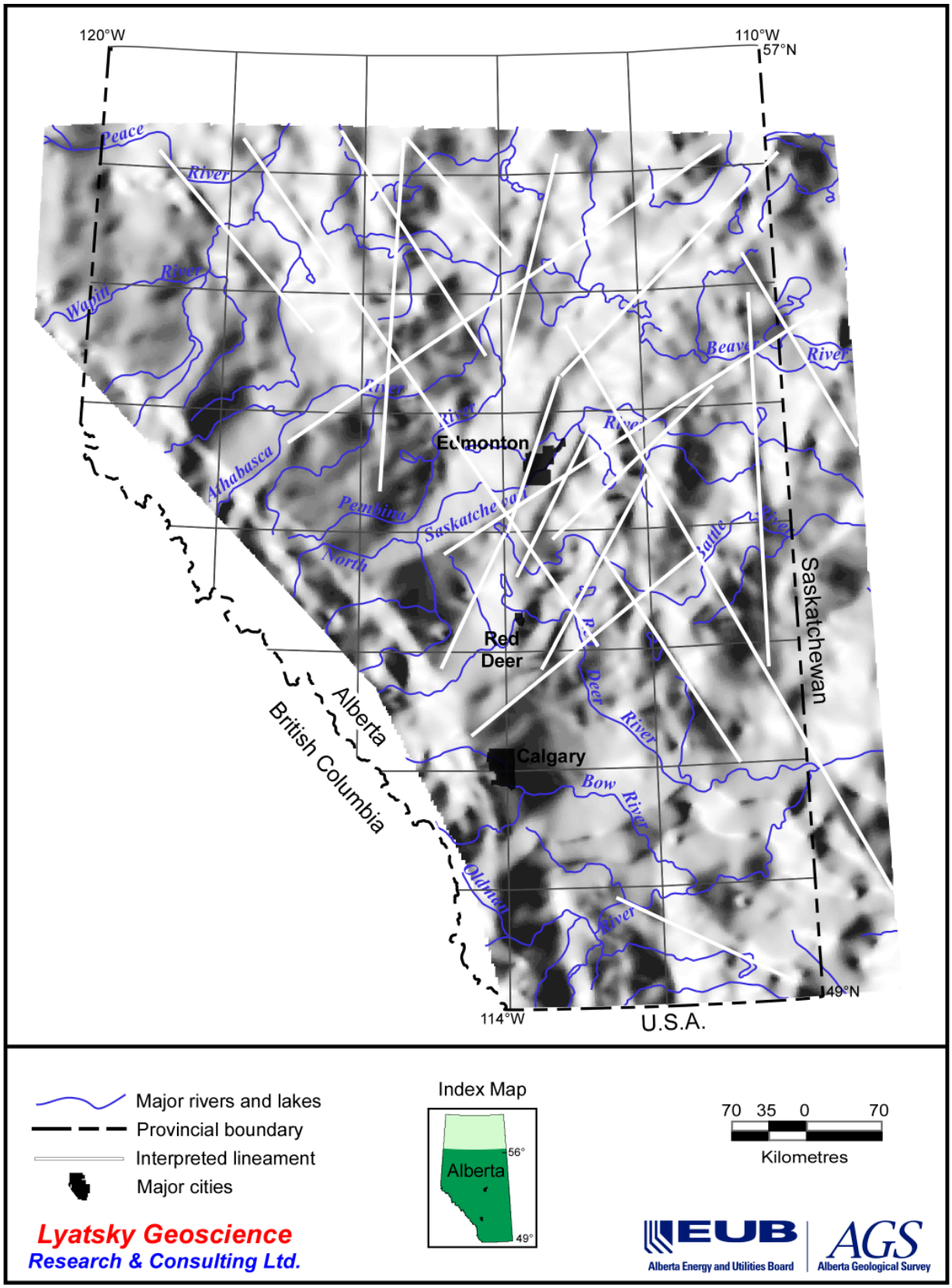

Map 14. Gravity shadowgram illuminated from the east with a 20° 'sun' inclination.

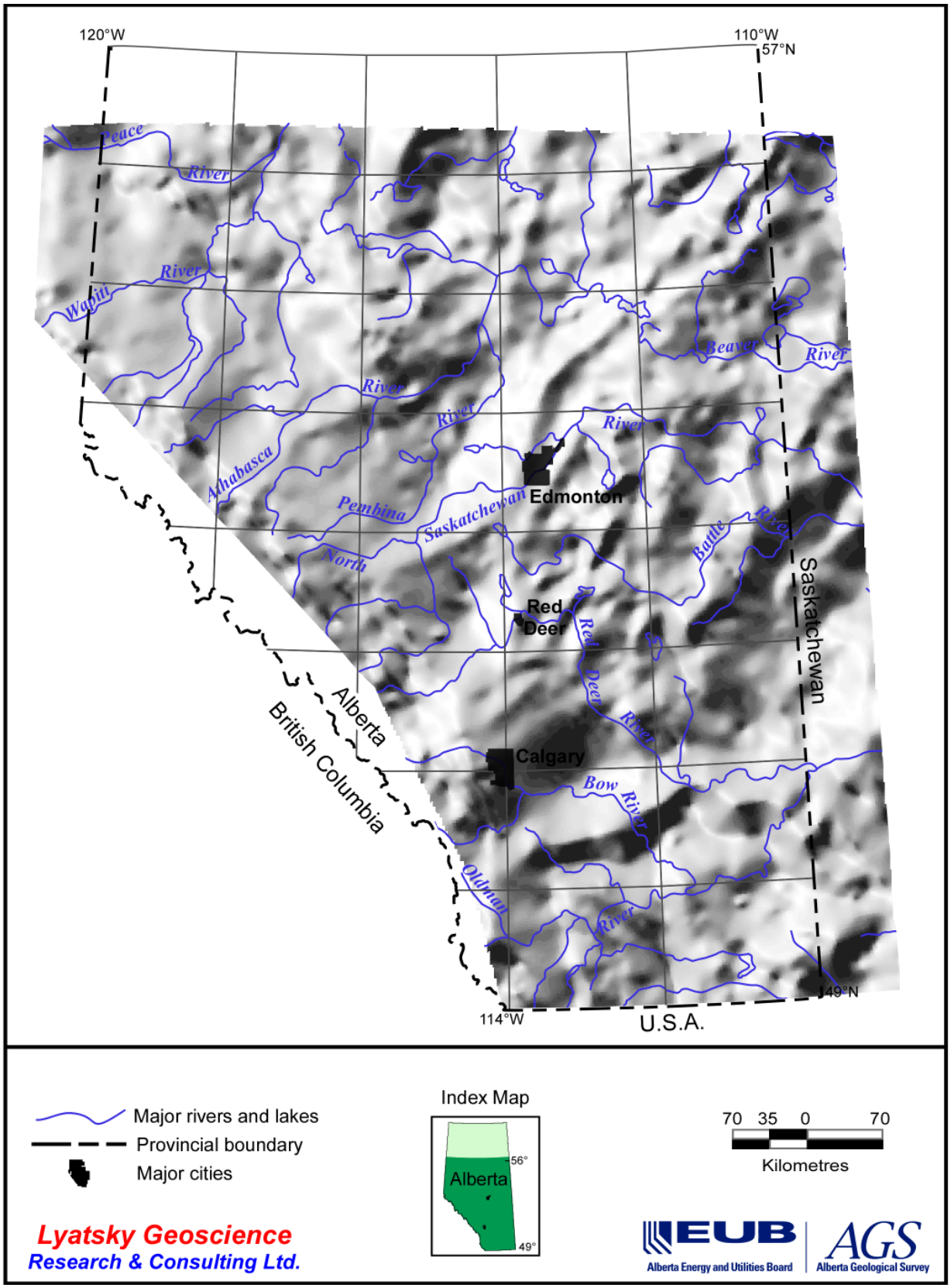

Map 15. Gravity shadowgram illuminated from the southeast with a 20° 'sun' inclination.

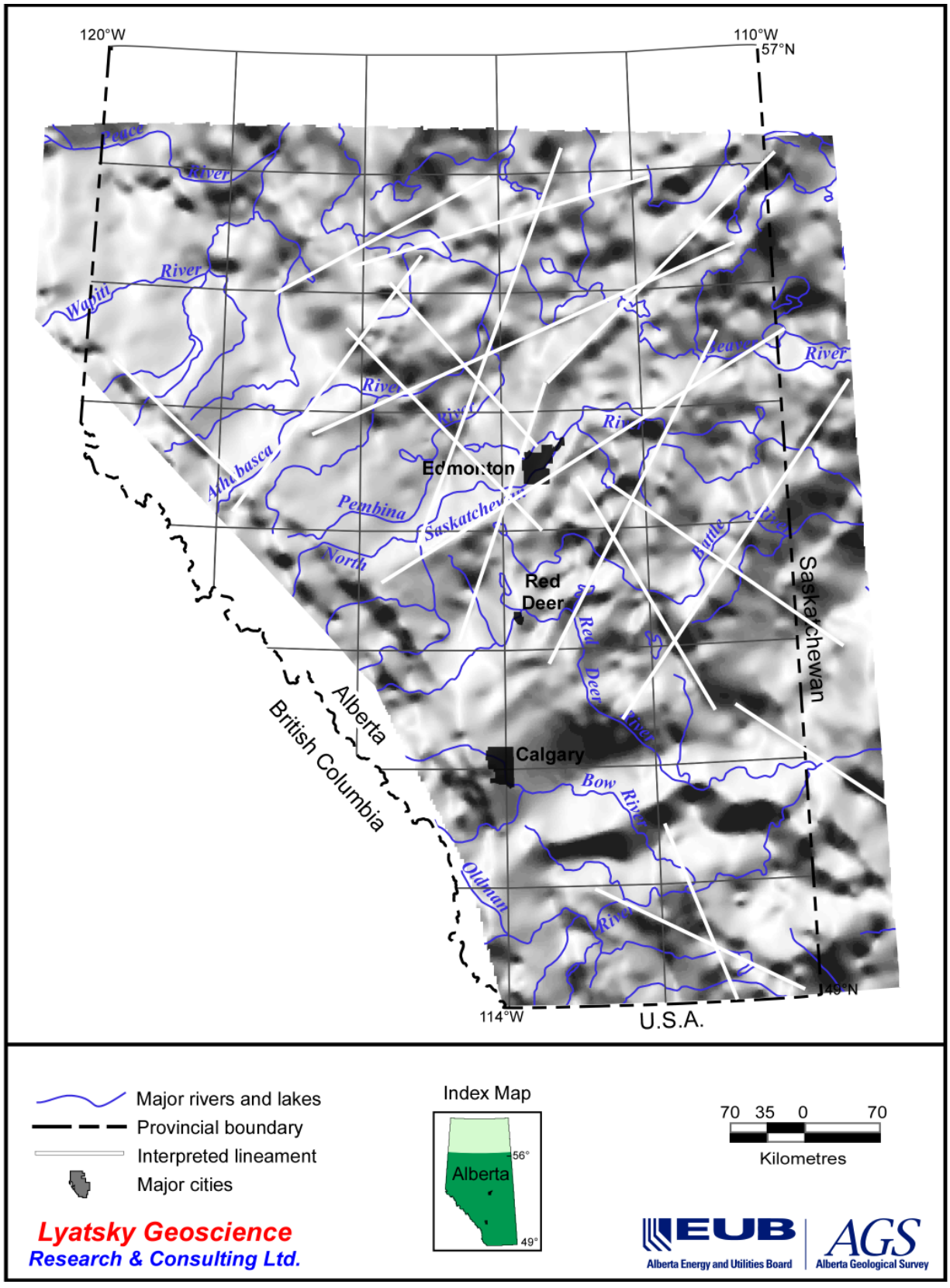

Map 16. Gravity shadowgram illuminated from the south with a 20° 'sun' inclination.

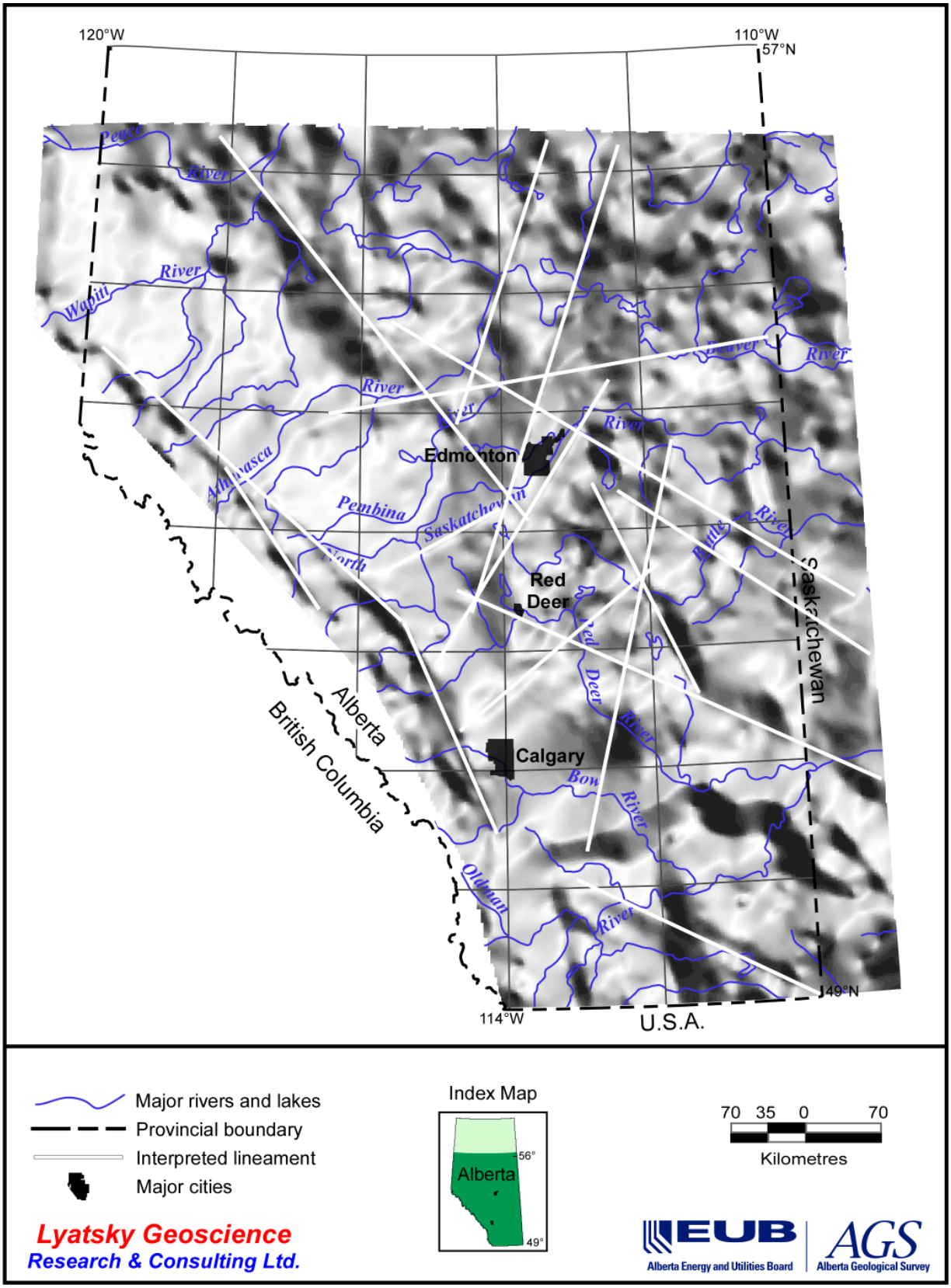

Map 17. Gravity shadowgram illuminated from the southwest with a 20° 'sun' inclination.

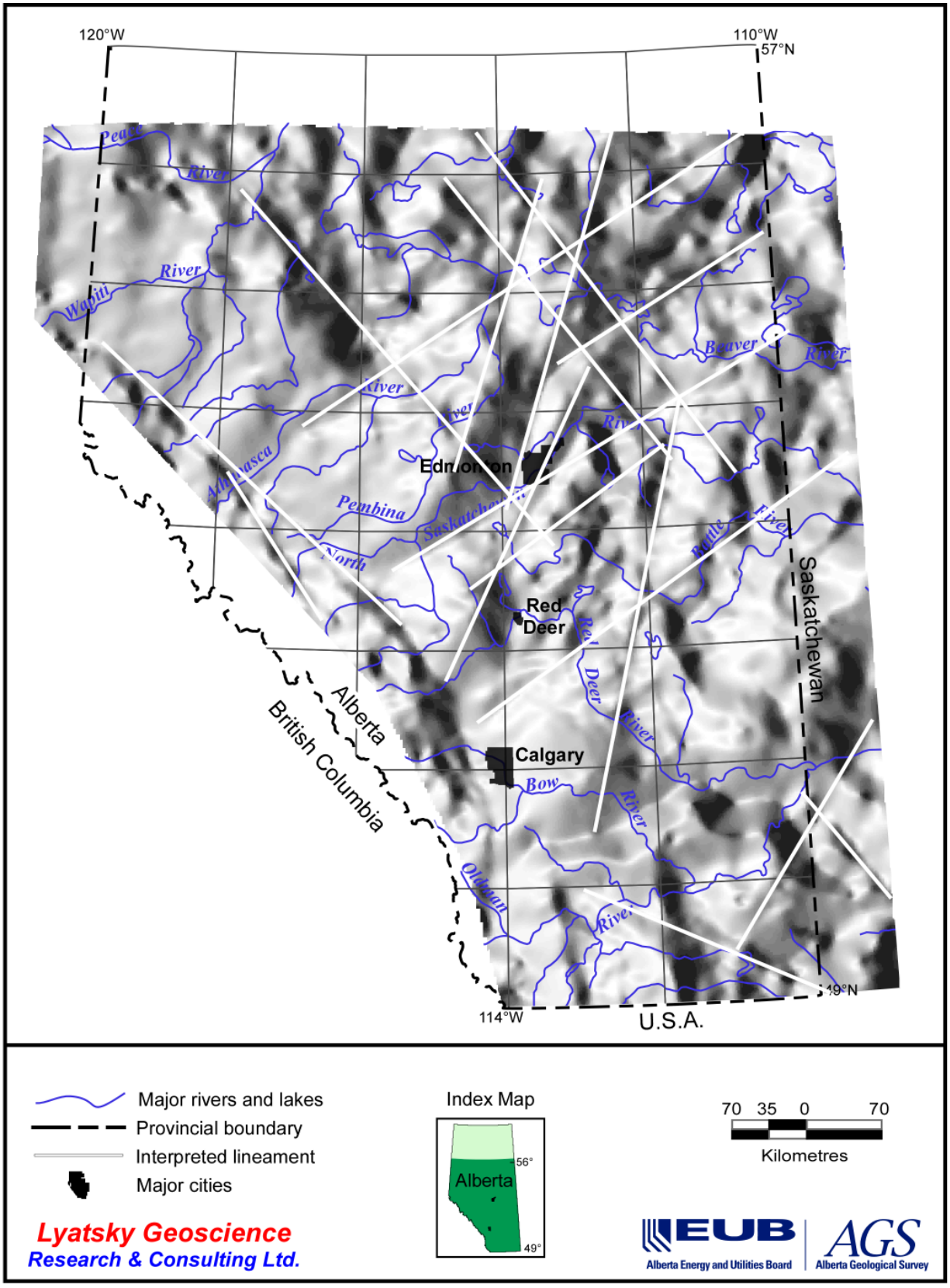

Map 18. Gravity shadowgram illuminated from the west with a 20° 'sun' inclination.

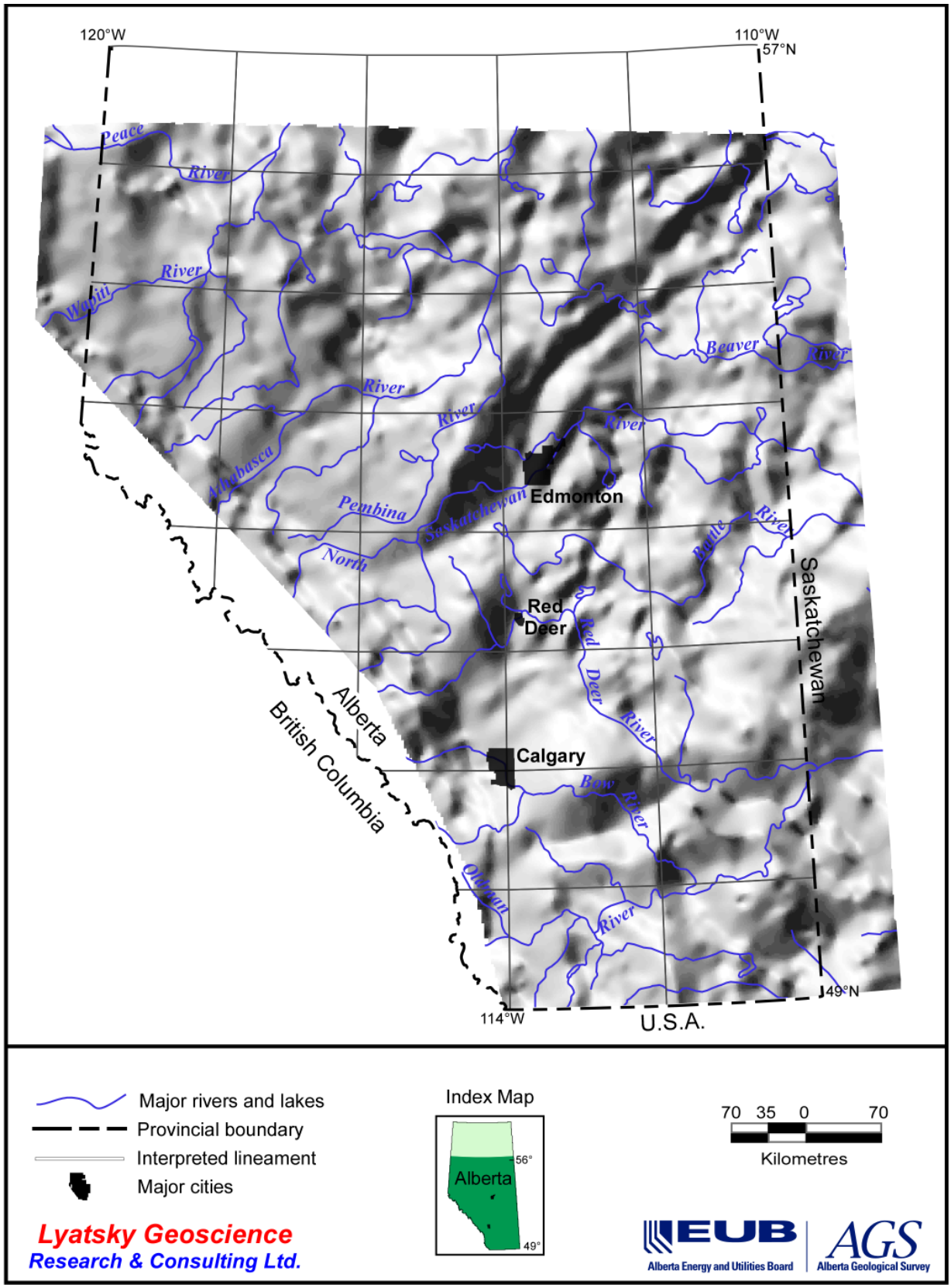

Map 19. Gravity shadowgram illuminated from the northwest with a 20° 'sun' inclination.

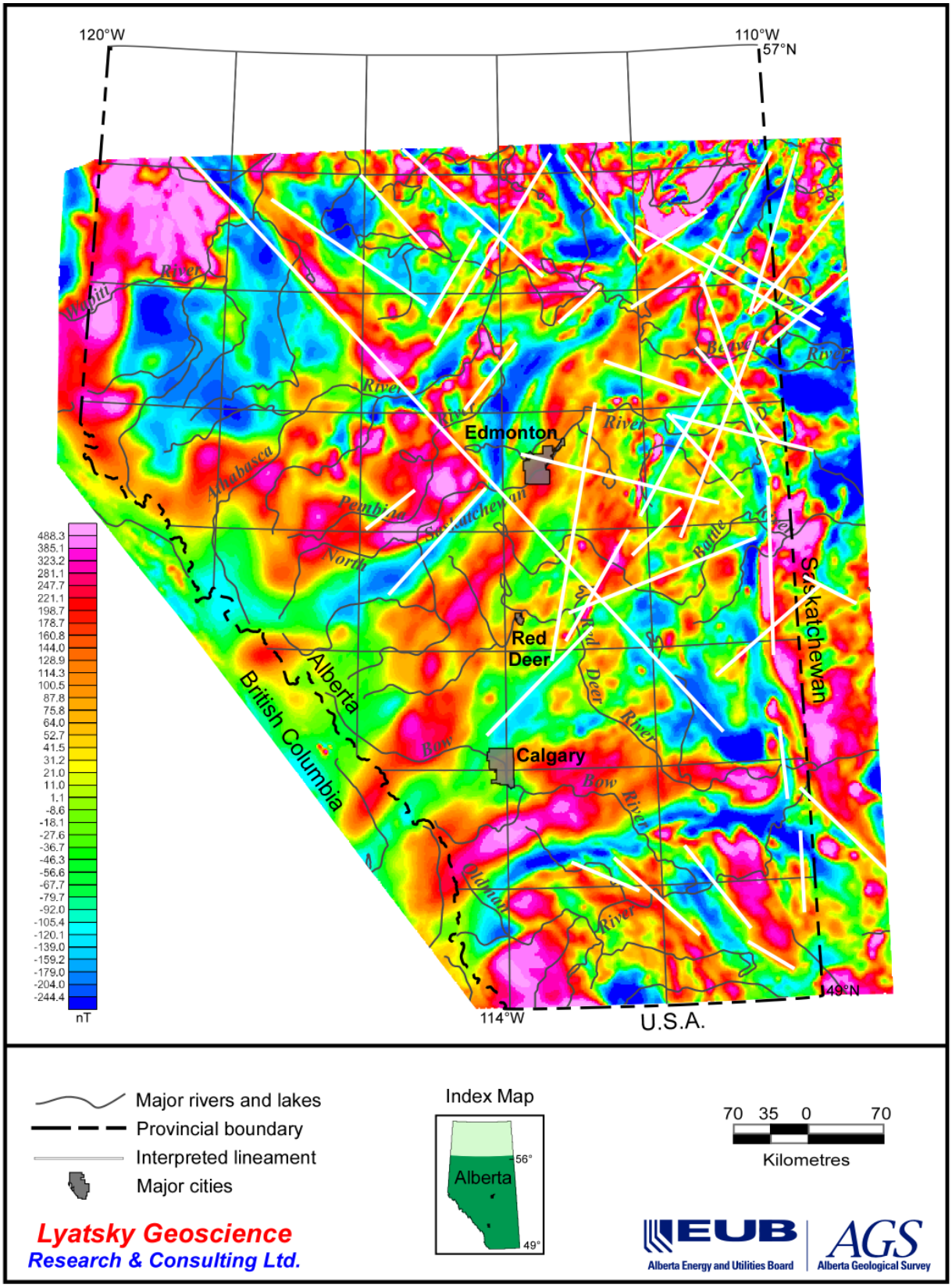

Map 20. Total-field magnetic map.

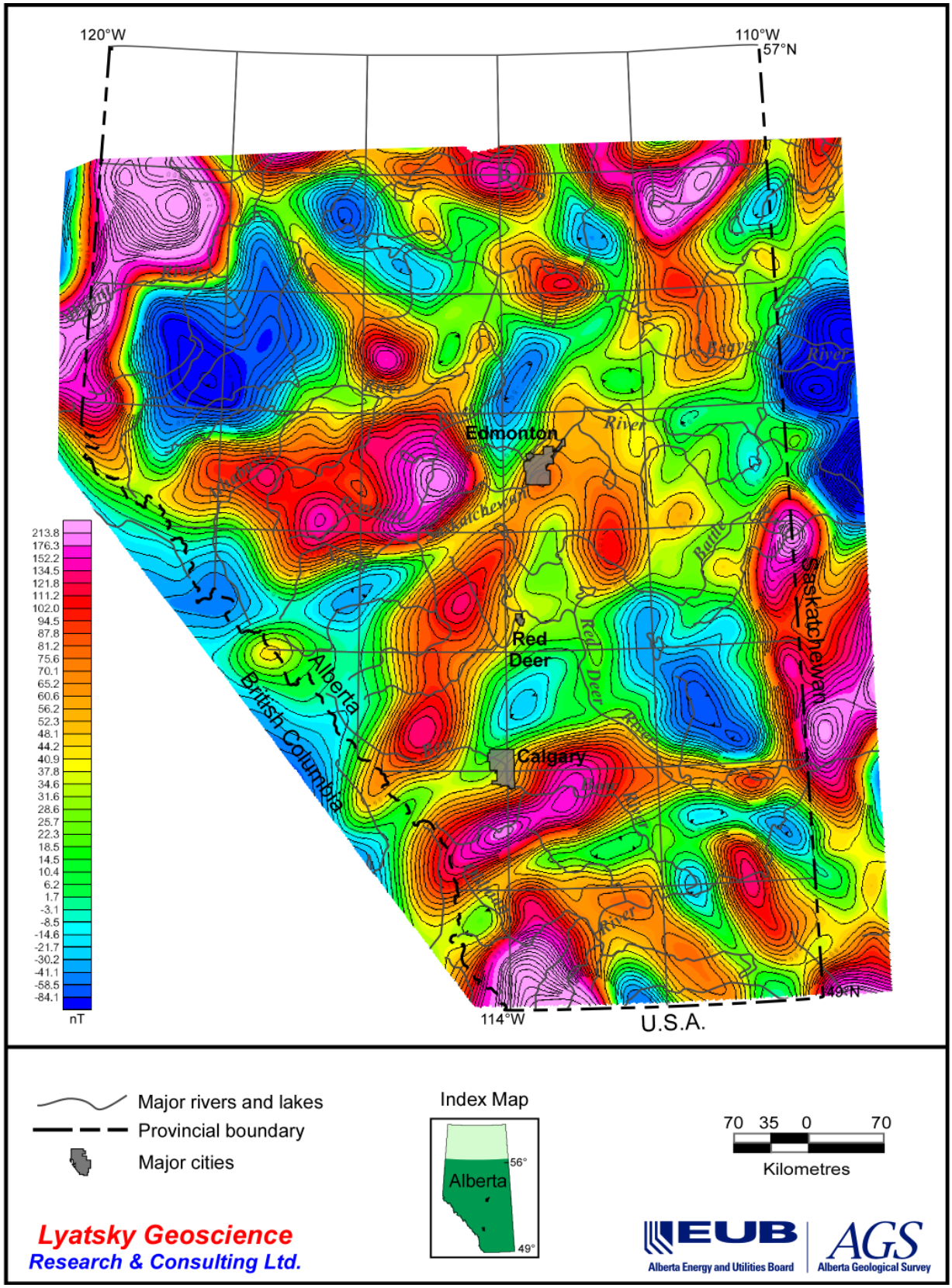

Map 21. Magnetic map upward continued to 20 km.

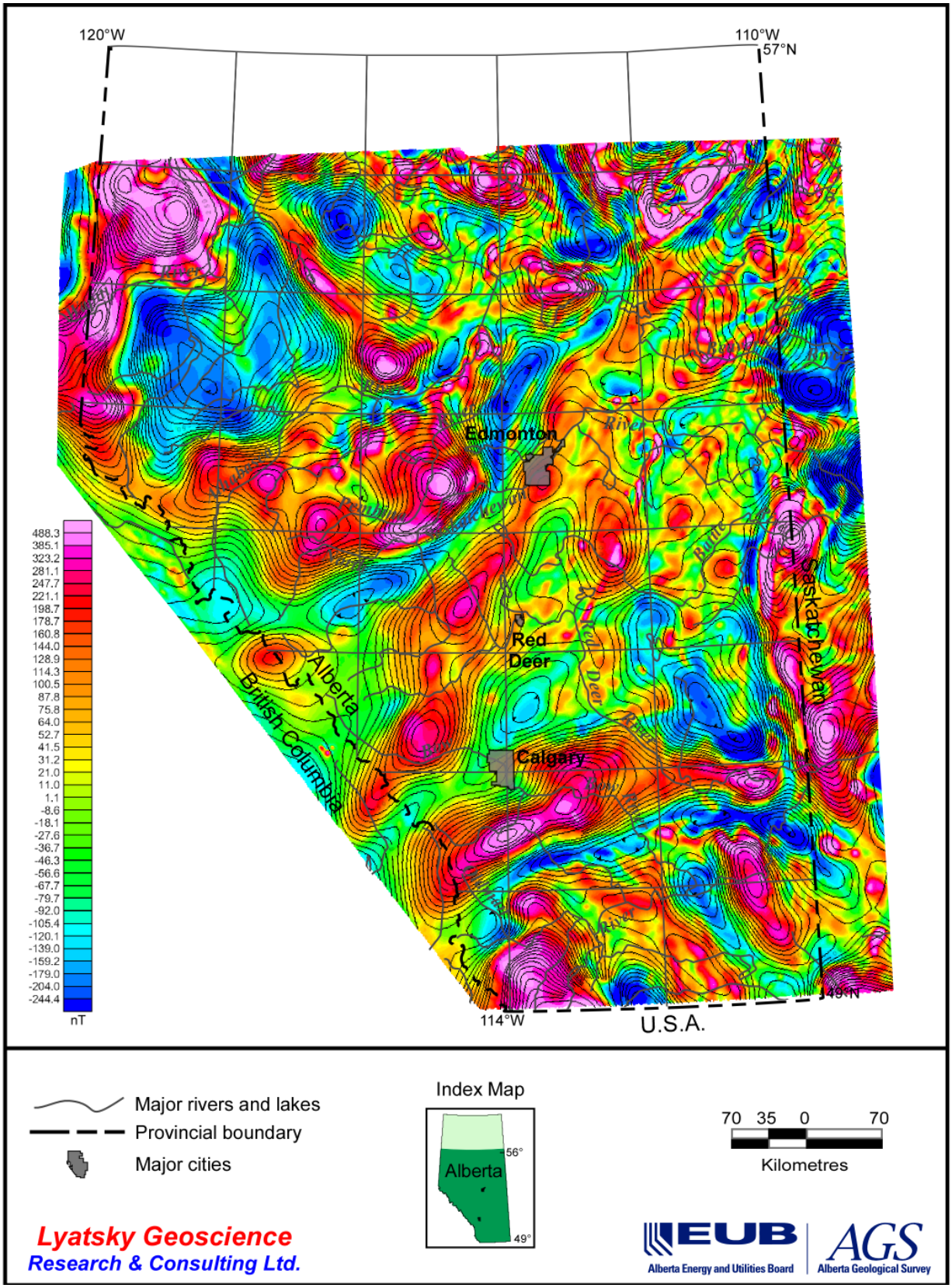

Map 22. Magnetic data with contours of the data upward continued to 20 km.

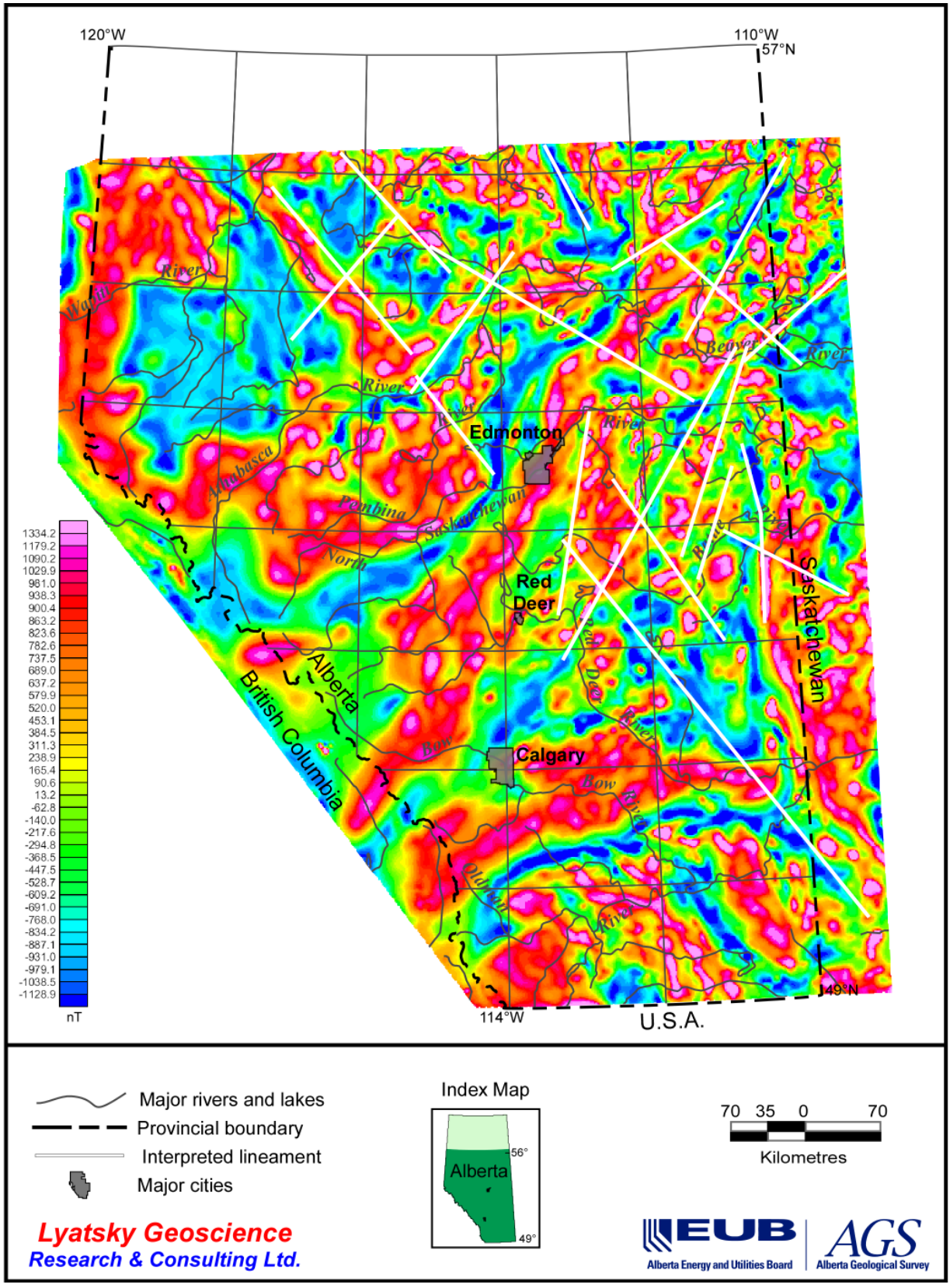

Map 23. Magnetic map with automatic amplitude gain (full AGC, window size= 29 grid cells).

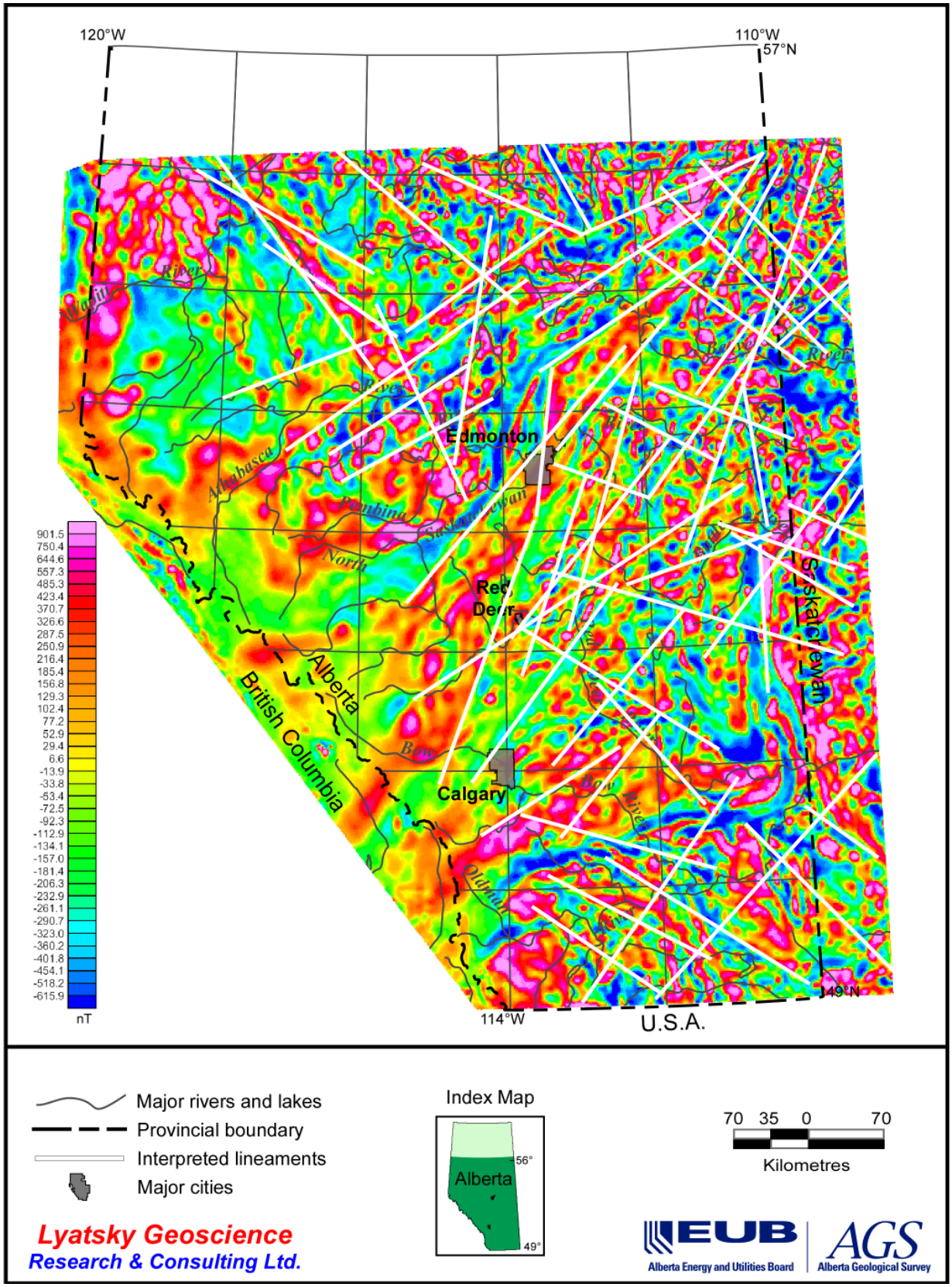

Map 24. Magnetic map with automatic amplitude gain (local AGC, window size=17 grid cells).

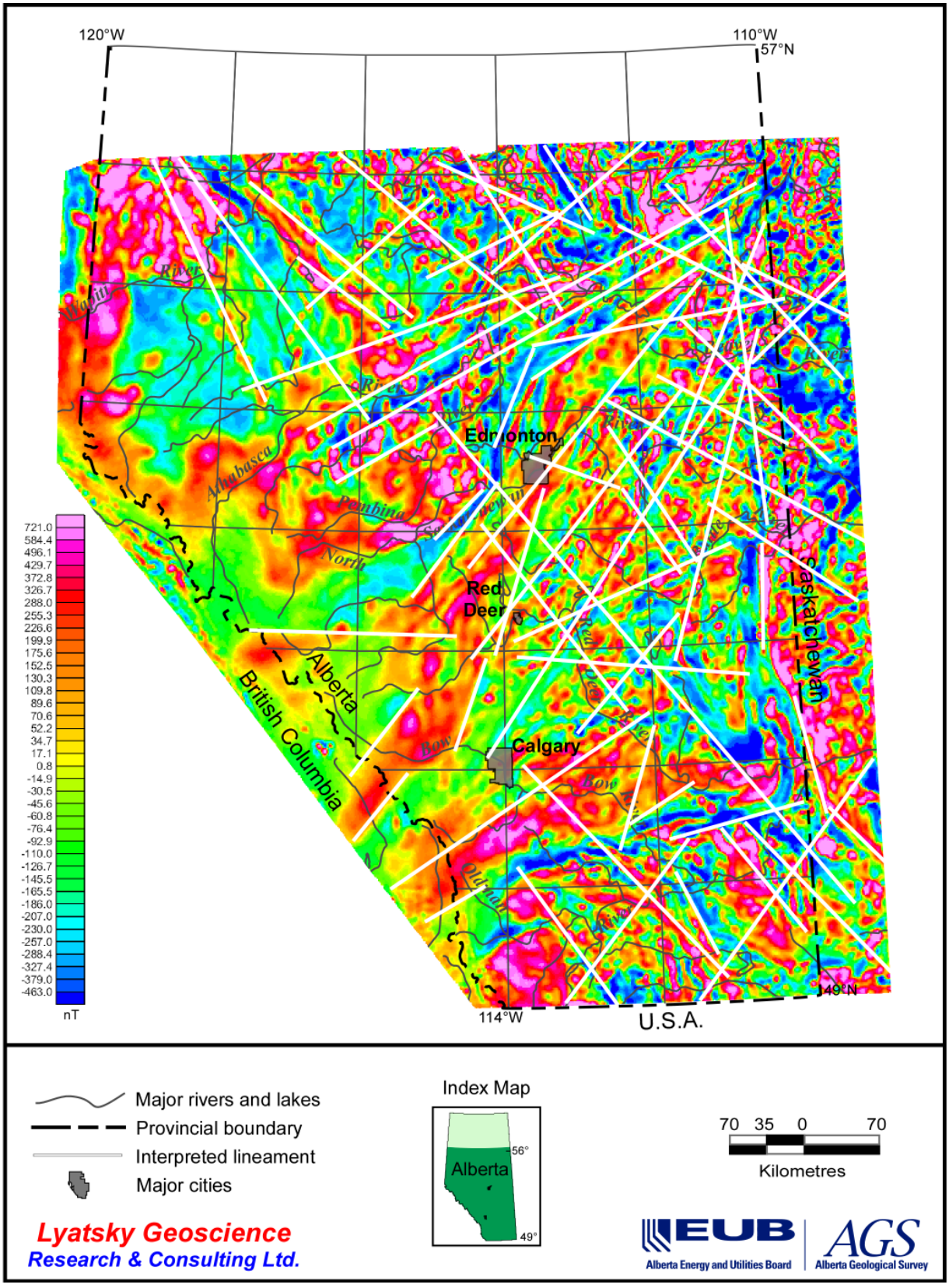

Map 25. Magnetic map with automatic amplitude gain (local AGC, window size=11 grid cells).

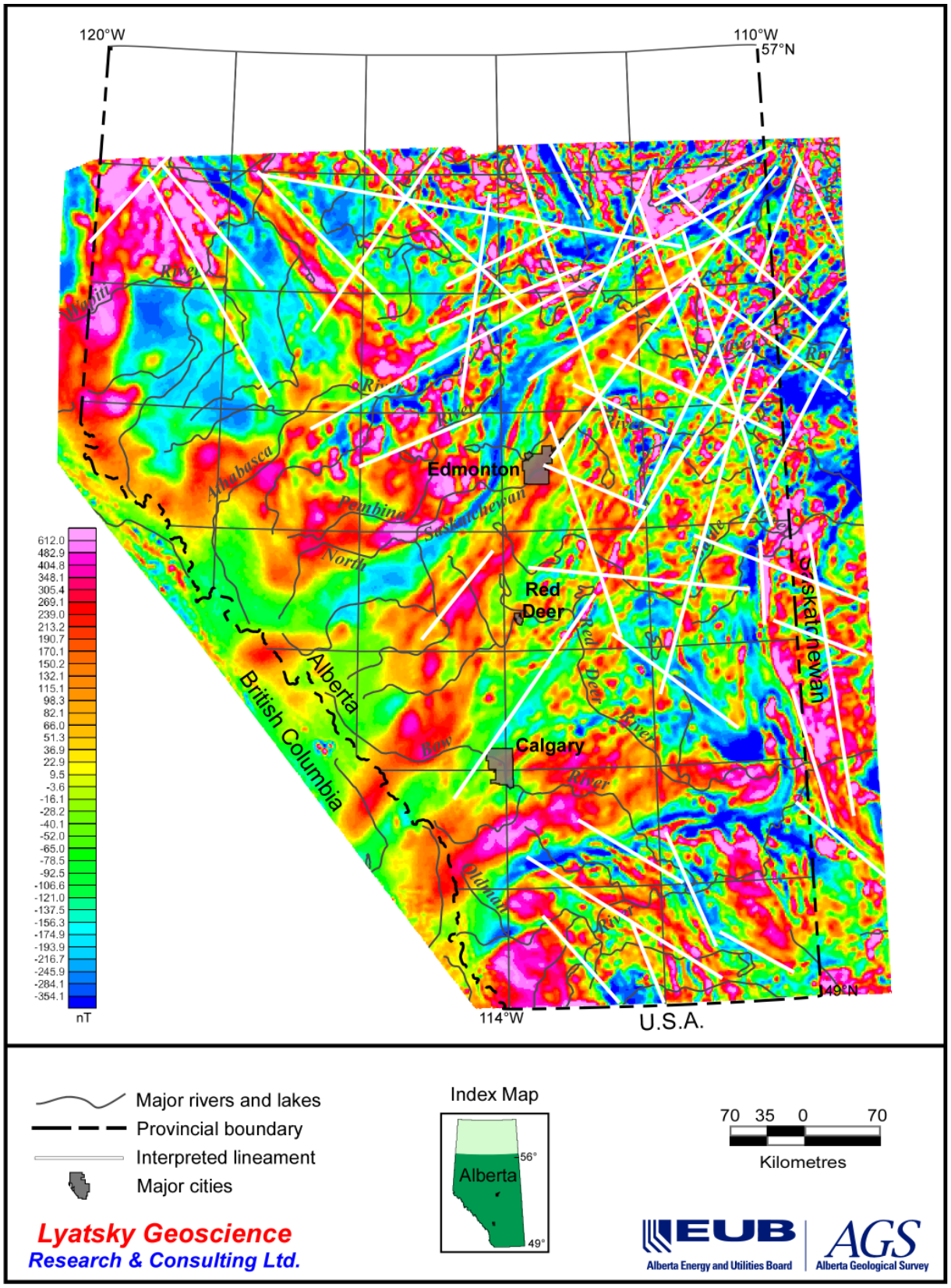

Map 26. Magnetic map with automatic amplitude gain (local AGC, window size=7 grid cells).

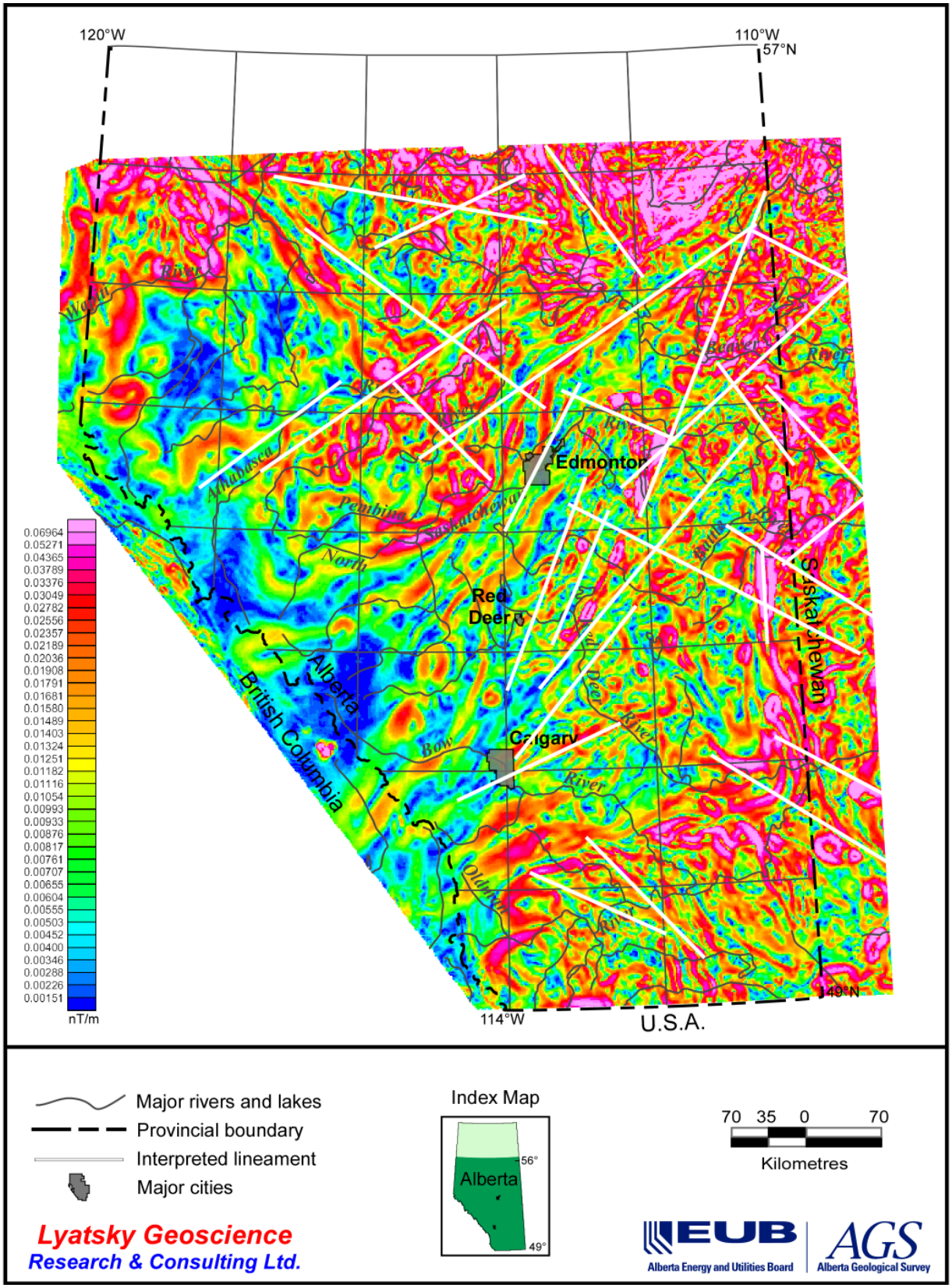

Map 27. Horizontal gradient of magnetic data.

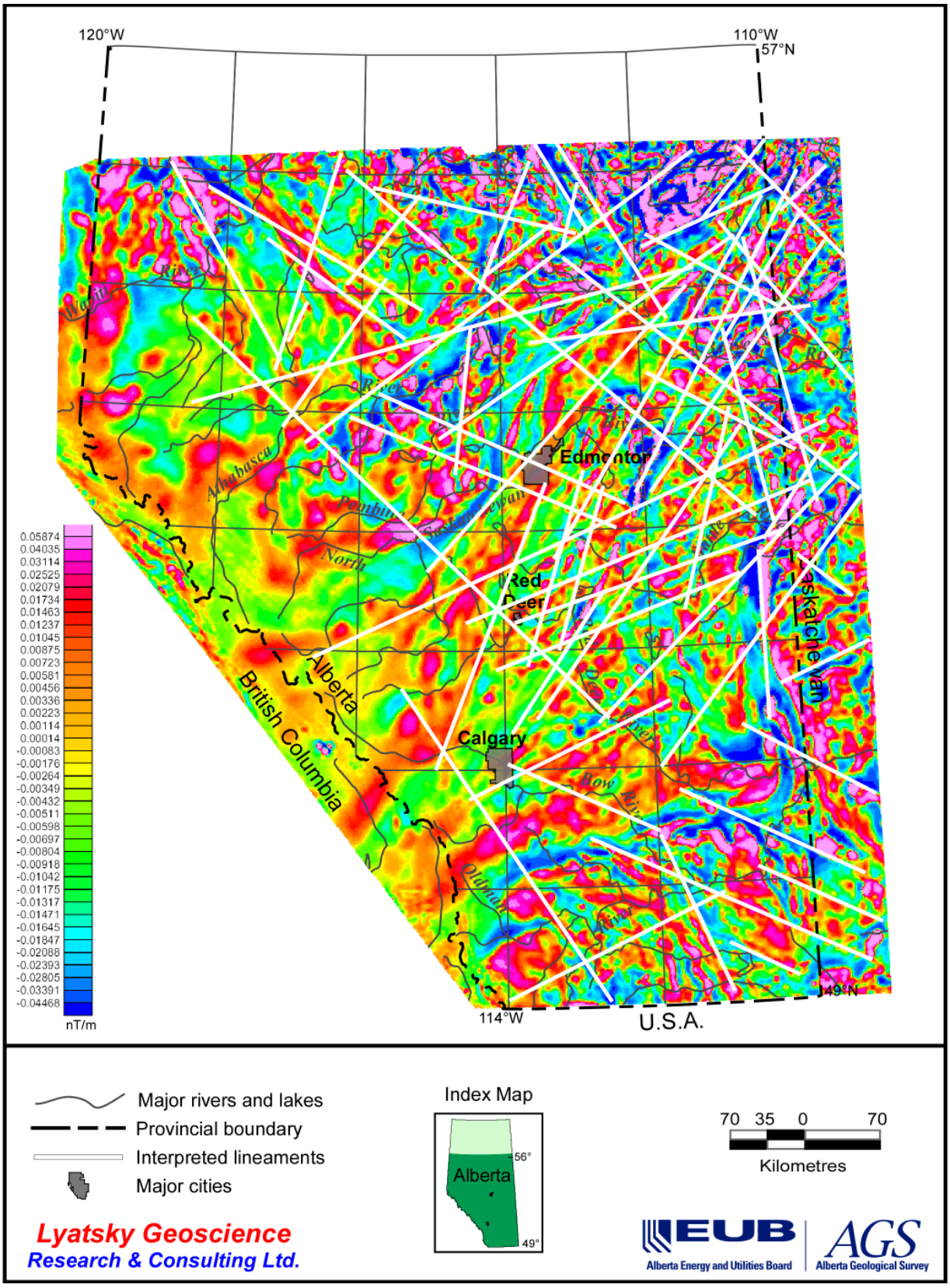

Map 28. First vertical derivative of magnetic data.

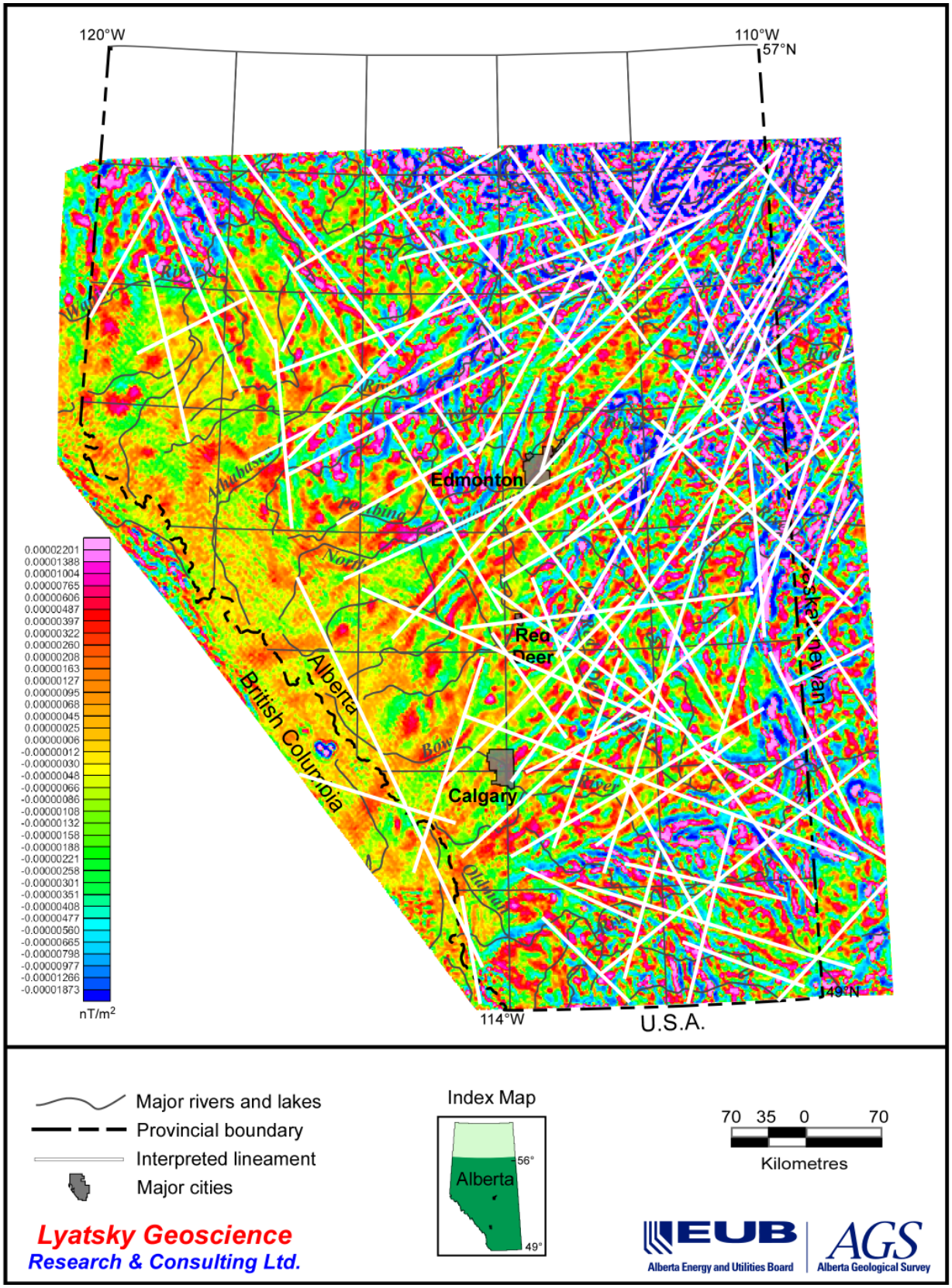

Map 29. Second vertical derivative of magnetic data.

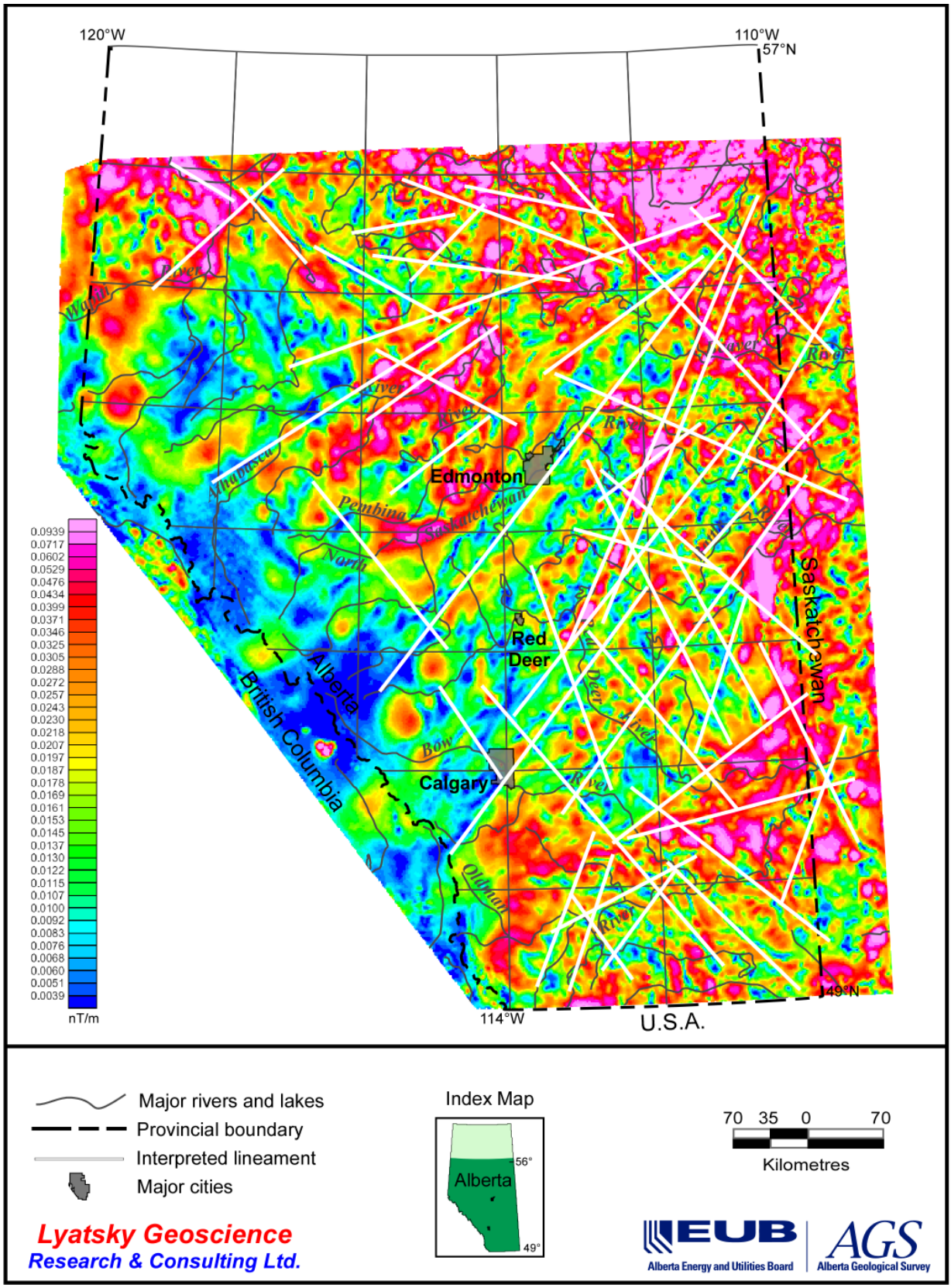

Map 30. Total gradient (analytic signal) of magnetic data.

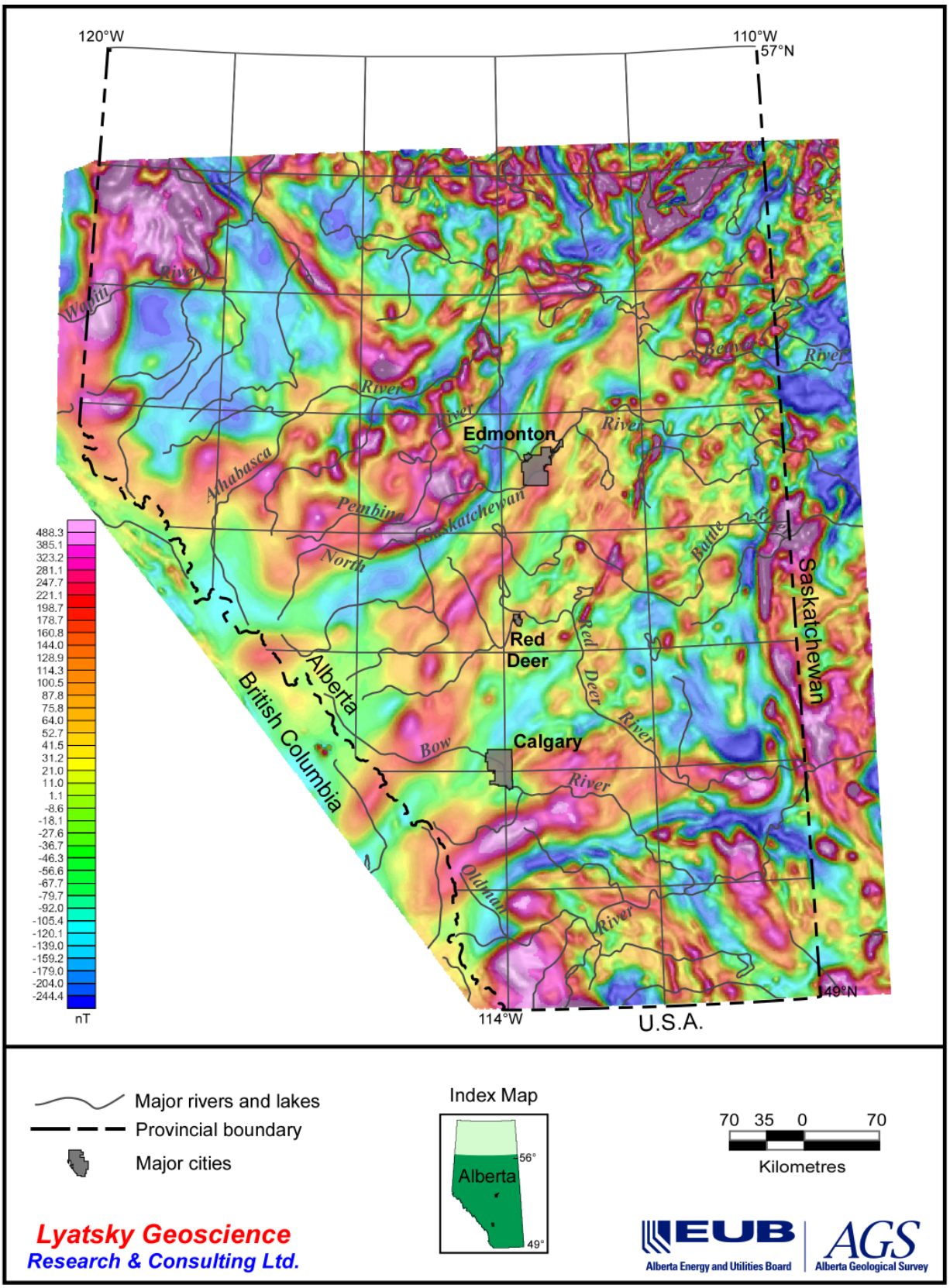

Map 31. Magnetic data with vertical shadowgram superimposed.

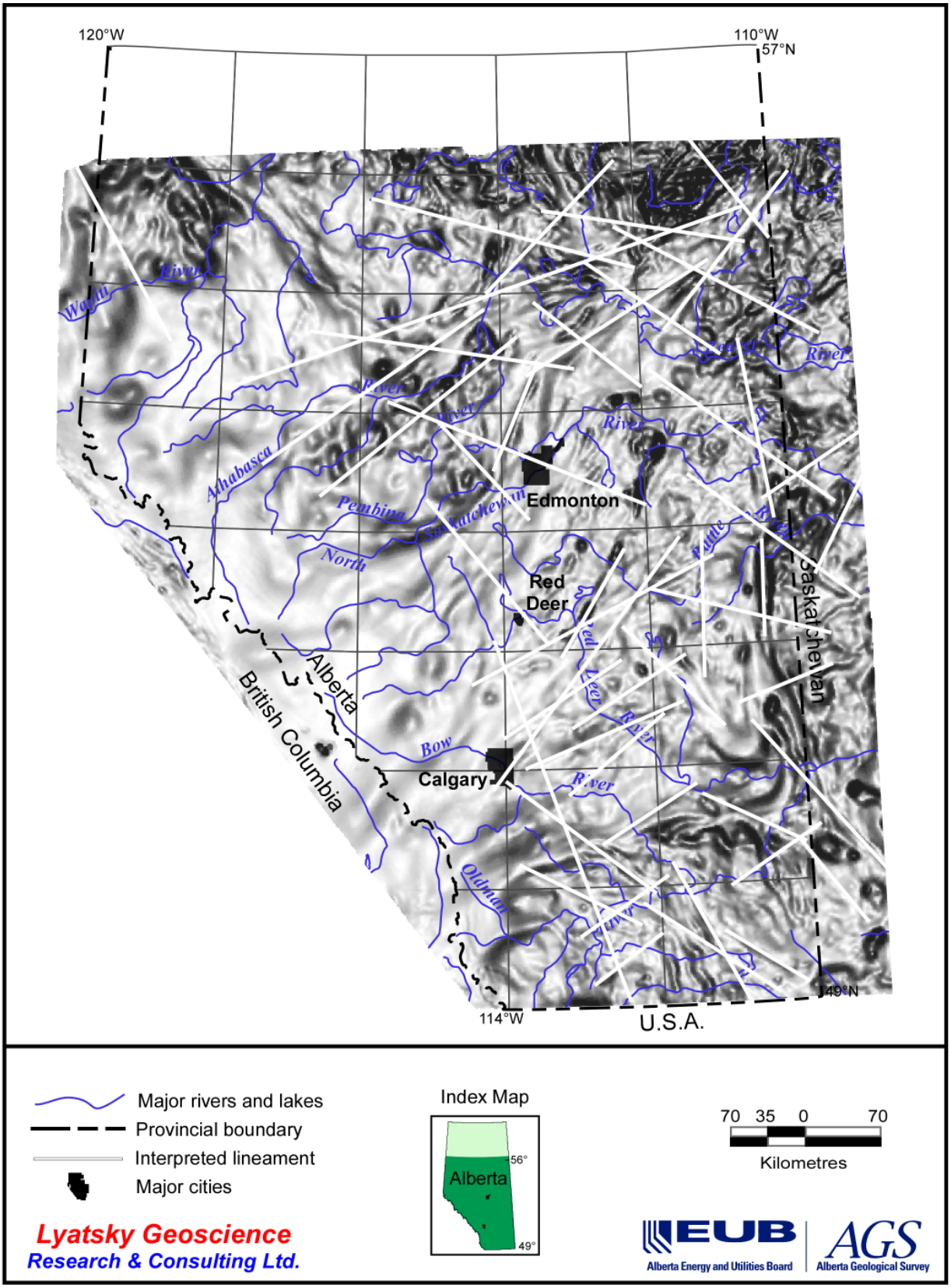

Map 32. Vertical-sun-angle shadowgram of magnetic data.

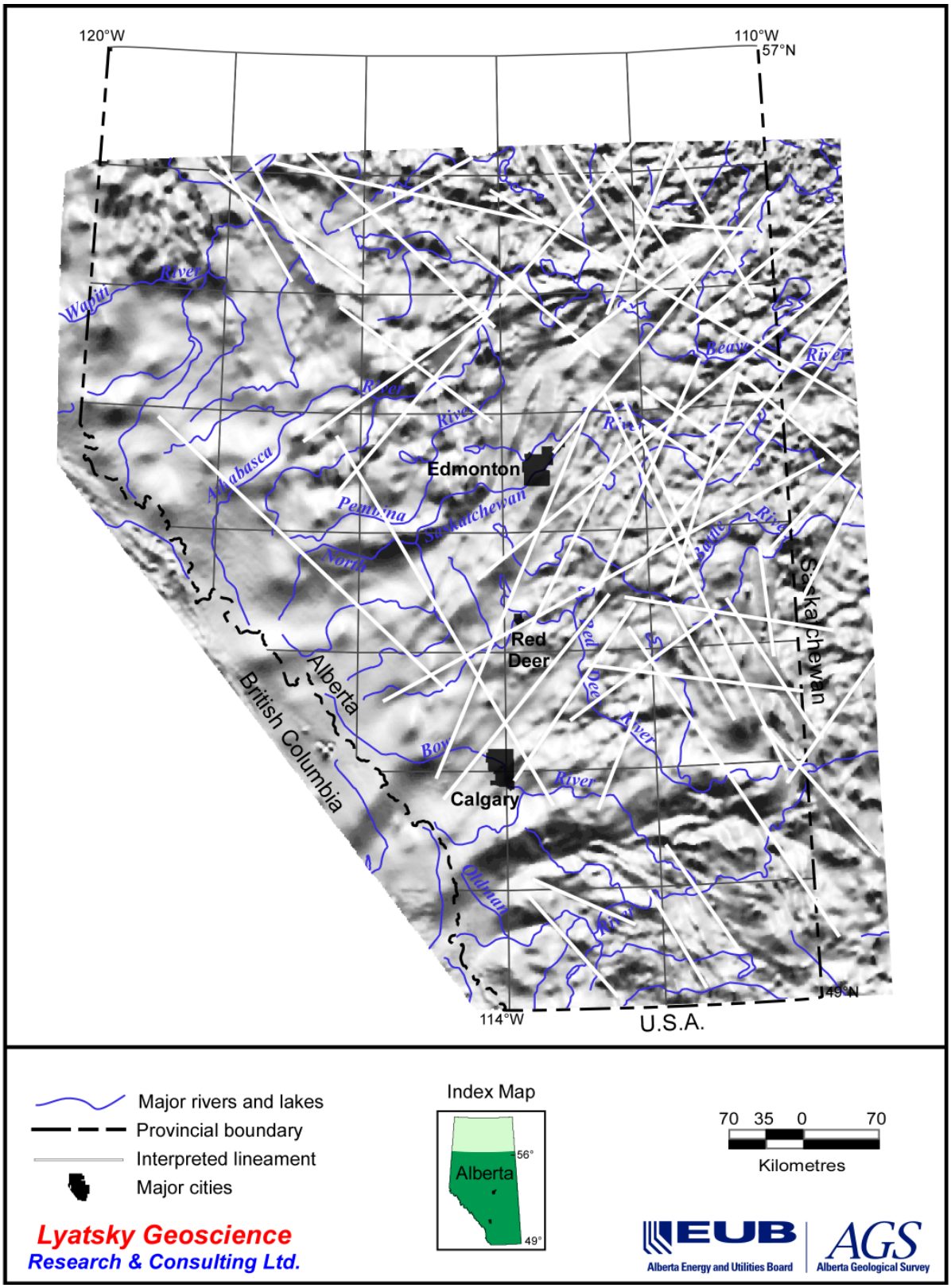

Map 33. Magnetic shadowgram illuminated from the north with 20° 'sun' inclination.

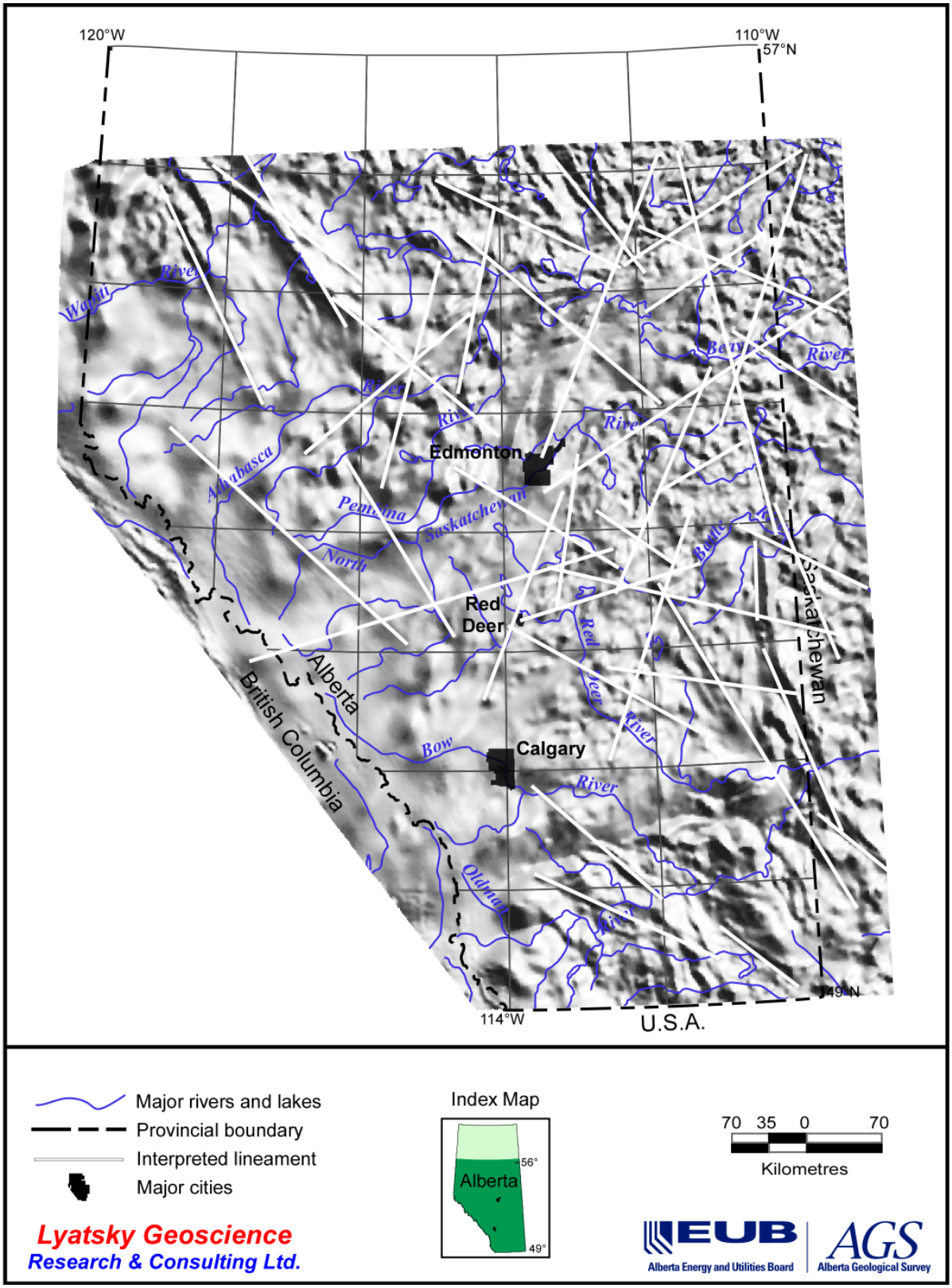

Map 34. Magnetic shadowgram illuminated from the northeast with 20° 'sun' inclination.

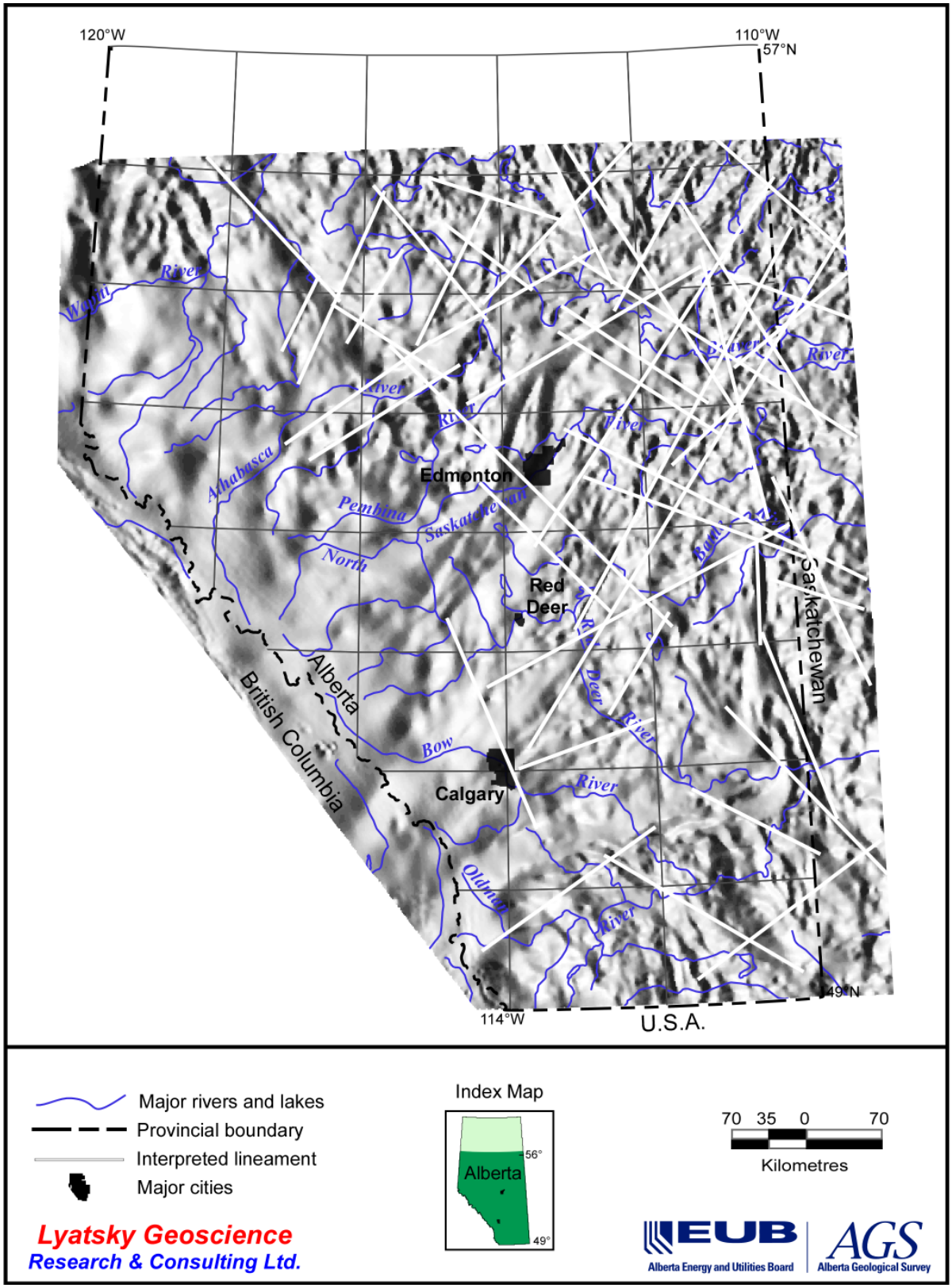

Map 35. Magnetic shadowgram illuminated from the east with 20° 'sun' inclination.

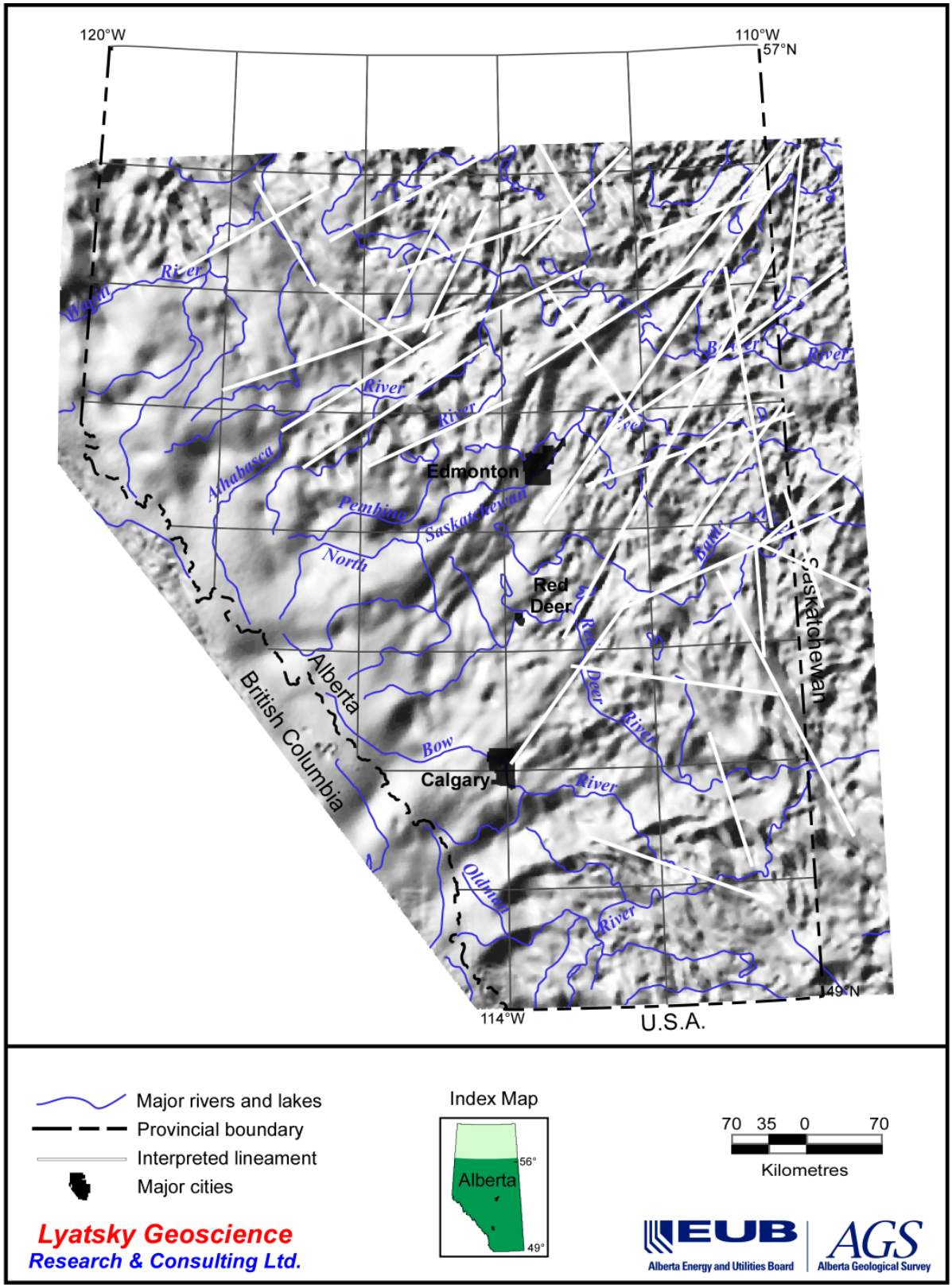

Map 36. Magnetic shadowgram illuminated from the southeast with 20° 'sun' inclination.

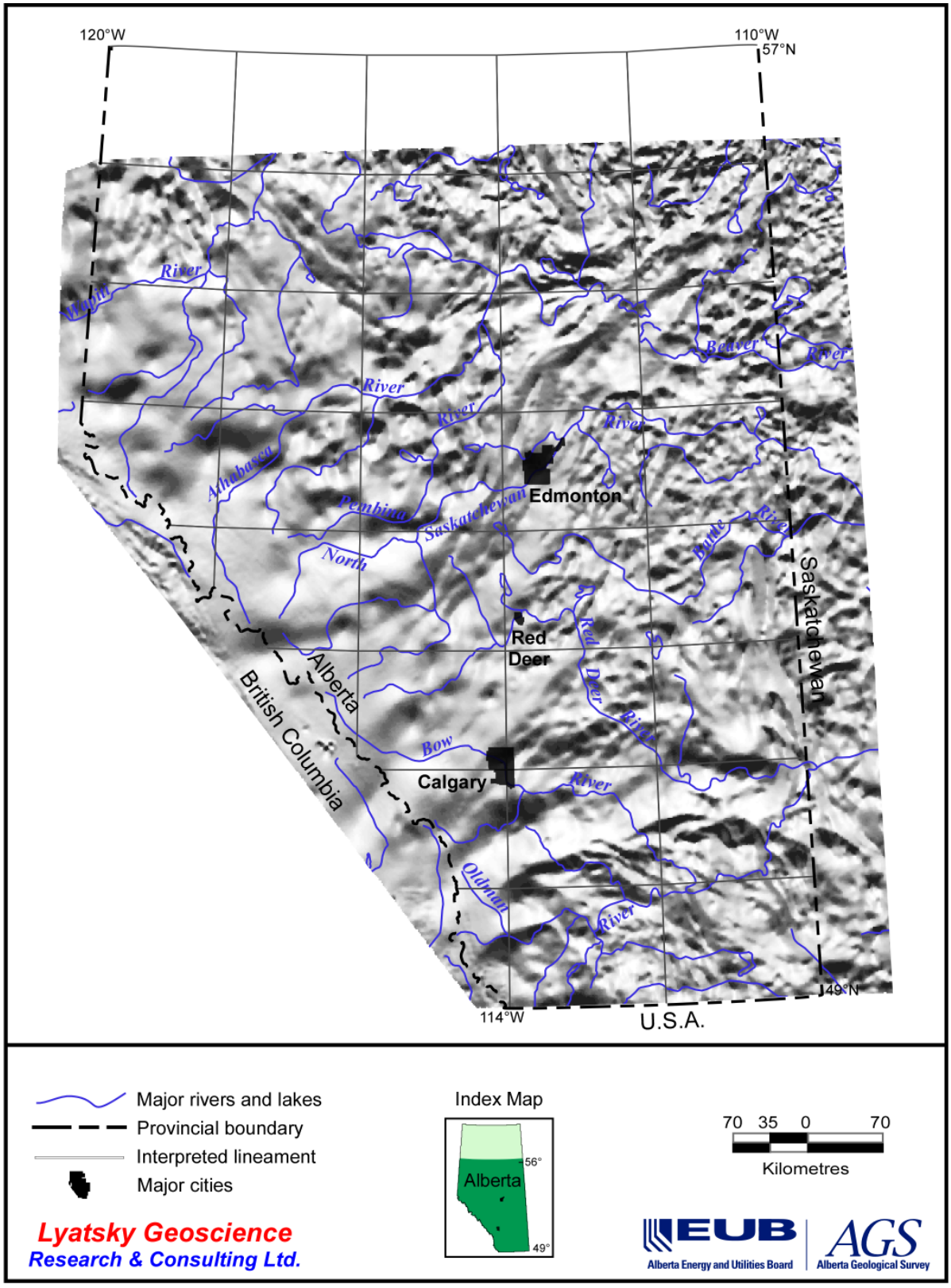

Map 37. Magnetic shadowgram illuminated from the south with 20° 'sun' inclination.

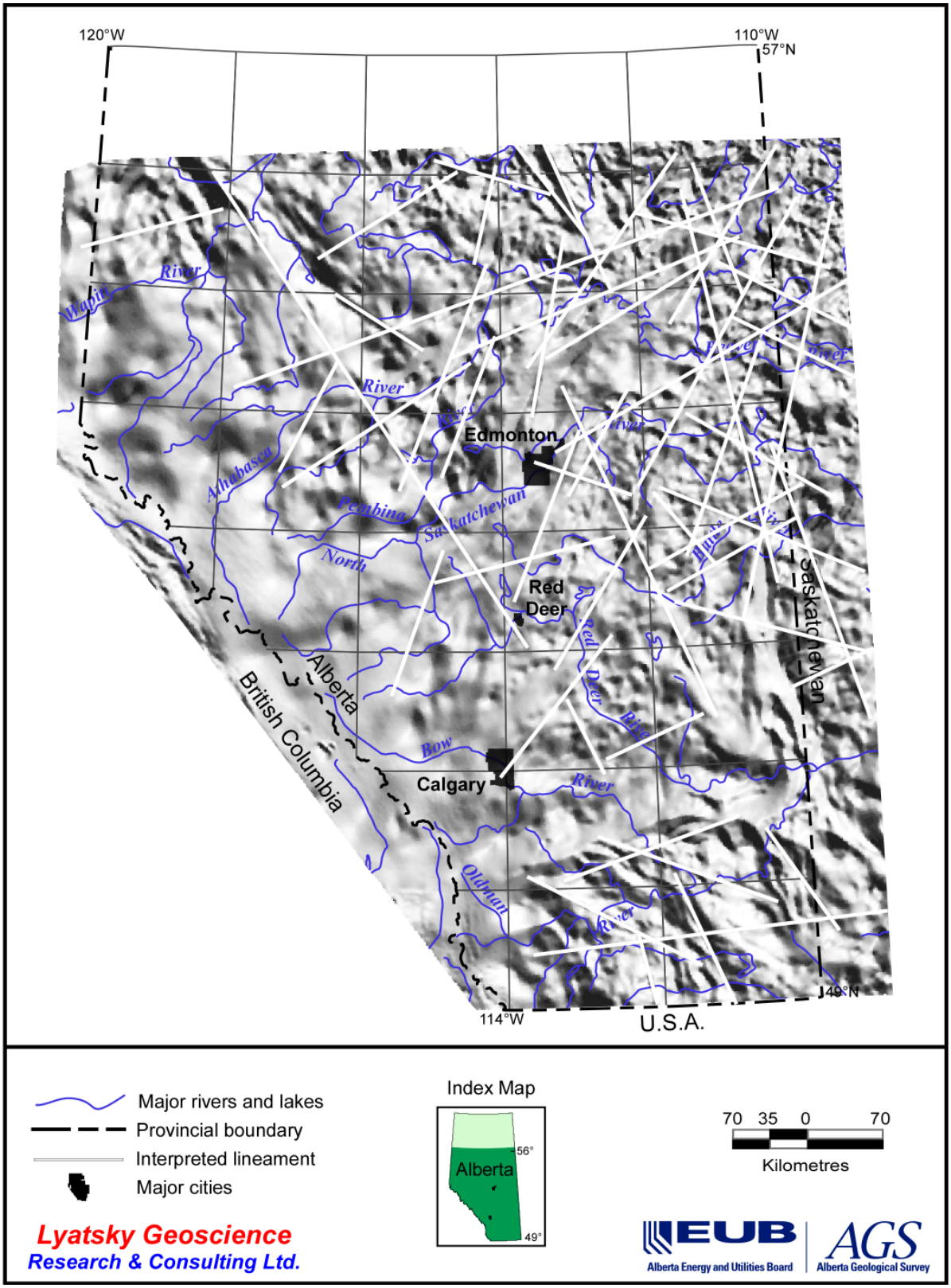

Map 38. Magnetic shadowgram illuminated from the southwest with 20° 'sun' inclination.

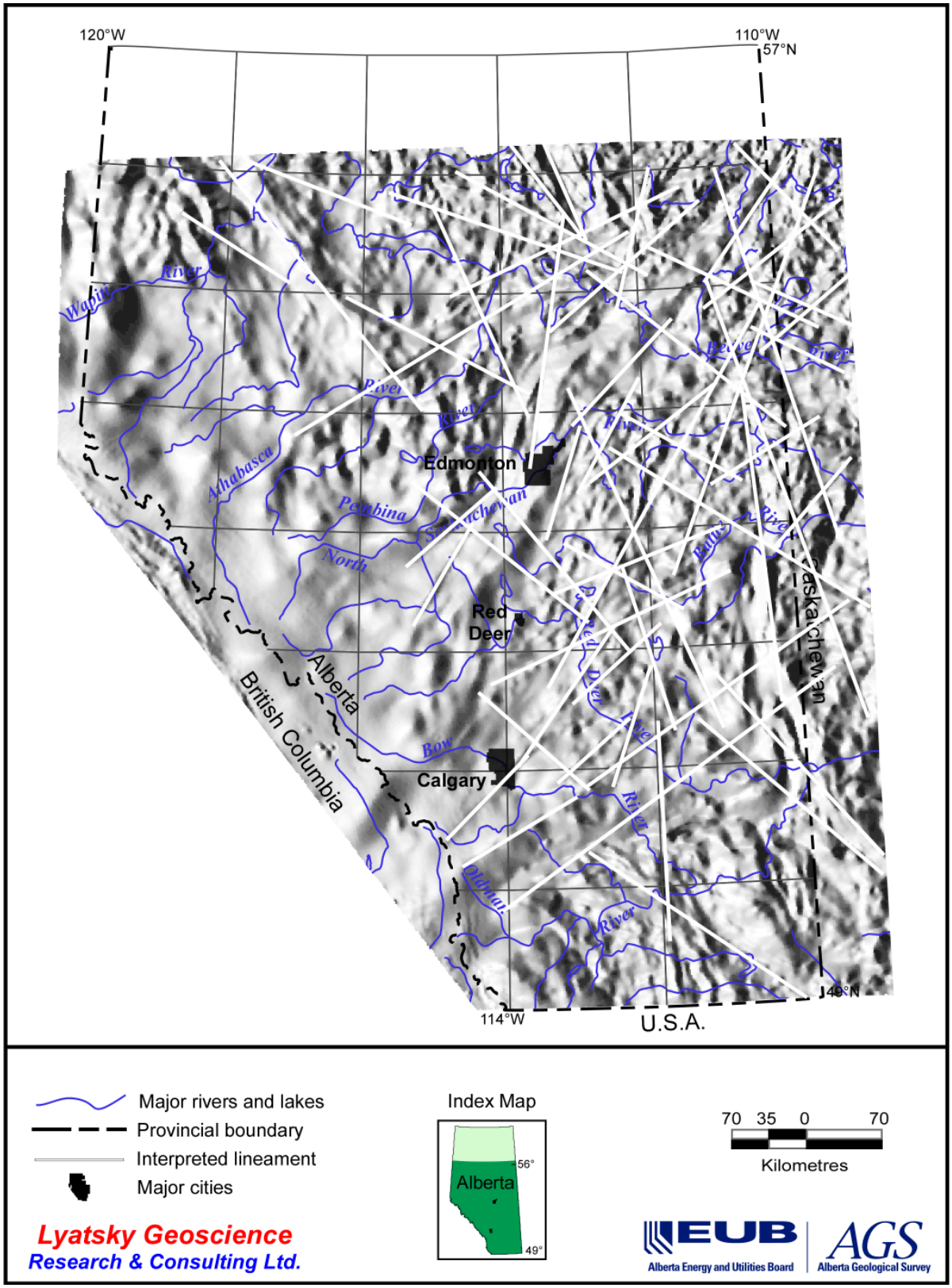

Map 39. Magnetic shadowgram illuminated from the west with 20° 'sun' inclination.

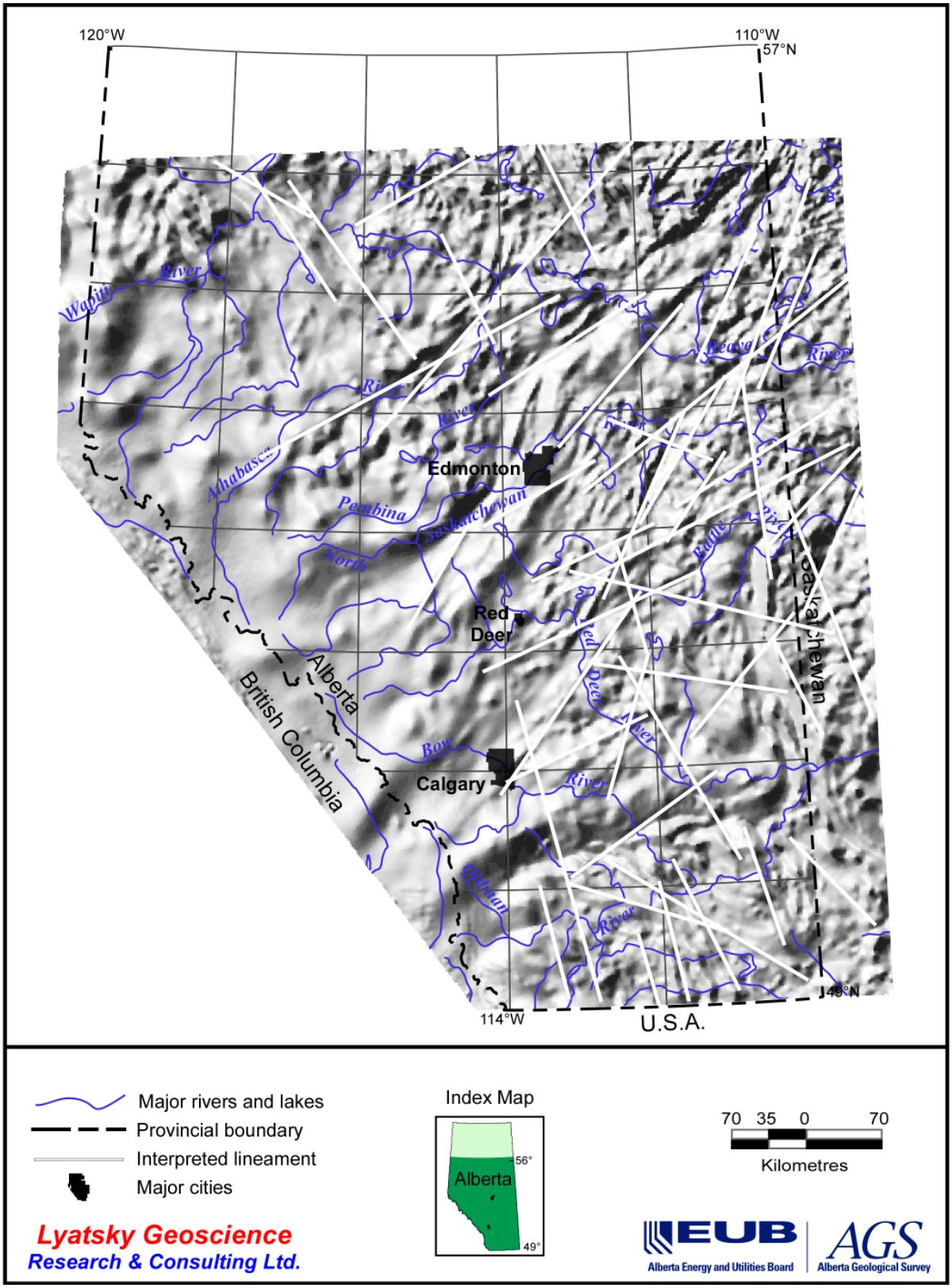

Map 40. Magnetic shadowgram illuminated from the northwest with 20° 'sun' inclination.

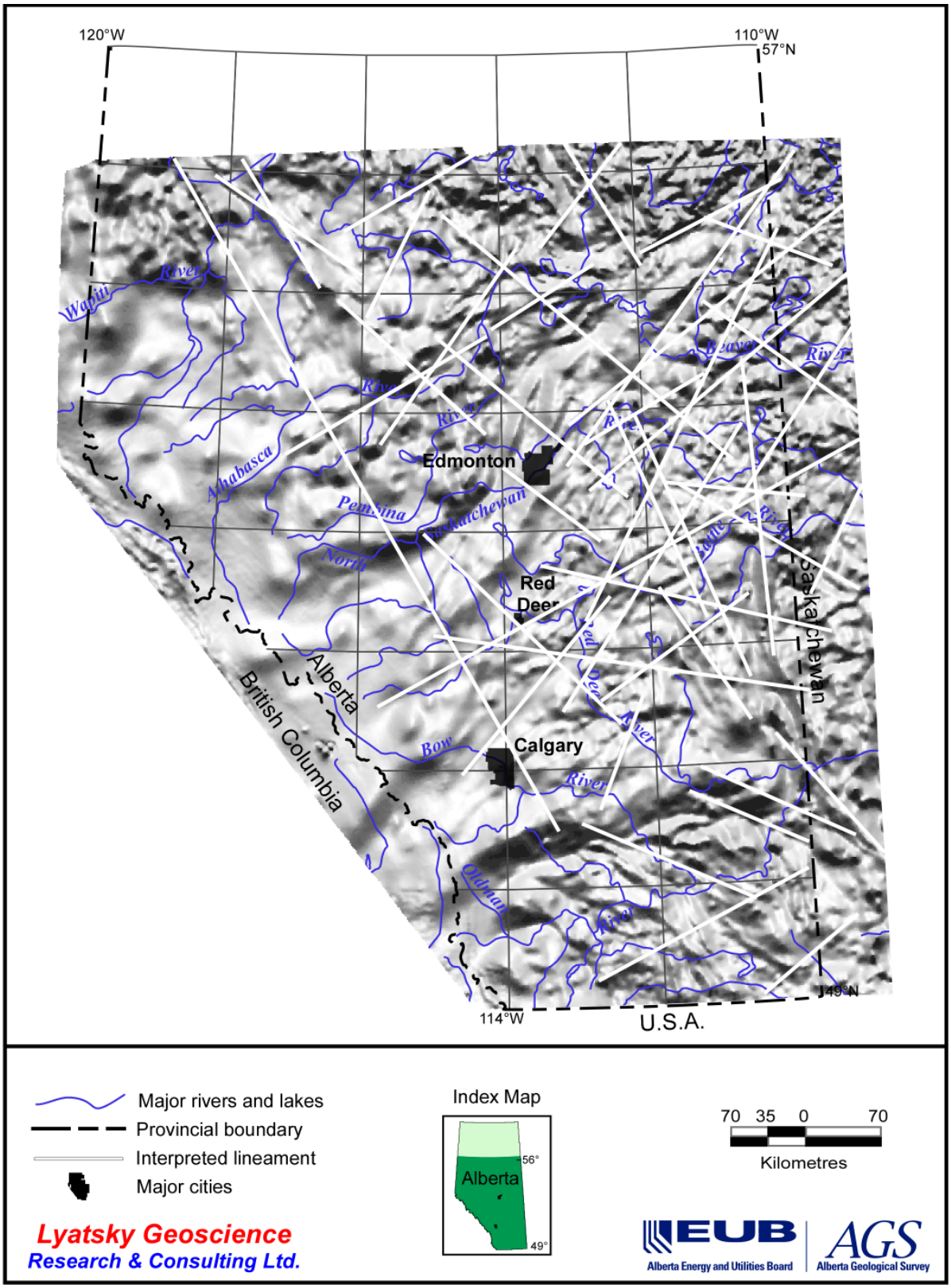

Map 41. Magnetic shadowgram illuminated from the north with 45° 'sun' inclination.

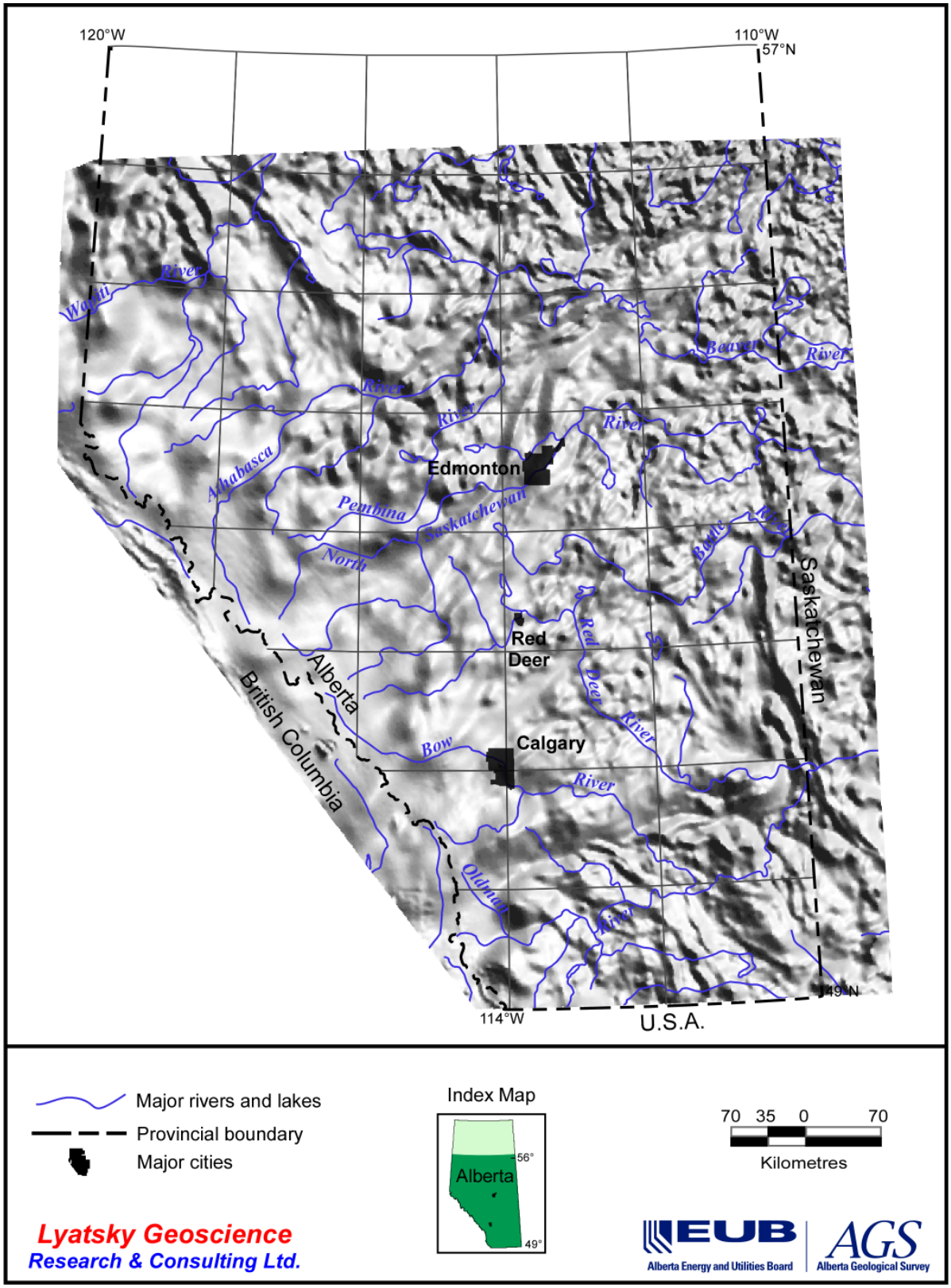

Map 42. Magnetic shadowgram illuminated from the northeast with 45° 'sun' inclination.

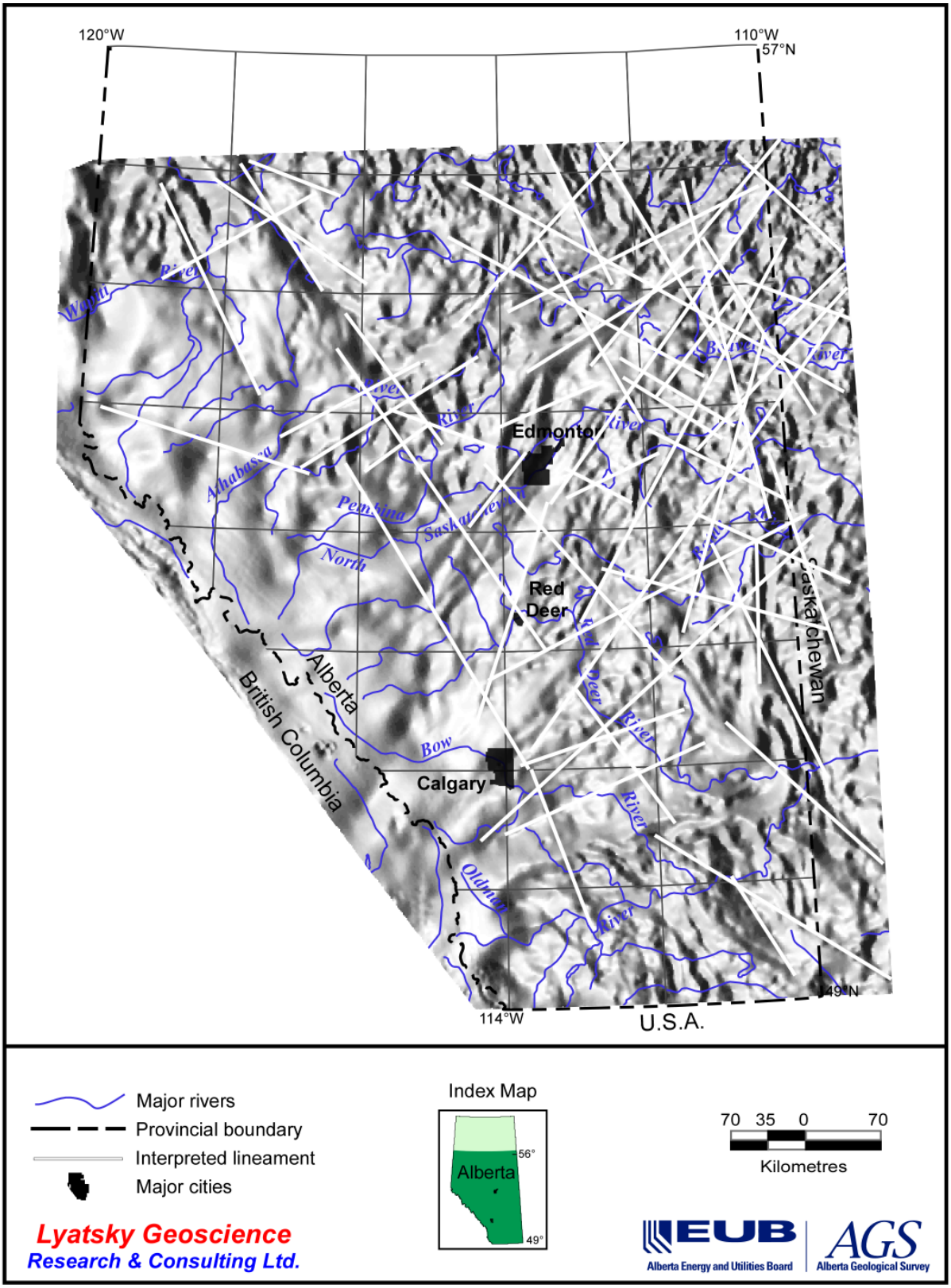

Map 43. Magnetic shadowgram illuminated from the east with 45° 'sun' inclination.

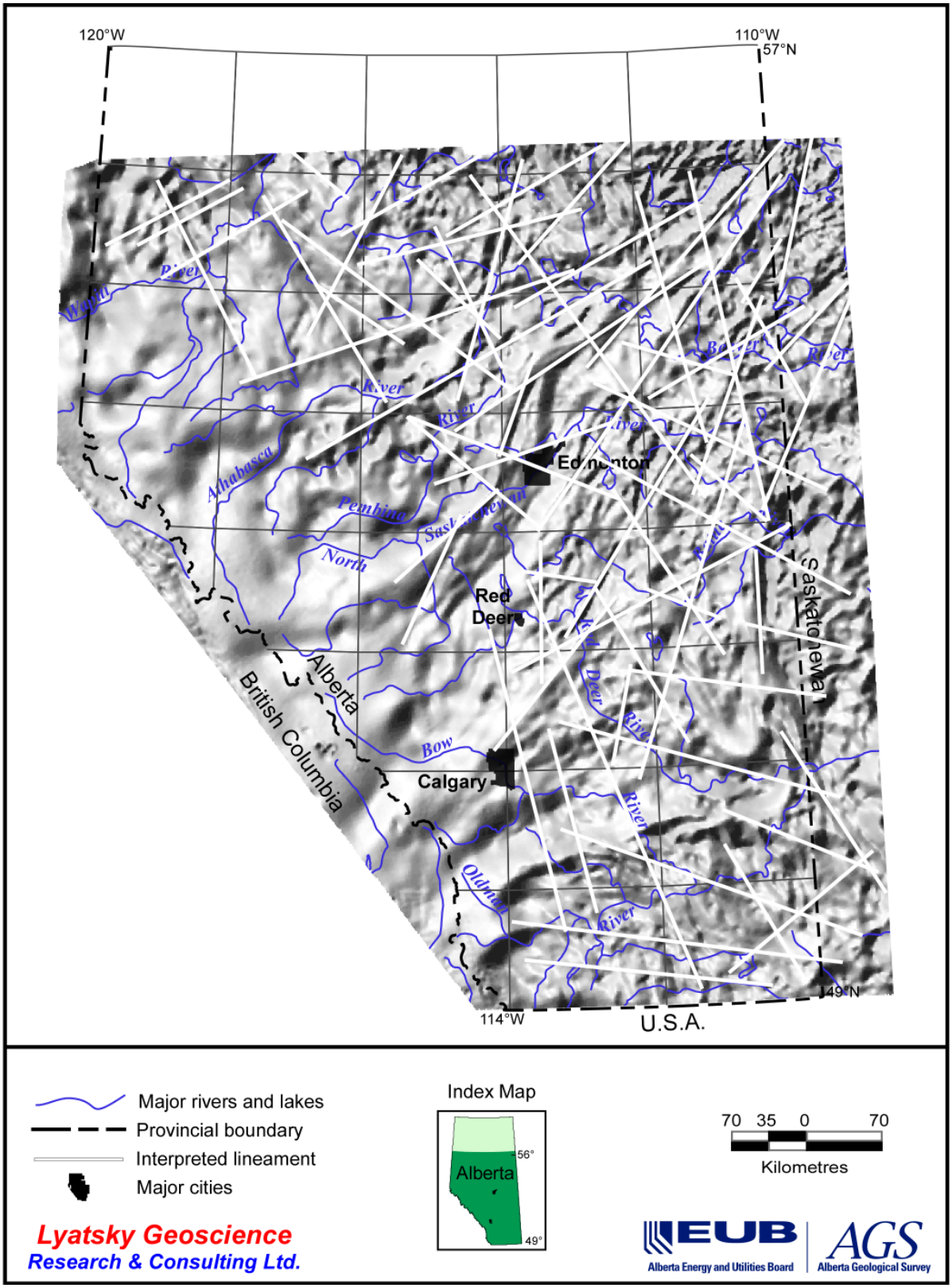

Map 44. Magnetic shadowgram illuminated from the southeast with 45° 'sun' inclination.

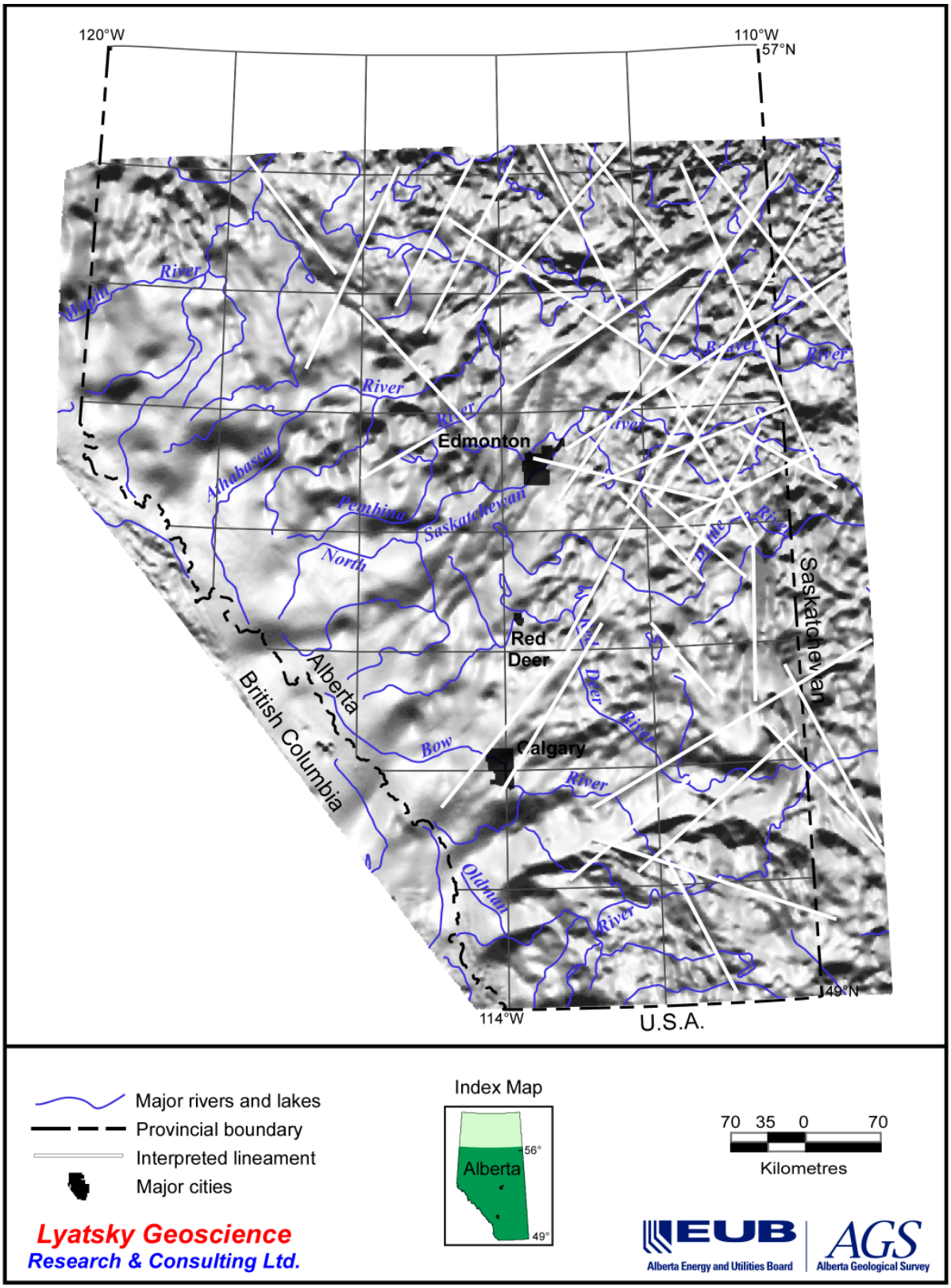

Map 45. Magnetic shadowgram illuminated from the south with 45° 'sun' inclination.

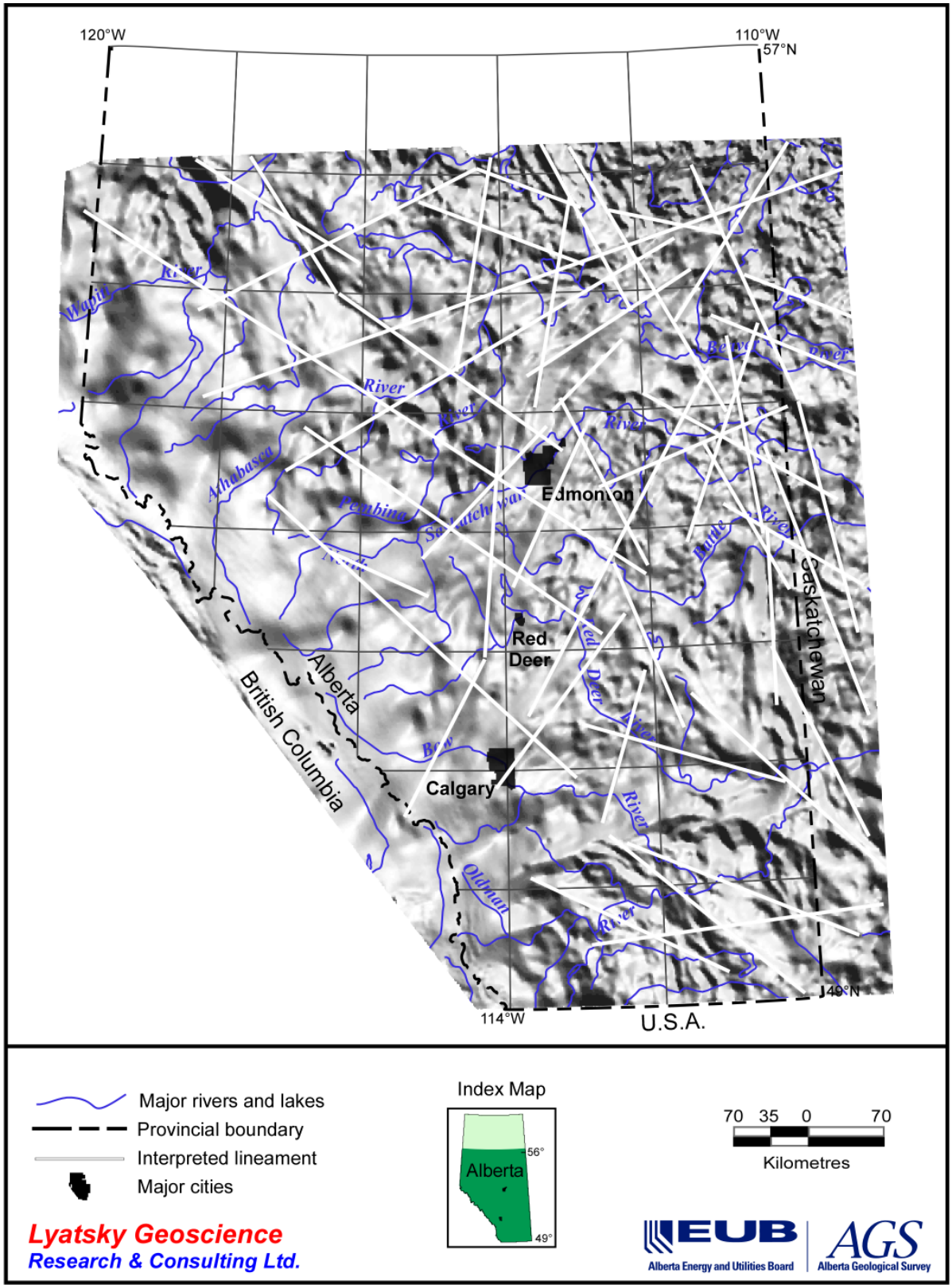

Map 46. Magnetic shadowgram illuminated from the southwest with 45° 'sun' inclination.

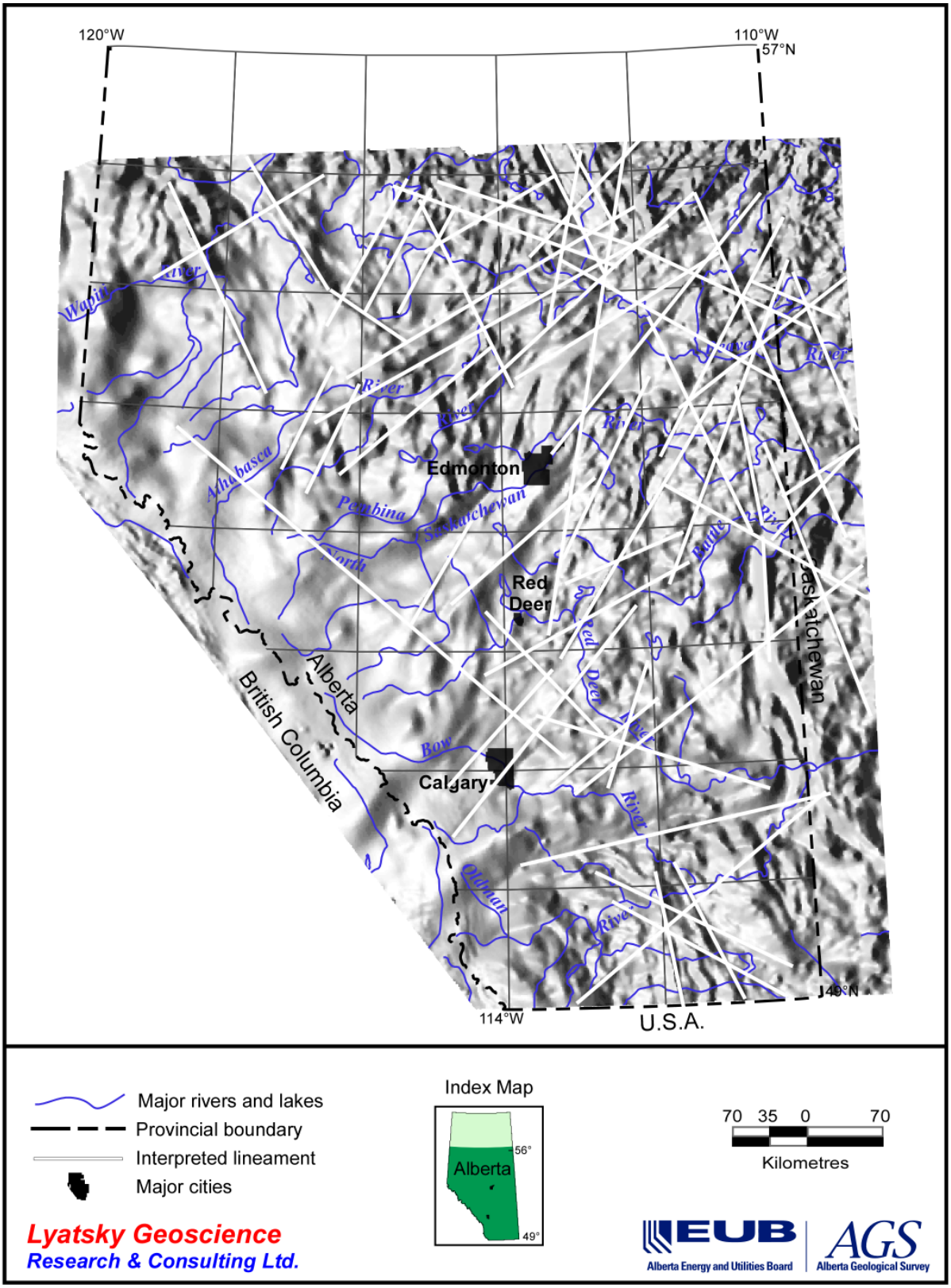

Map 47. Magnetic shadowgram illuminated from the west with 45° 'sun' inclination.

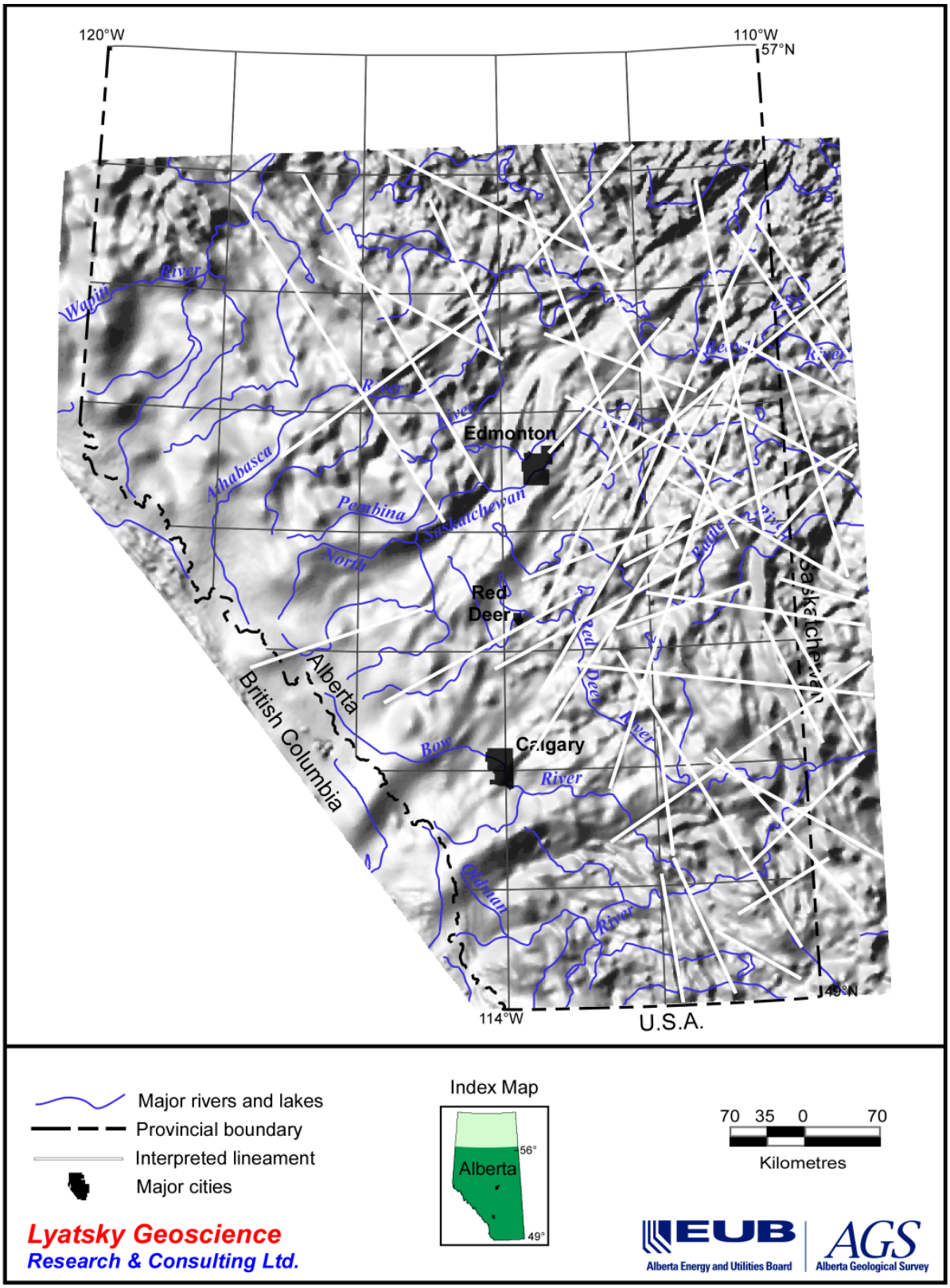

Map 48. Magnetic shadowgram illuminated from the northwest with 45° 'sun' inclination.

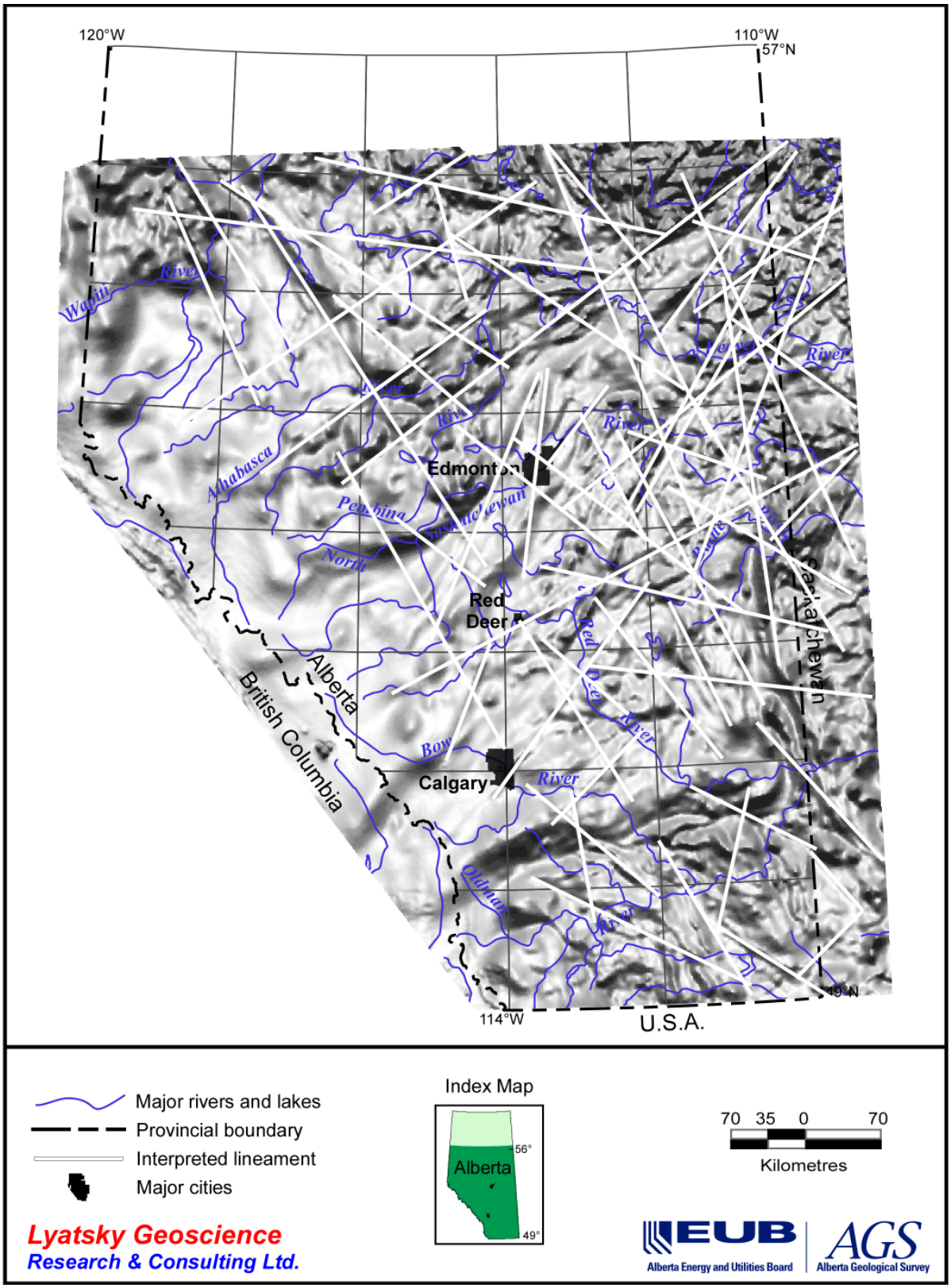

Map 49. Magnetic shadowgram illuminated from the north with 70° 'sun' inclination.

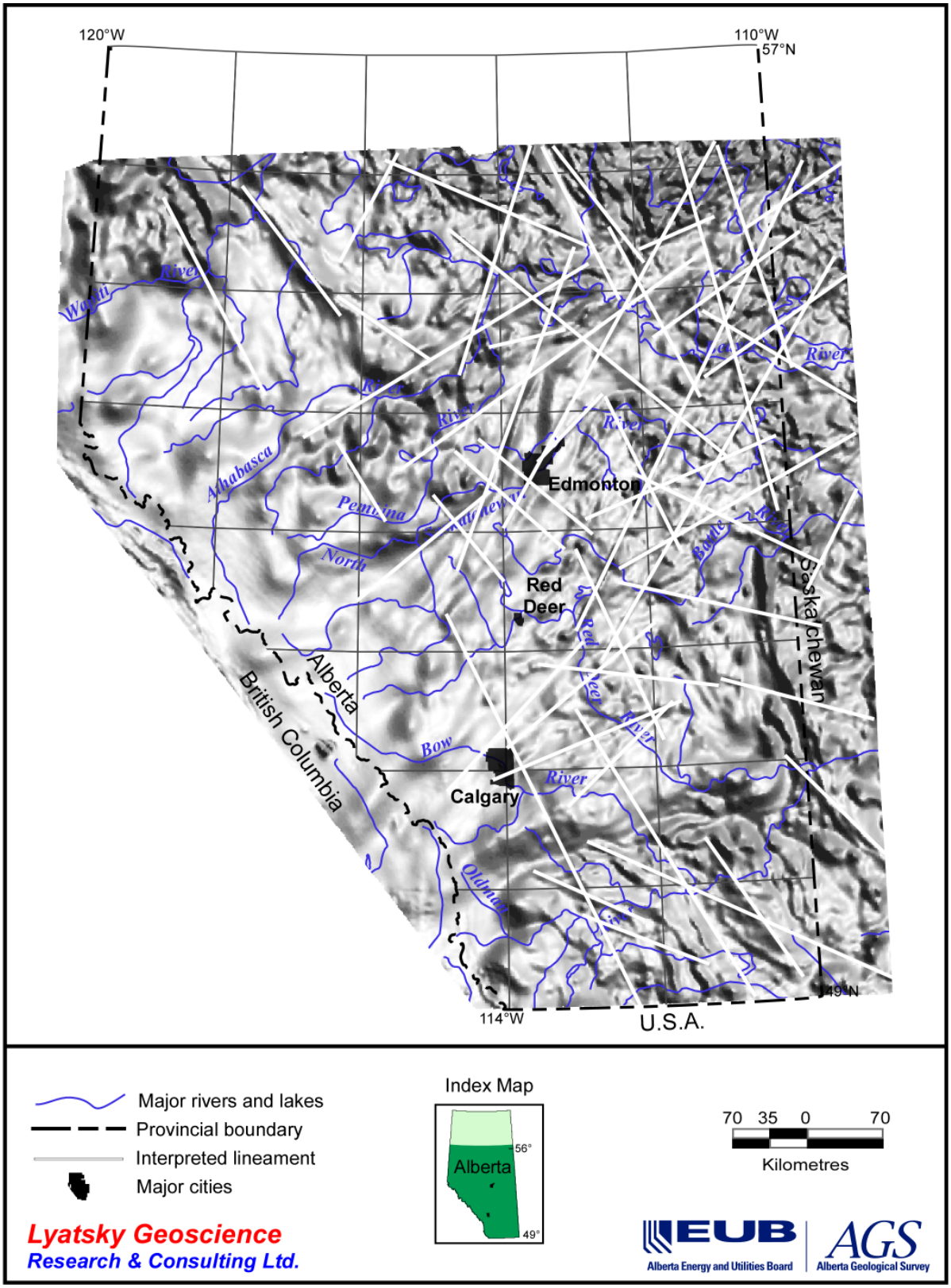

Map 50. Magnetic shadowgram illuminated from the northeast with 70° 'sun' inclination.

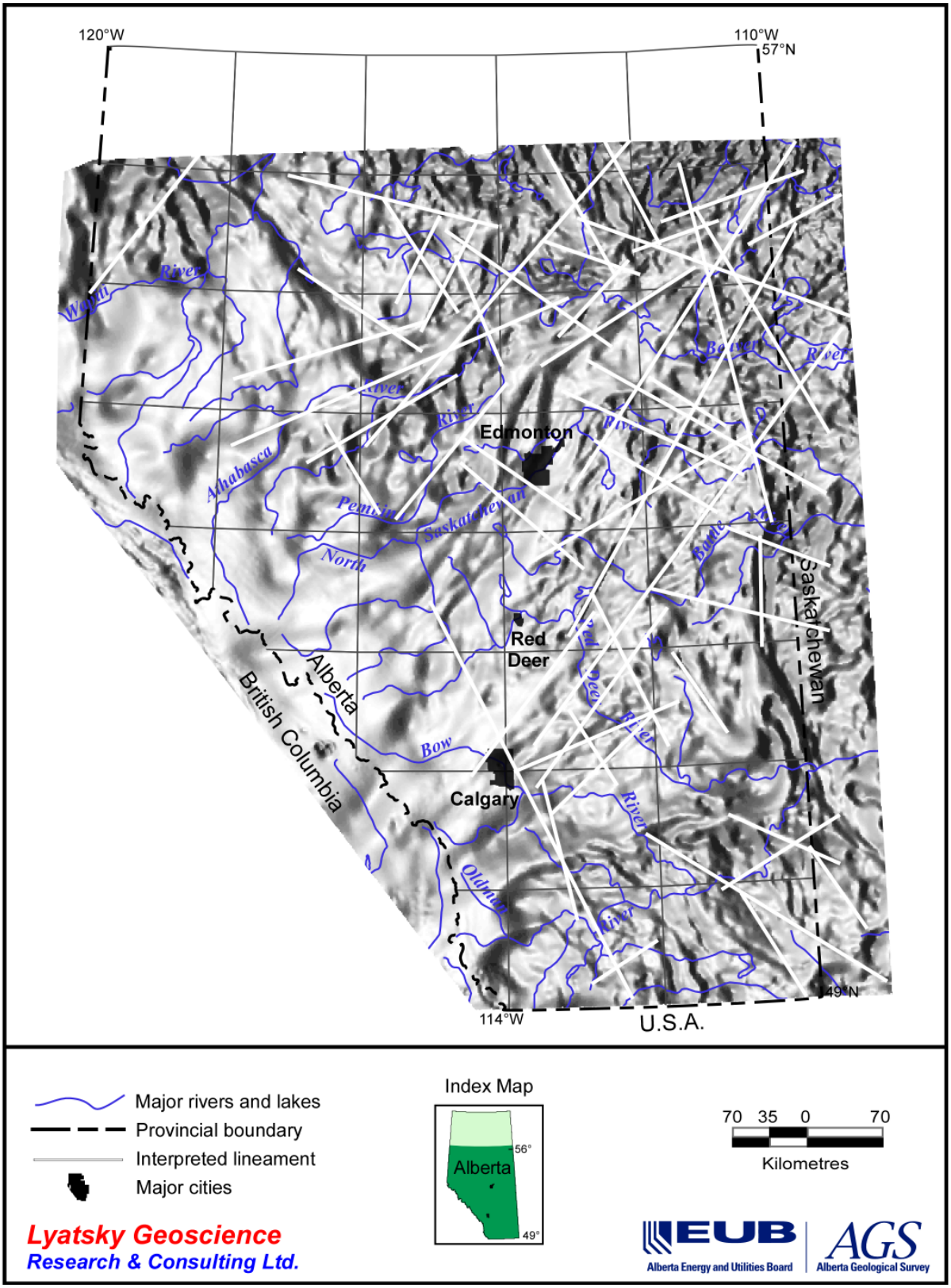

Map 51. Magnetic shadowgram illuminated from the east with 70° 'sun' inclination.

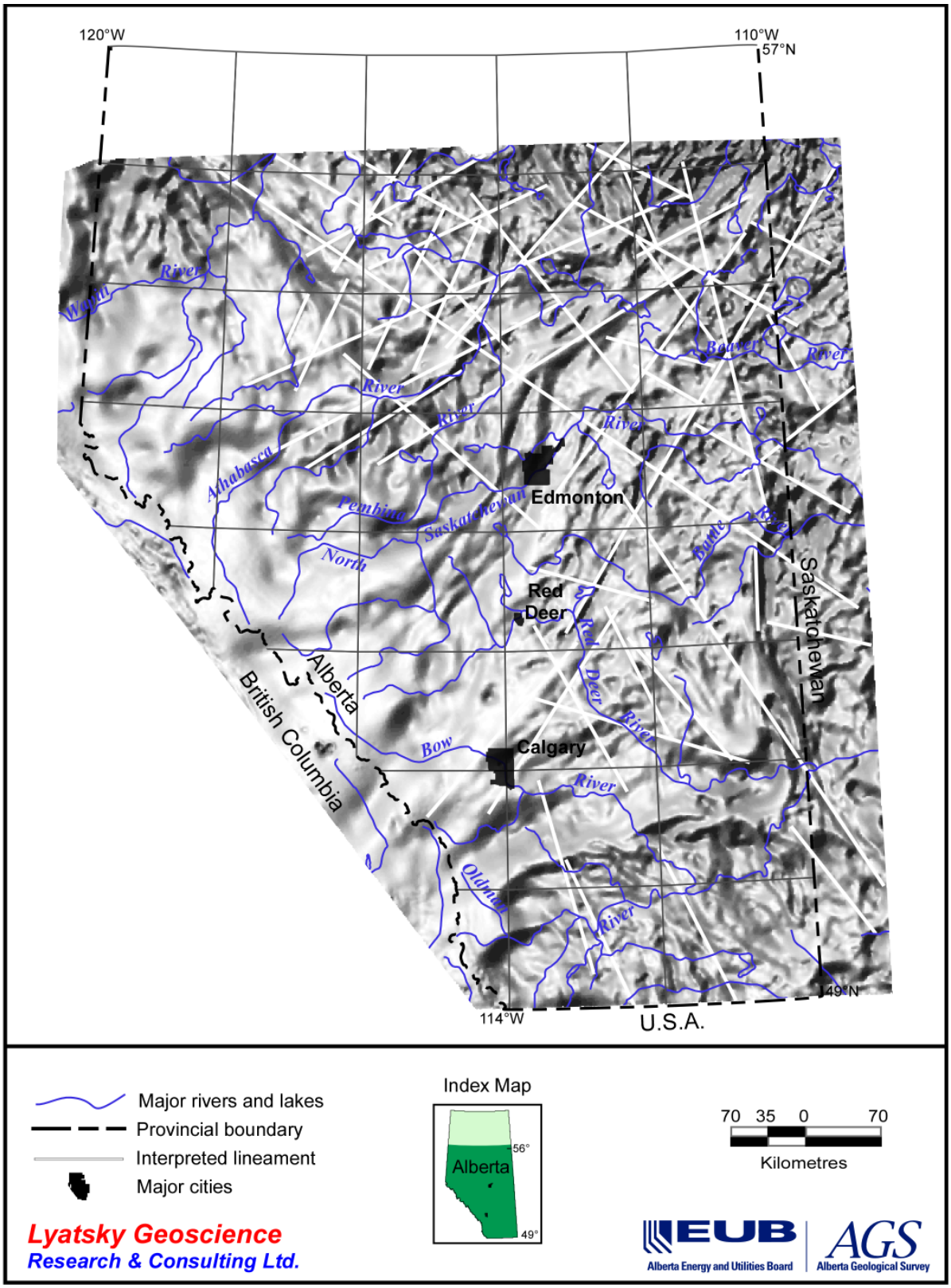

Map 52. Magnetic shadowgram illuminated from the southeast with 70° 'sun' inclination.

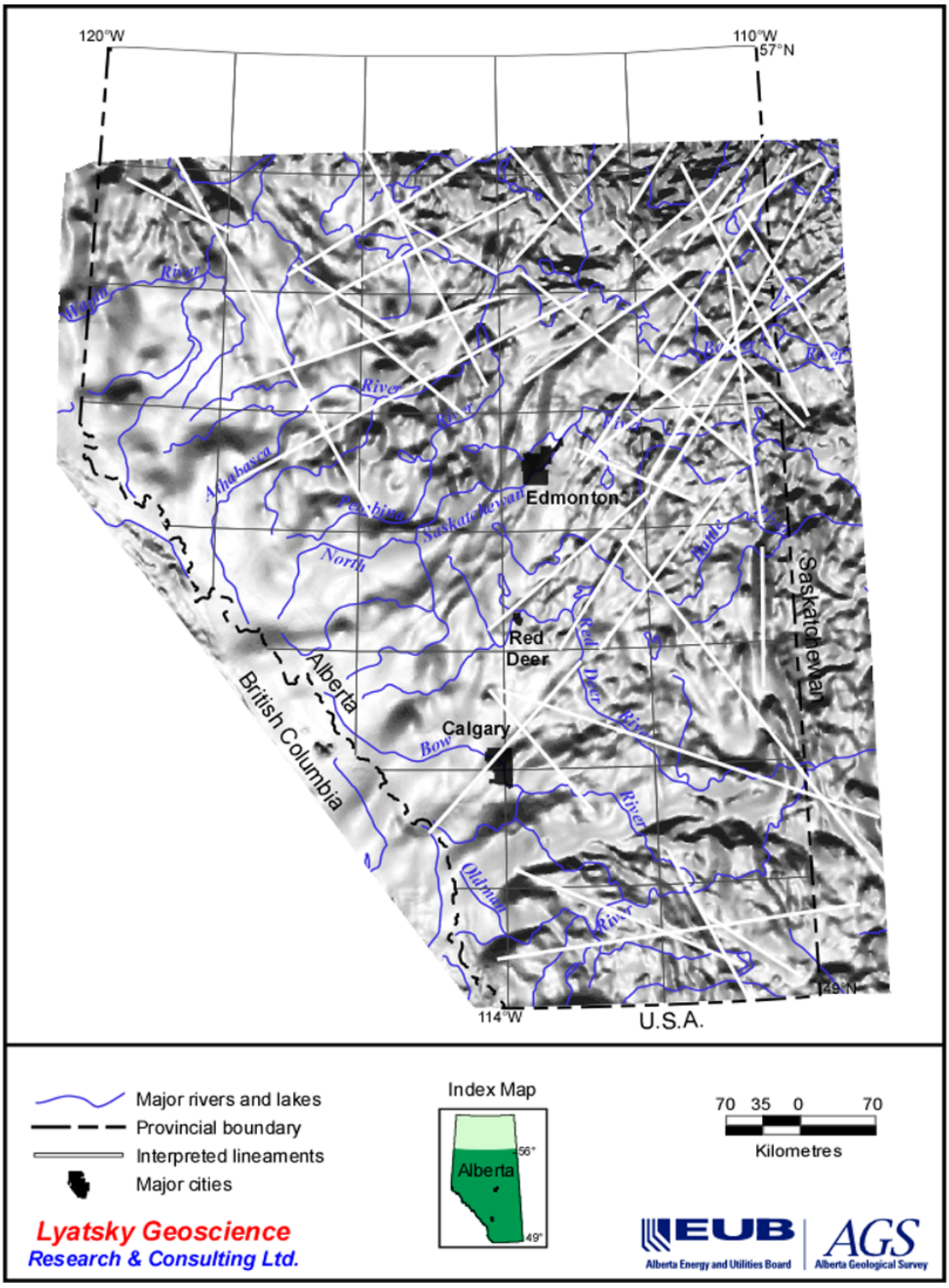

Map 53. Magnetic shadowgram illuminated from the south with 70° 'sun' inclination.

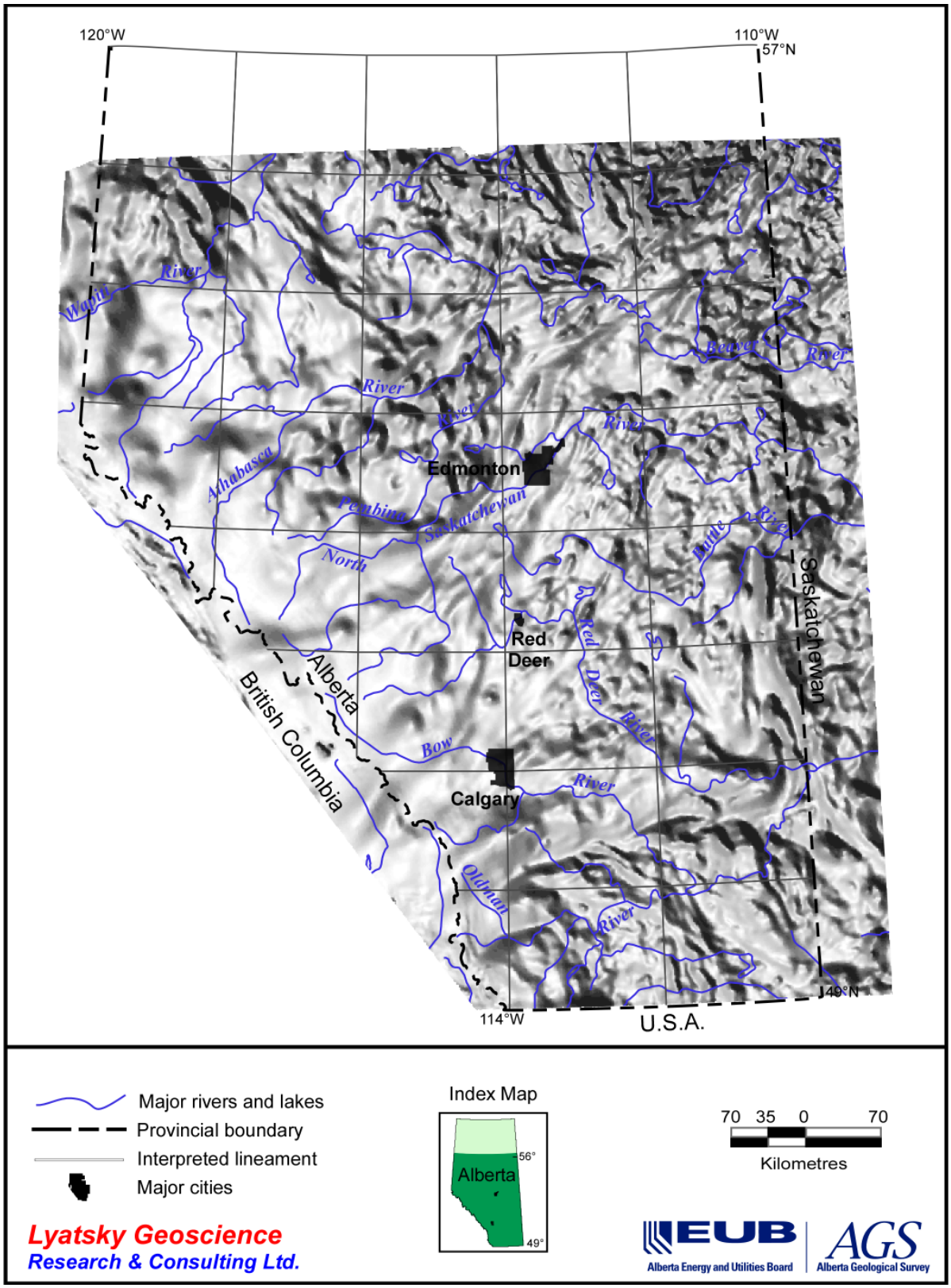

Map 54. Magnetic shadowgram illuminated from the southwest with 70° 'sun' inclination.

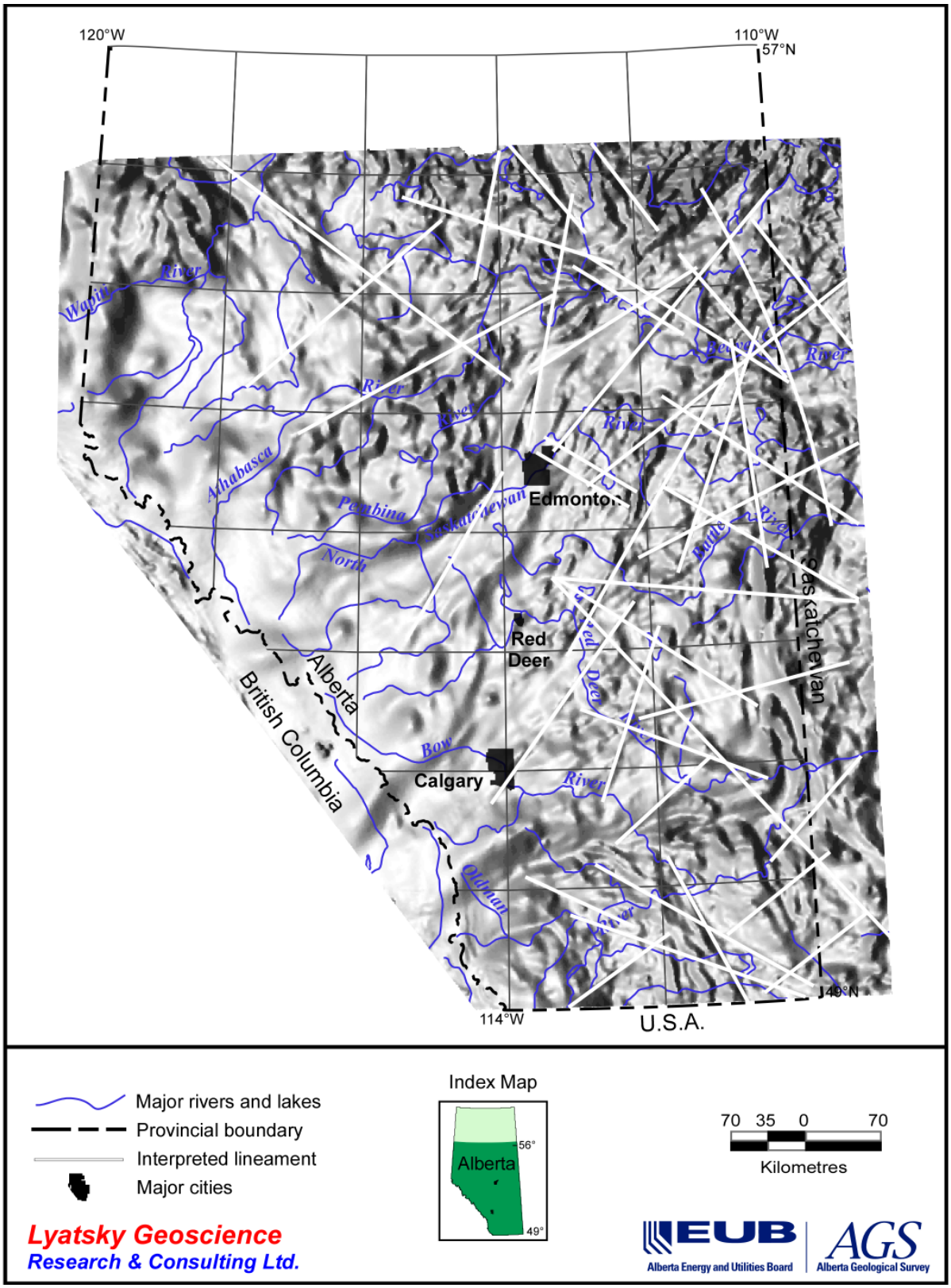

Map 55. Magnetic shadowgram illuminated from the west with 70° 'sun' inclination.

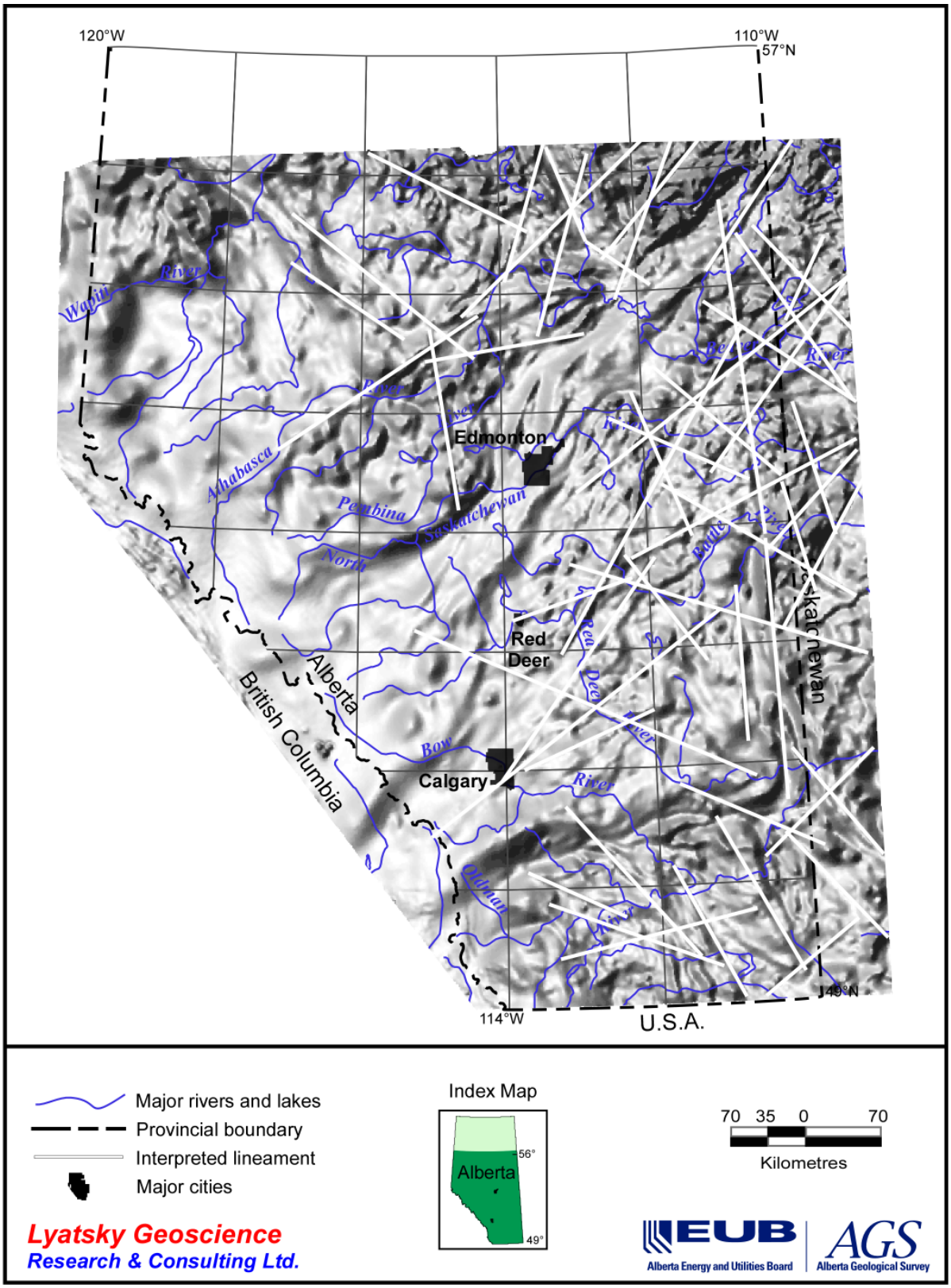

Map 56. Magnetic shadowgram illuminated from the northwest with 70° 'sun' inclination.